SZENT ISTVÁN UNIVERSITY

Development of hydrogel bio-anode with immobilized cells for improvement of performance of microbial fuel cells

DOI: 10.54598/000360

Ph.D. thesis

Truong Hoang Duy

2020

Doctoral School

Name: Doctoral School of Food Science

Field: Food Science

Head: **Prof. Livia SIMON-SARKADI D.Sc.**

Department of Food Chemistry and Nutrition Science

Faculty of Food Science, Szent István University

Supervisor: **Prof. Quang D. Nguyen Ph.D.**

Department of Brewing and Distilling

Faculty of Food Science, Szent István University

Assoc. Prof. Mai S. Dam Ph.D.

Institute of Biotechnology and Food Technology

Industrial University of Ho Chi Minh City, Vietnam

The applicant met the requirement of the regulations of the Szent István University and the thesis is accepted for the defense process.

…… ……

Signature of Head of Doctoral School Signature of Supervisor

Table of content

Abbreviations

ANOVA	Analysis of Variance
AEM	Anion Exchange Membrane
APS	Ammonium PerSulfate
BC	Bacterial Cellulose
BOD	Biological Oxygen Demand
BPM	Bipolar Exchange Membrane
CCD	Central Composite Design
CEM	Cation Exchange Membrane
CFU	Colony Forming Units
COD	Chemical Oxygen Demand
CV	Cyclic Voltammetry
HPLC	High-Performance Liquid Chromatography
I	Current
LB	Luria-Bertrani
MFC	Microbial Fuel Cells
MFCs	Microbial Fuel Cells system
OD	Optical Density
P	Power
PANI	Polyaniline
P_d	Power density
PEM	Proton Exchange Membrane
R	Resistor
SCE	Saturated Calomel Electrode
V	Voltage

List of figures

List of tables

1 INTRODUCTION AND OUTLINE

1.1 Introduction

Due to scarcity and adverse effects of fossil fuels, community are looking for an alternative energy source which is renewable and ecofriendly (Abbasi *et al.*, 2012; John *et al.*, 2011; Kothari *et al.*, 2012). In that context, it is believed that microbial fuel cells (MFC) is a two-fold solution to resolve the dilemma of energy crunch and negative environmental impacts of fossil fuels. MFC is an environmentally benign system, where microorganisms convert organic materials directly into electricity (Yong *et al.*, 2013). In MFC, electrons and protons are produced via anaerobic respiration of microorganism in anode chamber, and then while protons travel through the proton exchange membrane in the MFC to the aerobic cathode compartment, whereas electrons are transferred through the external circuit generating electricity. Despite it is very attractive technology (Jana *et al.*, 2010; Kim *et al.*, 2007; Rahimnejad *et al.*, 2011), however, the application still faces numerous limitations such as low power density, low electrical potential, cost of catalyst in cathodic chamber etc. (Hu, 2008; Oliveira *et al.*, 2013). There are various factors affecting the performance of MFCs such as microorganisms, substrate, mediator, electrode material and construction of MFCs (Logan *et al.*, 2006; Oh *et al.*, 2004; Park *et al.*, 2014). Engineering of electrodes may good direction to enhance the efficiency of MFCs (Huggins *et al.*, 2014) because of their electron production and transfer role. No doubt that the electrode biofilm and the electronic transport are important factors in improving the performance of MFCs (Picioreanu *et al.*, 2007).

Shewanella spp. is well-accepted by several research groups to produce electricity in the MFC. In the metabolic pathway, during the conversion of NAD^+ to NADH, CO_2 and organic acids, as well as H^+ and electrons are generated. Several strains of *Shewanella* produce mediators, such as riboflavin, flavin etc. to facilitate electron transfer to the anode (terminal electron acceptor) (Carmona-Martinez *et al.*, 2011). Interestingly, it was reported that bacterial cells can utilize both exogenous (externally added into the medium) or self-produced (endogenous) shuttle compounds as extracellular electron transporter (Velasquez-Orta *et al.*, 2010). In recent years, electron mediators or electron acceptors such as methylene blue, methyl red, humic acid, ferricyanide, riboflavin were used in most biological fuel cells to boost the electricity generation (Rahimnejad *et al.*, 2011; Wu *et al.*, 2013). The electron transfer rate could be enhanced by shuttling the electron from donor microorganism to acceptor electrode (Santoro *et al.*, 2017). In recent studies, riboflavin was used as an electron shuttle to transport electron to the anode. The important role of riboflavin in improving

electricity in the MFC was reported by several authors such as Wang *et al*. (2017); Wu *et al*. (2017); Yong *et al*. (2013); Zhang *et al*. (2017). The efficiency of application of mediator, however, strongly depends on its quality and actual quantity that can improved by new technique known as immobilization of mediators onto anode electrode. The advantage of this method was able to reuse the anode electrode with mediators and minimize their washing out in continuous operation (Wang *et al.*, 2017).

Carbon paper, cloth, foams or graphite rods, felt, foams, plates are commonly used as anode material in MFC (Logan, 2007c). For example, conductive polymer polyaniline (PANI) is one of materials that use to fabricate anode electrode because it played a great role in the energy storage (polyaniline based electrode materials for energy storage and conversion). Polyaniline is well known as a low cost, mechanical flexibility and stability material (Sapurina *et al.*, 2012). Szöllősi *et al*. (2017) used alginate/polyaniline/titanium-dioxide/graphite for the immobilization microorganism and make hydrogel bio-anode and an increase in electrical power of MFC was also reported. Bacterial cellulose (BC) is well known a non-toxic, low cost polymer, as well as it has some outstanding characteristics compared to plan cellulose such as renewability, ultrafine network structure, higher purity, water retention capability, porosity, biological interaction, mechanical strength (Dayal *et al.*, 2013; Vandamme *et al.*, 1998; Wang *et al.*, 2012a). Conducting polymers-cellulose composites including BC coated with conducting polymers is a new promising polymer and received interest in recent years because of their largely potential applications such as batteries, sensors and electrical devices. BC/PANI is a typical example for combination of BC and conducting polymer with the integration of several properties such as tensile strangle, biocompatibility, high surface areas and electrical conductivity (Kamalesh *et al.*, 2001; Li *et al.*, 2006). Müller *et al.*, (2012) as well as Wang *et al.*, (2012a) have been successful in fabrication of BC/PANI material with high electrical conductivity. In many researches, the PANI coated anode was successfully used in microbial fuel cells to enhance power density (Lai *et al.*, 2011; Logan *et al.*, 2006; Schröder *et al.*, 2003). Furthermore, the modified PANI polymers with the presence of titanium dioxide have generated enhanced current densities (Watanabe, 2008).

One of the main parts in MFCs is the anode, where exo-electrons are generated by the biocatalysts (bacteria) and transferred to the electrode. The performance of MFC is strongly affected by the quality and activity of microorganisms (Lovley, 2008) as well as quality and construction of the anode (Chen *et al.*, 2014). Additionally, its performance also depends on some factors affected the efficiency of electron transfer such as the distance between microorganism cells and electrode, the internal resistance, mediators etc.

1.2 Outline of dissertation

In the last decade, due to intensive development of conductive composites materials and application of mediators, the engineering of anode in the MFC has turned onto a new stage. New type of bio-anode can be formed applying conductive composite materials, mediators and it may lead to enhance efficiency of electron-transfer between bacteria cells and electrode, thus improvement of performance of MFC. Connecting to this field, my PhD research focused on development of hydrogel electrode with immobilized bacteria cells (bio-anode). Detailed tasks are following:

- Growth *of Shewanella xiamenensis* species bacteria
- Investigation of riboflavin production of *Shewanella xiamenensis*
- Fabrication and characterization of conductive hydrogel composites anode electrode
- Incorporation and immobilization of bacterial cells into hydrogel electrode
- Construction of MFC using hydrogel bio-anode with immobilized cells
- Stability and operational performance of MFC

2 LITERATURE REVIEW

2.1 Microbial fuel cells

2.1.1 General description

MFCs is one of the systems that is able to generate electric energy directly from organic wastes or in bioremediation (Palanisamy *et al.*, 2019; Szöllősi *et al.*, 2017). It contains an anode that uses bacteria to oxidize organic matters and generate current (Long *et al.*, 2019; Palanisamy *et al.*, 2019). In MFC, electrons and protons are produced via anaerobic respiration of microorganism in anode chamber. Then while protons travel through the proton exchange membrane in the MFC to the aerobic cathode compartment, whereas electrons are transferred through the external circuit. No doubt that microorganism and their potentiality to produce electron and proton play a notable role (Jana *et al.*, 2010; Kim *et al.*, 2007; Rahimnejad *et al.*, 2011) in the performance of MFC.

2.1.2 The history of MFC development

In 1910, the earliest MFC concept was introduced by Michael Cresse Potter, a professor of botany at the University of Durham, UK (Najafpour, 2015). The MFC system with the platinum electrodes was constructed using the living cultures of *Escherichia coli* and *Saccharomyces* to generate electricity (Du *et al.*, 2007). After the first innovation, there was no activity of research in MFC development for about 55 years until 1960s, when the US space program encouraged scientists to develop MFCs in turning organic waste into electricity in its long-haul space flights (Najafpour, 2015; Shukla *et al.*, 2004). In 1980s, it was discovered that the addition of electron mediators could greatly enhanced current density and power output (Du *et al.*, 2007). The outer layer of majority of microbial species are made of a non-conductive lipid membrane, peptidoglycans and lipopolysaccharides that prevent the direct electron transfer to the anode. Mediators can easily capture the electrons from the membrane. However, the electron mediators had several disadvantages such as toxicity such and solubility (Najafpour, 2015).

In 2007, the University of Australia and the Foster Brewing Company introduced the series of microbial cells with the total working volume of 10 L. The fuel was sewage from brewery. The waste was successfully converted to carbon dioxide and water while producing electricity (Gajda *et al.*, 2018; News, 2007).

2.1.3 Working principles of MFC

In an MFC, microorganisms grow on the anode and produce electrons, protons by oxidizing organic matter **(Eq. 2.1)** (Harnisch *et al.*, 2009). Electrons travel through a series of respiratory enzymes in the cells and make energy for the cells in the form of ATP (Logan, 2007b). Then, electrons are transferred to the anode, a terminal electron acceptor. After that, electrons flow through an external electrical circuit to cathode electrode, as a result producing electricity (Barua *et al.*, 2010; Kumar *et al.*, 2015a). The anode and cathode chambers are separated by a membrane. Protons are transferred internally through the membrane to the cathode. The cathode is sparged with air to provide dissolved oxygen for the reactions of electrons, protons and oxygen. Finally, water molecules are produced in cathode when electrons combine with protons and oxygen **(Eq. 2.2)**.

$$C_xH_yO_z + (2x - z)H_2O \rightarrow xCO_2 + (y + 4x - 2z)H^+ + (y + 4x - 2z)e^- \quad \textbf{(Eq. 2.1)}$$

$$6O_2 + 24H^+ + 24e^- \rightarrow 12H_2O \quad \textbf{(Eq. 2.2)}$$

A schematic of a dual-compartment MFC is demonstrated in **Figure 2.1**. The presence of oxygen in the anode chamber inhibits the generation of electricity, because oxygen capture electrons and protons as a combination in the cathode chamber. Thus, the system must be designed to keep the bacteria in anode chamber separated from oxygen (Najafpour *et al.*, 2011).

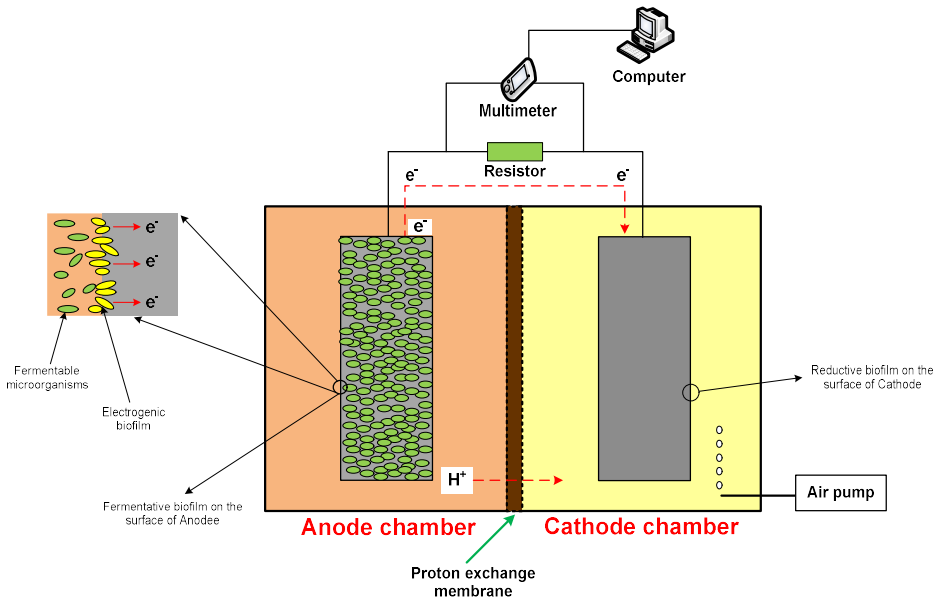

Figure 2.1. Schematic of the dual-compartment MFC with a biochemical reaction in the anode and cathode compartments (Logan, 2007b; Najafpour, 2015)

2.1.4 MFC construction

2.1.4.1 MFC components

A traditional MFC system consists of an anodic chamber and a cathodic chamber separated by a proton exchange membrane (PEM). Nowadays, there are many different designs are possible for MFCs: single compartment, dual compartment, and stacked MFCs that can be used for a specified purpose. One of the basic MFCs designs is "H" shape. It includes two bottles connected by a tube containing a separator which is usually a cation exchange membrane (CEM) such as Nafion, or a plain salt bridge. The key to this design is to choose a membrane that only allows protons to pass through (the CEM is also called a proton exchange membrane) (Logan *et al.*, 2006; Najafpour, 2015).

2.1.4.2 Single-compartment MFC system

Single-compartment MFC system consist of a cathode directly attached to a PEM allowing air oxygen to react at the electrode. Electrons are transferred to the cathode via the electrically conductive wire to complete the circuit (Liu *et al.*, 2004; Park *et al.*, 2003).

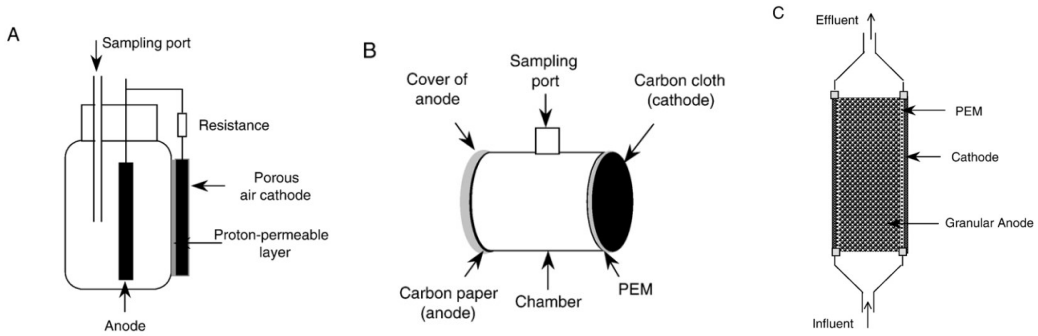

Figure 2.2. Schematics of different type of single-compartment MFC system: an MFC with a proton permeable layer coating the inside of the window-mounted cathode (A), an MFC consisting of an anode and cathode placed on opposite side in a plastic cylindrical chamber (B), and a tubular MFC with outer cathode and inner anode consisting of graphite granules (C) (Du *et al.*, 2007)

2.1.4.3 Dual-compartment MFC system

A dual-compartment MFC has anodic and cathodic chambers connected by a PEM, or a salt bridge, to allow protons to move across from the anode to the cathode. **Figure 2.3** shows the different dual-compartment MFC systems (Du *et al.*, 2007; Logan *et al.*, 2006; Najafpour, 2015). "H" shape **(Figure 2.3A)** systems are usually used for basic parameter research, such

as production using new materials, or types of microbial communities that arise during the degradation of specific compounds, but they typically produce low power densities (Logan *et al.*, 2006). **Figure 2.3C** showed the mini-MFC having a diameter of about 2cm was reported by (Ringeisen *et al.*, 2006). **Figure 2.3D** and **2.3E** are the up-flow mode MFC systems used for wastewater treatment with the fluid flowing continuously through porous anodes toward a membrane separating the anode from the cathode chamber (Logan *et al.*, 2006).

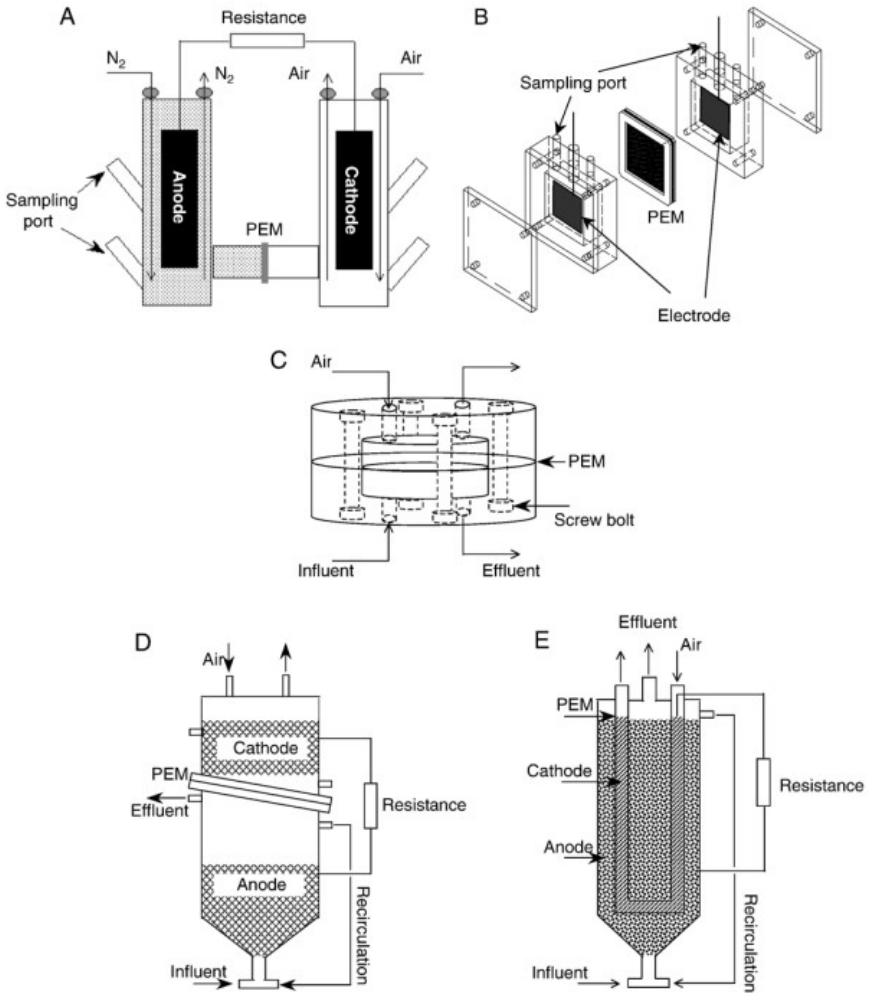

Figure 2.3. Schematics of a dual-compartment MFC: (A) "H" shape, (B) rectangular shape, (C) miniature shape, (D) upflow configuration with cylindrical shape, cylindrical shape with an U-shaped cathodic compartment (E) (Du *et al.*, 2007)

2.1.4.4 Stacked MFC system

Single compartment MFC system were used by many scientists but they showed the low efficiency. Therefore, a fuel cells stack was set up by connecting single MFCs in a series

and/or in parallel to enhance the efficiency of MFC system (Najafpour, 2015). **Figure 2.4** showed a stacked MFC consisting of six individual units. The MFCs were separated by rubber sheets, with the anode and cathode chambers (each 156 mL total volume, 60 mL liquid volume) containing graphite rods set into beds of graphite granules. By connecting several MFCs in series or in parallel can enhance voltage or current output. However, voltage reversal remains a large obstacle for successful increases in the voltage (Logan, 2007a).

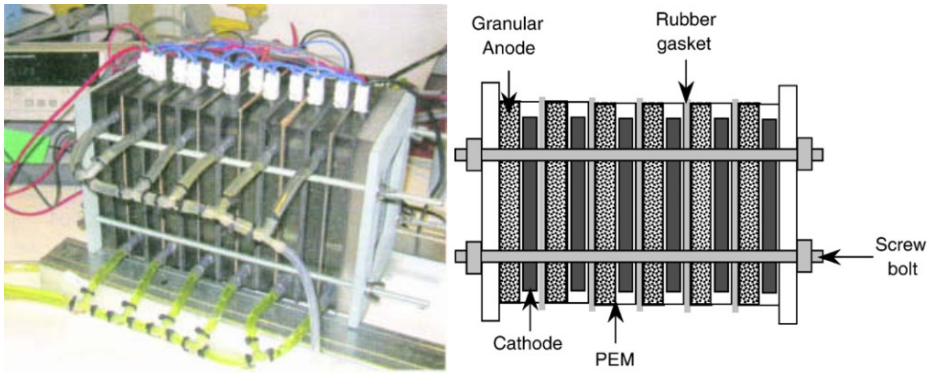

Figure 2.4. Stacked MFCs with 6 separate MFCs are joined in one reactor block
(Du *et al.*, 2007; Logan, 2007a)

2.1.5 MFC materials

2.1.5.1 Anode materials

The requirements of an anode material are: highly conductive, low resistance, non-corrosive, high specific surface area, high porosity, non-fouling, inexpensive, biocompatible, and chemically stable in the reactor solution (Logan *et al.*, 2006; Tanisho *et al.*, 1989). Noncorrosive metal such as stainless-steel mesh is one of materials can be used as anode (Logan *et al.*, 2006). However, bacteria must be able to attach to the material and achieve good electrical connections. In this case, noncorrosive metal apparently meet many requirements for an anode material, but may not be suitable for the attaching of bacteria (Logan, 2007c). The use of carbon materials such as felt, cloth, paper, fibers, foam for the MFC anode is very common (Logan *et al.*, 2006), because they have high conductivity, cheap, easy to handle, relatively defined surface areas and appear to be well suited for bacterial growth (Gil *et al.*, 2003; Logan *et al.*, 2006; Park *et al.*, 1999).

There are many factors affecting the efficacy of MFC and the anode electrode material is one of the crucial factors (Kalathil *et al.*, 2013). The requirements of anode materials

should have high surface area and porosity, large capacitance, excellent electrical conductivity, good biocompatibility (Wang *et al.*, 2020).

Nowadays, many studies were carried out and developed such as the addition ion metals, mediators into anode chamber or using conductive polymer materials to increase the anodic performance. In MFC, plain graphite and carbon-based materials are commonly used as electrode because of their high conductivity, durability, eco-friendliness and their flexibility to be shaped into various architectures (Logan *et al.*, 2007; Vargas *et al.*, 2013). However, their resistivity is typically 1000-fold higher than that of metals. To improve the catalytic and surface properties of these materials, anode materials should be modified (Kalathil *et al.*, 2013). He *et al.* (2013) used carbon felt or carbon cloth as a raw material for fabrication of polypyrrole- MnO_2 composites as free-standing electrode with supercapacitors. Yuan *et al.* (2016) also utilized MnO_2/polypyrrole/MnO_2 composite decorated on a carbon cloth that successfully improved the performance of MFCs. Lately, nanomaterials have attracted much attention. Xu *et al.* (2011) tested Fe nanoparticle-decorated graphite disks with six-fold higher average current densities than the plain graphite anode. However, carbon felt or carbon cloth has small pore sizes and microbes cannot access to the interior of anodes (Wang *et al.*, 2020). Kalathil *et al.* (2013) used a plain carbon paper modified with the carbon nanotube/MnO_2 nanocomposite and used it as anode for the MFC. The modified anode showed better electrochemical performance than that of plain carbon paper. Carbon nanotubes are promising electrode materials because of their high surface area, excellent electrical conductivity, chemical inertness and low internal resistance (Liang *et al.*, 2011). Anode was modified with carbon nanotube can increase the anode surface-to-volume ratio, improved the ability of the microbes to access and transfer electron to the anode (Liang *et al.*, 2011). Recently, some studies used porous sponge as a raw material instead of traditional materials (Xie *et al.*, 2012). Because sponge has a continuous 3D structure with large surface area (Wang *et al.*, 2020). Li *et al.* (2014) fabricated sponge/carbon nanotube/polypyrrole/manganese dioxide (S/CNT/PPy/MnO_2) composite as supercapacitor gained high capacitance.

Polyaniline, one of the conductive polymers, have received widely attention in anode material development. Many reports indicated that power density of MFC increased with using PANI-modified anode (Dumitru *et al.*, 2016). For example, the power density of MFC with carbon felt/PANI anode was 1.4-fold higher than unmodified anode (Li *et al.*, 2011). MFC used platinized carbon cloth/PANI anode got the higher current density than platinized carbon cloth (1.45 mA/cm^2 vs 0.84 mA/cm^2) (Schröder *et al.*, 2003). In addition, the

incorporation of modified anode with metal nanoparticles presents a potential for the improvement of MFC. **Table 2.1** showed the power output of MFC using different raw material anode modified by PANI and/or with TiO_2. Hen *et al.* (2018) used modified anode in MFC with the immobilization of bacterial cell and improvement of the efficiency of MFC was reported.

Table 2.1. The power density of different modified anodes in MFC

Anode material	MFC contruction	Bacteria	Power density P_{max}	References
Alginate/polyaniline/ TiO_2/graphite	DCMFC	*S. algae*	9.86 W/m^3 (graphite cloth anode: 2.88 W/m^3)	Szöllősi *et al.*, 2017
Carbon nanotube/ polyaniline	-	*E. coli*	42 mW/m^2	Qiao *et al.*, 2007
Carbon cloth/ polyaniline	DCMFC	-	5.16 W/m^3 (fresh carbon cloth anode: 1.93 W/m^3)	Lai *et al.*, 2011
Chitosan-nitrogen/ carbon nanotubes/ polyaniline	DCMFC	-	4.2 W/m^3 (carbon nanotube/sponge anode: 1.4 W/m^3)	Xu *et al.*, 2019
Graphite sheets/ polyaniline/graphene/ TiO_2 immobilized bacterial cell	DCMFC	*S. oneidensis*	79.3 mW/m^2 (graphite sheets/ polyaniline/graphene/TiO_2 nonimmobilized bacterial cell anode: 61 mW/m^2; plain carbon paper immobilized bacterial cell: 29.4 mW/m^2)	Han *et al.*, 2018

DCMFC: dual-chamber MFC

2.1.5.2 Cathode materials

Some materials such as carbon paper, cloth, graphite, woven graphite, graphite granules can be used for both cathodic or anodic electrode. In cathode, the electrons, protons and oxygen must all meet at a catalyst in a tri-phase reaction to achieve high efficiency, thus, the catalyst must be on a conductive surface, but it must be exposed to both water and air (Logan, 2007c). Protons produced in the anodes chamber migrate into the cathode chamber via the proton exchange membrane. The electrons travel to cathode electrode and transmit onto

oxygen (Rahimnejad *et al.*, 2015). Oxygen is the most suitable electron acceptor in cathode due to its accessibility, intense oxidation potential, availability and low cost (Logan *et al.*, 2006). Besides, potassium ferricyanide ($K_3[Fe(CN)_6]$) is usually used as an electron acceptor in cathodic chamber due to their low overpotential. However, it has a disadvantage namely the insufficient re-oxidation by oxygen, thus it must be regularly replaced (Rabaey *et al.*, 2005a).

2.1.5.3 Membrane

Membrane are primarily used in dual-compartment MFC system for separating the liquids between anode and cathode (Logan, 2007c). Both porous and non-porous membranes fabricated from polymers are commonly used in bio-electrochemical systems, but non-porous ones (charged), one of the selective ion-permeable membranes (cation, anion exchange or bipolar membrane), are mostly preferred (Bakonyi *et al.*, 2018). In the MFC system, proton migrates from the anode chamber to the cathode chamber via the cation exchange membrane (CEM) such as Nafion, Hyflon, Zirfon, Ultrex CMI 7000. Proton transport through membrane such as Nafion is due to its structure has the hydrophilic sulfonate group (negatively charged such as $-SO_3^-$, $-COO^-$, $-PO_3^{2-}$) attached the hydrophobic fluorocarbon group (Leong *et al.*, 2013; Oliot *et al.*, 2016; Sleutels *et al.*, 2017). While CEM or anion exchange membrane (AEM) allow only cation or anion move to the other side of MFC, bipolar membrane (BPM) allow both anion and cation move to the opposite side because it include a cation exchange layer and an anion exchange layer in each side of membrane (Oliot *et al.*, 2016).

2.1.5.4 Microbes

In the MFC system, microorganism(s) act as biocatalyst and through the microbial catabolism of organic substrate, they generate exo-electrons (Najafpour, 2015). *Geobacter* species and *Shewanella* species such as *Geobacter metallireducens, Geobacter sulfurreducens, Shewanella oneidensis, Shewanella putrefaciens* (Bond *et al.*, 2002; Min *et al.*, 2005; Park *et al.*, 2002; Ringeisen *et al.*, 2006) with their exo-electrogenous potential are widely (Tharali *et al.*, 2016), but, some other microorganisms for example *Escherichia coli, Lactobacillus plantarum, Proteus mirabilis, Streptococcus lactis* and *Saccharomyces cerevisiae* are also reported to be as good as catalyst in the MFC (Choi *et al.*, 2003; Grzebyk *et al.*, 2005; Najafpour *et al.*, 2011).

Shewanella spp. are a group of facultative anaerobic bacteria that can be found in marine and fresh-water environments (Tang *et al.*, 2009). They can also be used in MFCs

because of their electron generation and their versatile electron accepting capacities by oxidizing organic compounds. Additionally, *Shewanella* spp. have an important role for carbon cycling. Therefore, they can be used for the remediation of contaminated environments (Fredrickson *et al.*, 2008). There were many researches using *Shewanella* spp. in MFCs (Hasan *et al*., 2017; Li *et al*., 2016; Wang *et al.,* 2017). The ability to produce exo-electrons by *Shewanella xiamenensis* was reported by Szöllősi *et al.* (2014) and they also mentioned the potential of this species in MFCs.

2.1.6 Electron transfer and mediators

Electron transfer in the anode chamber is the key issue in understanding the theory of how MFC operation. Microorganisms play important roles in anode chamber and they utilize different substrates as a carbon source to generated electrons and protons (Liu *et al.*, 2004; Park *et al.*, 2014). For example, glucose can be used as a substrate and the electrons are generated according to **Eq. 2.3**. Degradation of 1 molecule glucose in an anaerobic condition will generate 24 electrons and 24 protons.

$$C_6H_{12}O_6 + 6H_2O \rightarrow 6CO_2 + 24e^- + 24H^+ \qquad \textbf{(Eq. 2.3)}$$

The electron transfer from microorganism to the electrode through an electron transport system that includes a series of components in the bacterial extracellular matrix or together with electron shuttles dissolved in the bulk solution (Du *et al.*, 2007). **Figure 2.5** illustrated the chemical compounds to be involved in the electron transfer from electron carriers in the intracellular matrix to the final electron acceptor (anode) in *Shewanella oneidensis* MR-1.

Microorganisms can be used in four ways for producing electrical energy (Shukla *et al.*, 2004):

1. Microorganism produce electrochemically active substances through fermentation or metabolism. Fuels are produced in separate reactors and transported to the anode of a conventional fuel cells. The microbial bioreactor is kept separated from the fuel cells.
2. Microorganism oxidized organic matter and produce fuel directly in the anodic of the fuel cells.
3. The mediator played as an electron shuttle, accepted electrons from the microorganisms and transport them to the anode of the fuel cells.
4. The ability of metal-reducing of microorganism created the communication electrically with the electrode surface directly.

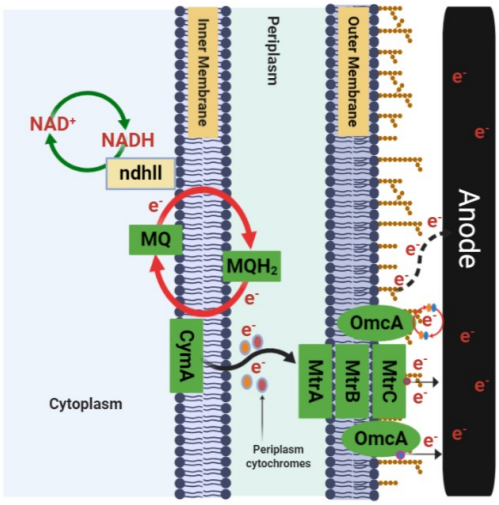

Figure 2.5. Summary of components proposed to be involved in the electron transport from cells to the anode in MFCs (*Shewanella oneidensis MR-1*) (CymA inner membrane tetraheme c-Cyts; MtrA periplasmic decaheme c-Cyts; MtrB β-barrel trans-OM protein; MtrC and OmcA two OM decaheme cCyts) (Du *et al.*, 2007; Li *et al.*, 2018)

Microorganisms can transfer electrons to anode in MFCs by three ways **(Figure 2.6)**, such as: transfer electron from bacterial to anode in the short-range through redox active protein present on the outer surface membrane of bacteria such as cytochromes; transfer electron via electron shuttles, mediators, for example, flavins and pyocyanin; transport electron to the anode in the long-range through microbial nanowires (Kumar *et al.*, 2015b). **Figure 2.6a** describes the electron transport via microbial-nanowires arising from the microorganisms. Some *Geobacter* and *Shewanella* strains can evolve conductive pili (microbial-nanowires) that allow microorganisms to use anode as an electron acceptor without contact directly. The conductive pili are connected to the membrane-bound cytochromes where the electron transfer from inside of microorganisms to outside. The electrons will follow the conductive pili to move to the anode. The second mode for transfer of electrons is indirect via soluble mediators **(Figure 2.6b)**. Oxidized mediators form catches electrons, then they are reduced and release electrons at the anode surface. In direct electron transfer **(Figure 2.6c)**, electrons can be transported via a physical contact of the bacterial cell membrane with the anode. Electrons inside of the microorganisms cell will be transferred to the outer membrane where c-type cytochromes allow the electron to move directly to anode external (Kim *et al.*, 2018; Kumar *et al.*, 2016).

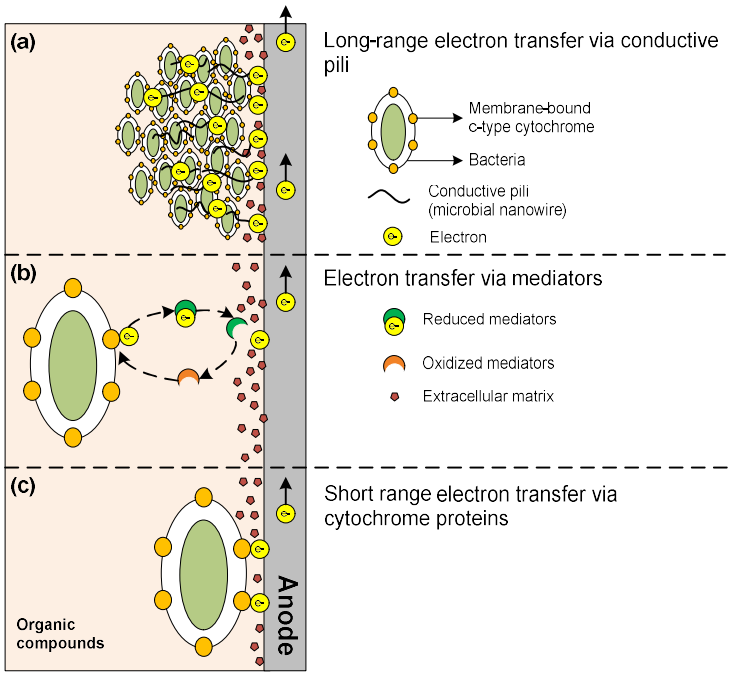

Figure 2.6. The mechanisms of electron transfers from microorganisms to anode in MFCs (Kumar *et al.*, 2015b)

Since 1980s, it's well known that current density and the power output of MFC system could be enhanced by the addition of electron mediators (Du *et al.*, 2007). Based on the application of electron shuttles, MFCs can be classified into two different categories: MFCs with mediator and mediator-less MFCs (Huang *et al.*, 2008). **Table 2.2** showed some constructions of MFCs together with microorganism, substrate and mediators (if any).

In mediator MFCs, some microorganisms have the outer layers composing of non-conductive lipid membrane, peptidoglycans and lipopolysaccharides or have no electrochemically-active-surface-proteins. These membranes can hinder the direct electron transfer to the anode electrode (Davis *et al.*, 2007). The presence of mediators accelerated the transfer electrons from microorganisms to the anode electrode. The working principle of these mediators was show in **Figure 2.7**. The mediators in an oxidized state can be reduced by crossing the outer cells lipid membranes and plasma wall capturing the electrons. Then, the mediators move to the anode and release the electrons and become in oxidized state again resulting increase in electrons transfer rate, and thus enhancement of the power output of MFCs (Bennetto *et al.*, 1983; Du *et al.*, 2007).

Table 2.2. List examples of MFCs with mediators or mediator-less and their substrates (Du *et al.*, 2007; Najafpour, 2015)

Microbes	Substrate	Mediator	References
Escherichia coli	Glucose sucrose	Methylene blue	Grzebyk *et al.*, 2005; Ieropoulos *et al.*, 2005; Schröder *et al.*, 2003
Geobacter metallireducens	Acetate	Mediator-less MFC	Min *et al.*, 2005a
Geobacter sulfurreducens	Acetate	Mediator-less MFC	Bond *et al.*, 2003a; Bond *et al.*, 2002
Gluconobacter oxydans	Glucose	HNQ, resazurin or thionine	Lee *et al.*, 2002
Mixed consortium	Glucose, sucrose	Mediator-less MFC	Thygesen *et al.*, 2009
Proteus mirabilis	Glucose	Thionine	Choi *et al.*, 2003
Pseudomonas aeruginosa	Glucose	Pyocyanin and phenazine-1-carboxamide	Rabaey *et al.*, 2005a; Rabaey *et al.*, 2004
Rhodoferax ferrireducens	Glucose, xylose, sucrose, maltose	Mediator-less MFC	Chaudhuri *et al.*, 2003; Liu *et al.*, 2006
Saccharomyces cerevisiae	Glucose	Thionine, neutral red, methyl blue, Ferric chelate	Najafpour *et al.*, 2011
Shewanella oneidensis	Lactate	Anthraquinone-2,6-disulfonate (AQDS)	Ringeisen *et al.*, 2006
Shewanella putrefaciens	Lactate, pyruvate, acetate, glucose	Mediator-less MFC, but incorporating an electron mediator like Mn (IV) or NR into the anode enhanced the electricity production	Kim *et al.*, 1999b; Kim *et al.*, 1999c; Park *et al.*, 2002

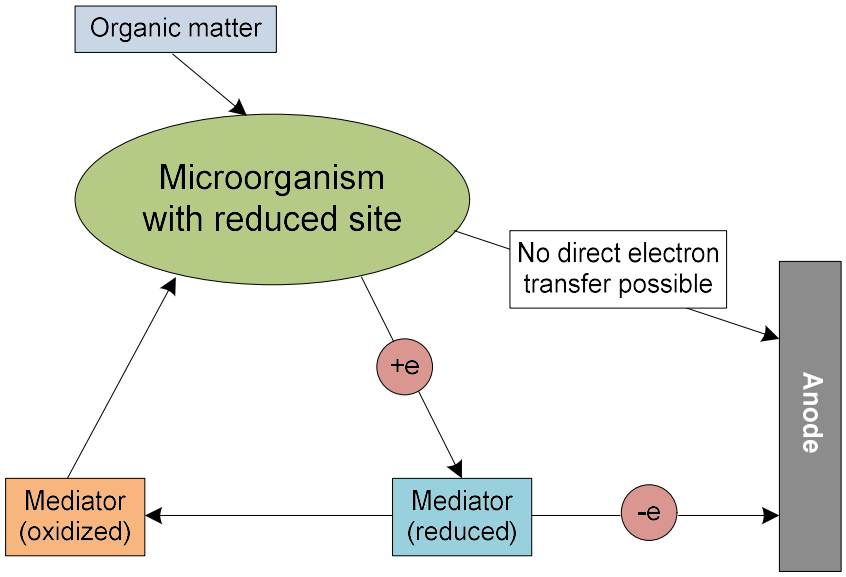

Figure 2.7. Working principle of redox mediators (Shukla *et al.*, 2004)

The mediator molecules should possess the following requirements (Du *et al.*, 2007; Ieropoulos *et al.*, 2005; Shukla *et al.*, 2004; Wilkinson, 2000):

- should cross the bacterial cells membrane easily to catch the reductive species inside the bacteria
- able to catch electrons from the electron carries of the electron transport chains
- able to escape from the bacterial cell membrane
- have a high rate of electrode reaction
- should be chemically stable in the electrolyte solution, should be easily soluble, and should not adsorb on the bacterial cells or electrode surface
- non-toxic to microbes or microbial decomposition
- low cost and be available

The mediators are classified in two groups, such as artificial mediators and self-generated mediators. Various chemicals are used as an artificial mediators (Bond *et al.*, 2003; Logan *et al.*, 2006) for example, thionine, benzyl viologen, potassium ferricyanide, 2,6-dichlorophenolindophenol, 2-hydroxy-1,4-naphthoquinone, phenazines, phenothiazines, phenoxazines, iron chelates, neutral red, methylene blue (Bond *et al.*, 2002; Ieropoulos *et al.*, 2005; Ikeda *et al.*, 2003; Logan, 2004; Logan *et al.*, 2006; Park *et al.*, 2000; Vega *et al.*, 1987). **Figure 2.8** showed the chemical compounds involved in the electron transportation from the metal reducing microorganisms to anode surface.

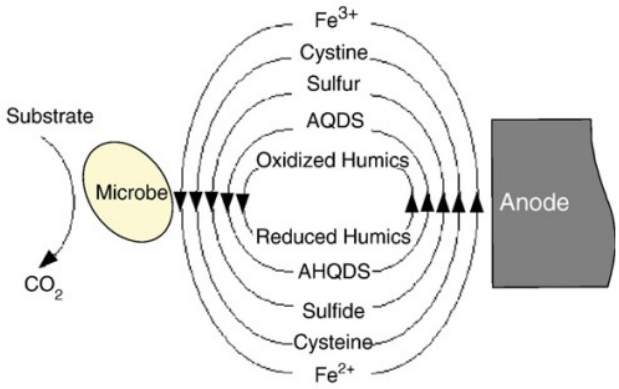

Figure 2.8. Model of various chemical compounds play as electron shuttles
(Du *et al.*, 2007)

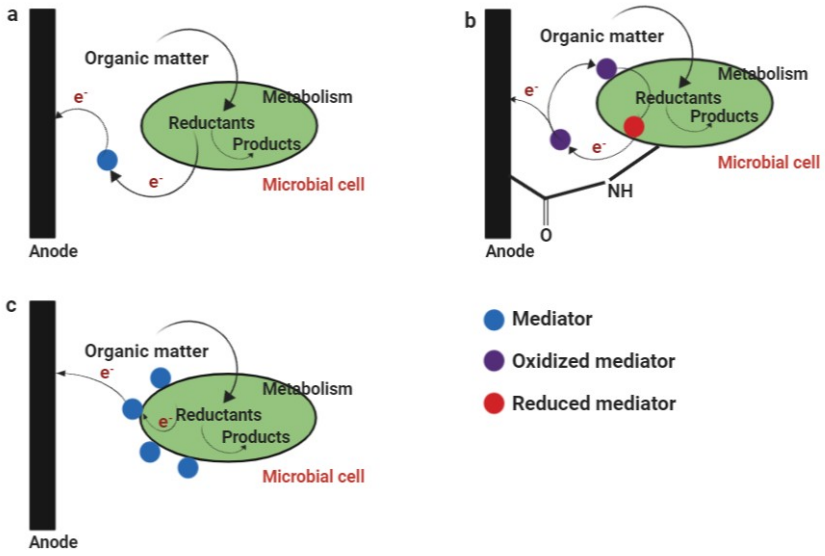

Figure 2.9. The different electron transport mode of the mediator: (a) mediators and bacterial cells are present in the solution phase; (b) bacterial cells are covalently attached to the anode surface; (c) mediators are covalently linked to the outer membrane of bacterial cells (Shukla *et al.*, 2004)

In the other hand, some microorganisms can produce extracellular compounds acted as mediators. (Rabaey *et al.*, 2005b; Reguera *et al.*, 2006) reported that *Pseudomonas* species in MFCs produced a material called phenazine which transports the electrons to the anode surface. The mediators can connect to the microorganism in three different ways **(Figure 2.9)**: **(a)** as diffusional mediator shuttling between the microbial suspension and the anode surface; **(b)** a diffusional mediator shuttling between the anode and microbial cells covalently linked

to the electrode. The amide bond was formed between the presence of -COOH groups of the electrode surface and the amino groups of the microbial membrane via covalent linking; **(c)** mediator adsorbed on the microbial cells transporting electron from the cells membrane to the anode surface (Shukla *et al.*, 2004).

In mediator-less MFCs, electricity can be generated by some microorganisms without any mediators. Because of some limitations of mediator such as application cost and toxicity, mediator-less MFCs may have advantages including non-toxic and cheaper (Flimban *et al.*, 2019). Some metal-reducing bacteria such as *Shewanella putrefaciens*; *Rhodoferax*; *Geobacter sulfurreducens*; *Geobacter metallireducens*; *Aeromonas hydrophila*; and *Klebsiella pneumoniae* (Chaudhuri *et al.*, 2003; Fan *et al.*, 2016; Kim *et al.*, 1999a; Kumar *et al.*, 2015a; Pham *et al.*, 2003; Zhang *et al.*, 2008) were reported to be good biocatalyst in the MFC. Fe(III)-reducing bacteria are found to be electrochemically active because of their cytochromes in the outer membranes (Kim *et al.*, 1999b; Kim *et al.*, 2002). In the glucose medium with the presence of Fe(III), the stoichiometry of glucose utilization and Fe(III) reduction can be explained in the **Eq. 2.4** (Chaudhuri *et al.*, 2003; Shukla *et al.*, 2004). In this reaction, utilisation of one glucose molecule, the microorganism can reduce totally 24 mol Fe^{3+} generating $24e^-$ and $24H^+$. It exhibits high reducing capacity of electrochemically active bacteria.

$$C_6H_{12}O_6 + 6H_2O + 24Fe(III) \rightarrow 6CO_2 + 24Fe(II) + 24H^+ + 24e^- \qquad \textbf{(Eq. 2.4)}$$

2.1.7 Application

2.1.7.1 Wastewater treatment

Wastewater treatment is one of the most well-known application of MFCs (Najafpour, 2015). Since 1991 many studies focused in this area **(Table 2.3)**. Rabaey *et al*. (2006) reported that MFCs using specific microbes were excellent techniques to remove sulfides from wastewater. Puig *et al.* (2011) used MFC in landfill leachate treatment and electricity production under high levels of nitrogen concentration.

In terms of ingredient of wastewater, it is divided into organic and inorganic wastes. Communal wastewater contains a mixture of organic matter that microorganisms in MFCs can use as fuel and oxidize these releasing electrons (Du *et al.*, 2007; Habermann *et al.*, 1991; Shukla *et al.*, 2004). In some cases, MFCs can even achieve 50 – 90% solids removal from wastewater, reducing restatements costs (Holzman, 2005). Additionally, up to 90% of COD

(Chemical Oxygen Demand) was removed in some cases (Puig *et al.*, 2011; Wang *et al.*, 2012b) with coulombic efficiency as high as 80% (Kim *et al.*, 2005) while the organic molecules such as acetate, propionate, butyrate were thoroughly broken down to CO_2 and H_2O (Du *et al.*, 2007). MFCs also are used for treatment of inorganic wastes (Najafpour, 2015). In 2006, some special microbes were used in MFC system to remove sulfides in wastewater (Rabaey *et al.*, 2006).

Table 2.3. MFC system with wastewater treatment (Najafpour, 2015)

Component eliminate	Maximum power	Anode material	Cathode material	Removal efficiency	Location of removal	References
COD	371 mW/m^2	Graphite plate	Graphite plate	95	Anode chamber	Oh *et al.,* 2005
COD	225 mW/m^2	Graphite plate	Graphite plate	92	Anode chamber	Min *et al.,* 2005b
Carbon	34.5 W/m^3	Granular graphite	Granular graphite	100	Anode chamber	Virdis *et al.,* 2008
COD	7.6 mW	Graphite felt	Graphite felt	90	Anode chamber	Moon *et al.,* 2005
Dye	15.73 mW/m^2	Graphite plate	Graphite plate	93	Anode chamber	Yadav *et al.,* 2012
Nitrogen	34.6 W/m^3	Granular graphite	Granular graphite	67	Cathode chamber	Virdis *et al.,* 2008
Copper	339 mW/m^3	Graphite plate	Granular graphite	96	Cathode chamber	Tao *et al.,* 2011
COD	26 mW/m^2	Graphite plate	Graphite plate	80	Single chamber	Liu *et al.,* 2004b

2.1.7.2 Generation of bioelectricity

MFC an attractive technology is able to generate electricity by using biochemical energy stored in the chemical compounds in a biomass with the aid of microorganisms (Logan, 2007b; Najafpour, 2015). In the report of Chaudhuri *et al.* (2003), *R. ferrireducens* was used in the mediator-less two-chambered glass vessel MFC system to generate electricity with difference of anode materials such as graphite rod (6.5×10^{-3} m^2), graphite foam (6.5×10^{-3} m^2), and fine woven graphite felt (20×10^{-3} m^2). Increasing the surface area of anode for microbial colonization increased current output. For example, 3-fold higher (~0.57 mA; 620 mV) current output was produced when using graphite felt instead graphite rod. Porous graphite foam electrodes, having almost the same geometric surface area as that of graphite

rods, generated 2.4-fold more current (~0.45 mA; 445 mV) with glucose as the fuel than did the graphite rods. In addition, their result (Chaudhuri *et al.,* 2003) also showed that *R. ferrireducens* can convert even over 80% of glucose to electrons making current in comparation with 0.04% of *Clostridium butyricum* in the report by Park *et al.* (2001). Rosenbaum *et al.* (2006) demonstrated the MFC system with the high coulombic efficiency (97%) with current density up to 6 mA/cm, when oxidized formate with the catalysis of Pt black. Rabaey *et al.* (2003) constructed a MFC system containing a mixed bacterial culture utilizing glucose as carbon source. Higher electron recovery as electricity of up to 89% at powers up to 3.6 W/m^2 of plain graphite electrode surface was reported in their research. Recently, there are many approaches to studying the electricity generation of MFC, **Table 2.4** showed the performance of MFCs with difference of bacteria and electrode type.

Table 2.4. The power density of MFCs based on difference of bacteria and electrode type (Rabaey *et al.*, 2005b)

Bacteria	Substrate	Electrode type	Mediator	Power density (W/m^3)	References
Proteus vulgaris	Glucose	Glassy carbon	Thionine	18	Delaney *et al.*, 2008
Proteus vulgaris	Glucose	Glassy carbon	Thionine	9.0	Choi *et al.*, 2003
Escherichia coli	Lactate	Woven graphite	Mn(IV) was immobilized in/on electrode matrix	7.6	Choi *et al.*, 2003
Shewanella putrefaciens	Lactate	Woven graphite		0.08	Kim *et al.*, 2002
Geobacter sulfurreducens	Acetate	Plain graphite		0.35	Bond *et al.*, 2003
Pseudomonas aeruginosa	Glucose	Plain graphite		8.8	Rabaey *et al.*, 2005a

However, MFC power generation is very low because of the low rate of electron transport (DeLong *et al.*, 2002; Tender *et al.*, 2002). To solve this problem, a simple solution is to save the generated electrons in rechargeable devices and use them as needed. “EcoBot I” is the product can accumulate the energy generated by the MFC and worked in a pulsed manner (Ieropoulos *et al.*, 2003). In addition, Willkinson *et al.* (2000) was also used MFC

system to provide energy for the operation of robots namely “Gastrobots”, a class of intelligent machines, self-feeding the biomass collected by themselves.

2.1.7.3 Biosensor

Another application of MFC technology it used as a biosensor for pollutant analysis and process monitor (Chang *et al.*, 2004; Chang *et al.*, 2005). The correlation between BOD and coulombic yield provides suitable method for determination of BOD in a wastewater (Chang *et al.*, 2004; Kim *et al.*, 2003). MFC with *Shewanella* sp. was reported to be good detector of the BOD of wastewater (Lovley, 2006). Lactate up to 50 mM was measured by MFCs biosensor containing *S. putrefacien*s (Najafpour, 2015). The MFC based BOD biosensor with the microbes enriched even worked for duration of 5 years without any process maintenance (Kim *et al.*, 2003).

2.2 Biopolymers

2.2.1 Hydrogel

Hydrogel products which constitute a polymeric materials group have three-dimensional network with the hydrophilic structure of which retains a large amount of water/biological fluids without dissolution in aqueous state water/biological fluids (Ahmed, 2015). The formation of these hydrogels were occurred by the interaction between polymeric chain networks and water/biological fluids (Pyarasani *et al.*, 2019). Hydrogels are insoluble in water because they have the cross-linking with the ionic interaction, covalent and hydrogen bonding between the polymeric networks and water molecules (Peppas *et al.*, 2000). Either natural or synthesis polymers can be used to prepare hydrogels (Ahmed, 2015).

The hydrogel products can be classified on different ways (**Table 2.5)**. The major groups are classified based on physical state, ionic charge, structure, cross-linking method, and hydrogel preparation methods.

2.2.2 Conducting polymer

Conducting polymer is sort of polymer belonging to group of artificial polymers with spatially extended π-bonding system, possess ability to conduct electrons (Wijsboom *et al.*, 2009). Conducting organic polymer was presented by Shirakawa *et al.* (1977) several decades ago. Today, there are over 25 organic conducting polymers that have been reported (Ateh *et al.*, 2007).

Table 2.5. The classification of hydrogel products (Ahmed, 2015)

Major groups	Name	References
Classification based on source	- Natural hydrogel: collagen, gelatin, starch, alginate, and agarose - Synthetic hydrogel: using chemical polymerization methods	Wen *et al.* 2013
Classification according to polymeric composition	- Homopolymeric hydrogels: polymer network derived from a single species of monomer, which is a basic structural unit comprising of any polymer network - Copolymeric hydrogels: polymer network comprised of two or more different monomer species with at least one hydrophilic component, arranged in a random, block or alternating configuration along the chain of the polymer network. - Multipolymer Interpenetrating polymeric hydrogel: made of two independent cross-linked synthetic and/or natural polymer component, contained in a network form, one component is a cross-linked polymer and other component is a non-cross-linked polymer.	Iizawa *et al.,* 2007; Maolin *et al.,* 2000; Yang *et al.,* 2002
Classification based on configuration	- Amorphous (non-crystalline) - Semi-crystalline: A complex mixture of amorphous and crystalline phases - Crystalline	Ahmed, 2015
Classification based on type of cross-linking	- Chemically cross-linked networks: have permanent junctions. - Physical cross-linked networks: the polymer chains are entangled together by hydrogen bonding, hydrophobic interaction, and crystallite formation	Hacker *et al.,* 2015
Classification according to network electrical charge	- Nonionic (neutral) - Ionic (including anionic or cationic) - Amphoteric electrolyte (ampholytic) containing both acidic and basic groups - Zwitterionic (polybetaines) containing both anionic and cationic groups in each structural repeating unit	Ahmed, 2015

As can be seen in the **Table 2.6**, the double and single bonds are arranged alternately, or conjugated segments coupled with atoms providing p-orbitals for a continuous orbital overlap (e.g. N, S) forming a conjugated structure of polymers. The conjugated structure makes an orbital system that allows the charge carriers to move through a continuous overlapping of π-orbitals along the polymer backbone (Dai, 2004).

Table 2.6. Some conjugated conducting polymers (Dai, 2004)

Polymer	Structure	Date conductivity discovered	Conductivity (S/cm)
Polyacetylene and analogues			
Polyacetylene	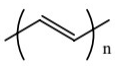	1977	$10^3 – 1.7 \times 10^5$
Polypyrrole	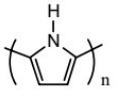	1979	$10^2 – 7.5 \times 10^3$
Polythiophene	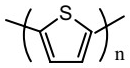	1981	$10 – 10^3$
Polyphenylene and analogues			
Poly(paraphenylene)	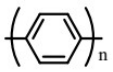	1979	$10^2 – 10^3$
Poly(p-phenylene vinylene)	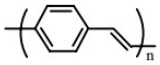	1979	$3 – 5 \times 10^3$
Polyaniline	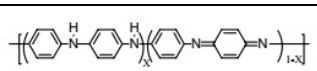	1980	30 – 200

Polyaniline is well-known a popular conducting polymer because of cheap, availability and easy to synthetize. Polyaniline is a phenylene-based polymer with -NH- group on either side of the phenylene ring (John *et al.*, 2008). Polyaniline can be synthesized by chemical and electrochemical oxidation methods. In the chemical method, it can be fabricated by aqueous, emulsion, interfacial polymerization technique (Bhadra *et al.*, 2009; Stejskal *et al.*, 2010). Ammonium peroxydisulfate has currently been used for the oxidation of aniline to polyaniline in water (Trchová *et al.*, 2006) or in the acidic aqueous medium (Stejskal *et al.*, 2002). Stejskal *et al.* (2017) oxidized 0.2 M aniline with 0.25 M ammonium peroxydisulfate in water at room temperature to form polyaniline **(Figure 2.10)**.

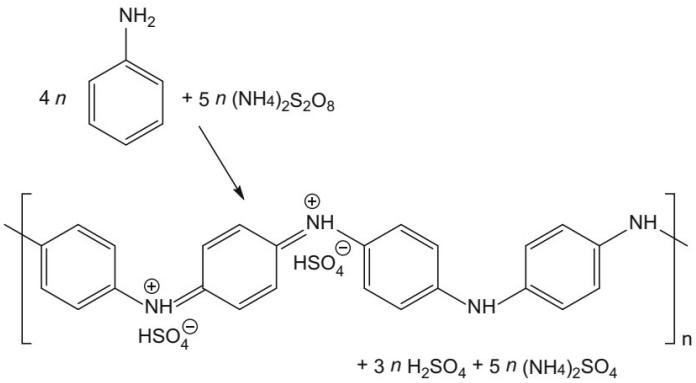

Figure 2.10. Shema for synthesis of polyaniline from aniline by oxidation with ammonium persulfate (Stejskal, 2017)

2.2.3 Conducting polymer hydrogels

Conducting polymer hydrogels are gels containing a conducting polymer along with a supporting polymer as constituents, and they are swollen with water or electrode solution (Stejskal, 2017). These hydrogels provide a great interface between the electronic transporting (electrode) and the ionic transporting phases (electrolyte) in both the natural and synthesis biological systems (Pyarasani *et al.*, 2019). Additionally, these materials include the benefits features of both the hydrogels and organic conductors (Pyarasani *et al.*, 2019; Stejskal, 2017). Some properties of conducting polymer hydrogels exhibit following (Ansari *et al.*, 2018; Stejskal, 2017):

- mixed electrical conductivity (electronic and ionic conductivity)
- electrochemical reversibility between redox forms of conducting polymer
- the transition between salt–base forms in conducting polymers
- good flexibility and mechanical integrity
- non-toxicity and biocompatibility
- porosity and high specific surface area
- controlled morphology and macroscopic homogeneity.

2.2.3.1 Preparation of conducting polymer hydrogel

Conducting polymer hydrogels can be prepared by many methods. The final material consists of conducting polymers as physically entrapped within the hydrogel matrix (Ansari *et al.*, 2018).

2.2.3.1.1 Within hydrogel matrix

Conducting polymer hydrogel are made by embedding conducting polymer in cross-linked water-soluble polymer matrix and swollen with water or aqueous solutions of electrolytes (Ansari *et al.*, 2018; Stejskal, 2017). The addition of conducting polymers into a gel matrix appeared in good chemical stability, thermal stability and the electrical conductivity. The natural polysaccharides such as starch, cellulose, chitosan, alginate and their derivatives have been used in preparation conducting hydrogels in different conditions (Sharma *et al.*, 2016). Polyaniline, polypyrrole and poly(3,4-ethylenedioxythiophene) have been used as conducting polymers (Ansari *et al.*, 2018; Stejskal, 2017). The synthesis of conducting polymer hydrogels is started by the preparation of hydrogels made of cross-linked water-soluble polymer, and then polymerization of monomers such as aniline, pyrrole, 3,4-

ethylenedioxythiophene, etc. are diffused into a hydrogel matrix. Monomer-containing hydrogel is immersed in the oxidant solution (Ansari *et al.*, 2018). **Table 2.7** shown the oxidant and hydrogel matrix using for preparation of some conducting polymer hydrogel with different monomers (Stejskal, 2017).

Table 2.7. Hydrogel matrix and oxidant of some conducting polymer hydrogels (Stejskal, 2017)

Hydrogel matrix	Oxidant	References
Polyaniline hydrogels		
Alginate, sodium salt	Ammonium peroxydisulfate (APS), Electrooxidation (EO)	Srinivasan *et al*., 2015 Kim *et al*., 2004
Cellulose	Silver nitrate, EO	Wan and Li, 2016 Shi *et al*., 2014a, b
Gelatin	APS	Wu *et al*., 2016
Pectin	APS	Zhao *et al*., 2016
Poly(vinyl alcohol)	APS	Wang *et al*., 2015a
Polypyrrole hydrogels		
Cellulose	Iron(III) chloride, Iron(III) nitrate and silver nitrate	Liang *et al*., 2015 Zhou *et al*., 2015
Phytic acid	APS	Tang *et al*., 2015
Polyacrylamide	APS, EO, Iron(III) chloride	Castro *et al*., 2015 Saha *et al*., 2015 Sun *et al*., 2011
Poly(acrylic acid)	APS	Smirnov *et al*., 2011
Poly(3,4-ethylenedioxythiophene) hydrogels		
Polyacrylamide	Iron(III) nitrate	Dai *et al*., 2010b
Poly(acrylic acid)	Iron(III) nitrate	Dai *et al*., 2009
Poly(styrene-4-sulfonate) sodium salt	Iron(III) nitrate, Iron(III) toluenesulfonate	Dai *et al*., 2015 Kishi *et al*., 2014
Poly(N,N-dimethylacrylamide)	Iron(III) toluenesulfonate	Kishi *et al*., 2014

2.2.3.1.2 In the presence of water-soluble polymer

This method is done only in one step. Conducting polymer hydrogel is made by the oxidation/polymerizations of aniline or pyrrole in the presence of water-soluble polymers, stabilizers and yield colloidal dispersions. When conducting polymer hydrogel is synthesized, hydrogen bonding and/or chain entanglements, or both are formed, where cross-linked

network and ionic bonds have a negligible role in their formation (Dispenza *et al.*, 2006; Stejskal *et al.*, 2005). When the reactants and/or stabilizer are high concentration, hydrogels are produced (Ansari *et al.*, 2018; Stejskal, 2017). Słoniewska *et al.* (2014) used 0.5 M ammonium peroxydisulfate oxidize 0.5 M aniline in 0.5 M poly(sodium 4-styrenesulfonate) aqueous solution to produce a soft and sticky hydrogel. In the oxidation of aniline in the presence of poly(sodium 4-styrenesulfonate) at a low concentration of stabilizer, colloidal dispersion were obtained and hydrogels are created only after the concentration of reactants is increased (Jia *et al.*, 2012).

2.2.3.1.3 Penetration of hydrogel with a conducting polymer

In this method, conducting polymer in solution or colloidal form, followed by their penetration into the preformed hydrogel (Ansari *et al.*, 2018; Stejskal, 2017). This method has the disadvantage of the limited solubility of conducting polymer. In addition, the compatibility of two polymers is also a limitation, solutions containing two different polymers tend to separate into coexisting phases. However, if there is a strong interaction between both polymers, conducting polymer can penetrate into hydrogel favorably (Mawad *et al.*, 2016). Martínez *et al.* (2015) successfully fabricate nanocomposite by loading polyaniline into a preformed hydrogel matrix (*N*-methylpyrrolidone). The conducting polymer hydrogels could be used in a pressure sensor because their electronic conductivity will be changed when they were applied by pressure.

2.2.3.1.4 In the presence of a conducting polymer

The particles of conducting polymers are dispersed in reaction mixture used for the preparation of a hydrogel. The cross-linking is formed by the presence of the physical gelation, chemical or radiation (Ansari *et al.*, 2018; Stejskal, 2017). The limitation of this method is the appearance of sedimentation in the forming of cross-linking because conducting polymer particles are insufficient dispersion and inhomogeneity (Ansari *et al.*, 2018). Zhang *et al.* (2009) prepared conducting polymer hydrogel by dispersing polyaniline nanofibers at 75^0C into agarose solution and cooling to ambient temperature. Baniasadi *et al.* (2015) used PANI-coated graphene in chitosan solution at 40 $^{\circ}$C to get conducting polymer hydrogel after temperature decrease. Lee *et al.* (2016) as well as Castro *et al.* (2015) used polypyrrole or poly(3,4-ethylenedioxythiophene) incorporated into polyacrylamide gel or gelatin/chitosan gel to prepare conducting polymer hydrogel.

2.2.3.1.5 Simultaneous polymerization/oxidation

The conducting polymer hydrogels are prepared when both the hydrogel and conducting polymers are produced in the same experiment. The process of polymerization and gelation/cross-linking does not necessarily occur at the same time (Ansari *et al.*, 2018; Stejskal, 2017). Dai *et al.* (2008) used iron(III) nitrate in the presence of poly(styrenesulfonic acid) with the oxidative polymerization of 3,4 ethylenedioxythiophene to produce conducting polymer hydrogel. Tang *et al.* (2008) mixed aniline, acrylamide and potassium peroxydisulfate solution at 80 °C. In this case, polyacrylamide and polyaniline were produced simultaneously and swelled in water to produce a hydrogel.

2.2.3.2 Application of conducting polymer hydrogel

Biosciences and energy conversion and storage are two main research streams of conducting polymer hydrogels. In biomedicine field, conducting polymer hydrogel are applied in biosensors and biostimulation, electrostimulated drug-release devices, and neural prostheses (Guiseppi-Elie, 2010; O'Connor *et al.*, 2015). The biodegradability of conducting polymer hydrogels is poor (Stejskal *et al.*, 2012), but they can be combined with biodegradable polymers, such as pectin to suit their application-wearable electronics (Zhao *et al.*, 2016). Some main applications of conducting polymer hydrogel are listed below.

2.2.3.2.1 Biosensor

Zhai *et al.* (2013) prepared polyaniline hydrogel for glucose enzyme biosensor based on Pt nanoparticles/polyaniline hydrogel heterostructures. According to the authors, this sensor has the average response time 3s and works well in the range of 0.01 – 8 mM glucose. The high sensitivity could be attributed to the 3D porous structure of hydrogel and synergic catalytic activity of Pt nanoparticles. In addition, Słoniewska *et al.* (2014) fabricated urea biosensor from such hydrogel that was prepared by the polymerization reaction of aniline monomer in polyaniline-poly(styrene sulfonate) solution. This sensor revealed high sensitivity for urea in the 10^{-4} – 0.1 M concentration. Besides, the same research group used polyaniline-poly(styrene sulfonate) hydrogel to attach horseradish peroxidase covalently by carbodiimide reaction resulting in fast responses with the low detection limit of H_2O_2 (Jabłońska *et al.*, 2017).

2.2.3.2.2 Supercapacitor

Using polyaniline hydrogel as electrodes in supercapacitors was reported in many research (Dou *et al.*, 2016; Guo *et al.*, 2015; Jayakumar *et al.*, 2015). Hu *et al.* (2017) used polyvinyl alcohol–polyaniline hydrogel to fabricate all-solid-state flexible supercapacitor by physical mixing method and exhibited 11.3 mF/cm^2 specific capacitance. Huang *et al.* (2016) prepared polyvinyl alcohol–polyaniline hydrogel by the freezing–thawing method and the specific capacitance of this electrode material is 105 F/g. Liu *et al.* (2018) reported hydrogel mediated polyaniline-polyacrylic acid-carbon nanotube electrode material for supercapacitor applications. The specific capacitance is 612.5 F/g at 0.5 A/g and cycling behavior of 81.5% retention after 1500 cycles. Polyaniline hydrogel containing nickel oxide (Zhang *et al.*, 2015), silicon nanoparticles (Oh *et al.*, 2015) were also used as electrodes in lithium-ion battery.

2.2.3.2.3 Microbial fuel cell

Due to excellent electrochemical properties and other advantageous features of both hydrogels and organic conductors (Tang *et al.*, 2015), conducting polymer hydrogel attracts attention in microbial fuel cell application. Tang *et al.* (2015) synthesize conductive polypyrrole hydrogels/carbon nanotubes (CPHs/CNTs), and this composite was used as anode in the MFC. Phytic acid was used as the gelator and dopant to synthesize the CPHs/CNTs composite. MFCs with CPHs/CNTs anode had a maximum power density of 1898 ± 46 mW/m^2, while the MFCs with bare graphite felt only exhibited a maximum power density of 871 ± 33 mW/m^2. In their research, CPHs/CNTs exhibited good material as electron transferrer in MFC. Kumar *et al.* (2014) fabricated graphene oxide/carbon nanotube composite hydrogels by dispersion of carbon nanotubes and graphene oxide in the poly(N-isopropylacrylamide) hydrogel matrix and use it as anode in MFC. Graphene oxide exhibits oxygen function groups that allow graphene oxide can be reactive with organic and inorganic chemicals such that hybrids materials or soft materials can be synthesized (Compton *et al.*, 2010). Moreover, graphene oxide is also used to disperse carbon nanotubes through π-π stacking interactions (O'Connell *et al.*, 2001). In MFC, poly(*N*-isopropylacrylamide)/graphene oxide/carbon nanotube composite hydrogels anode exhibited higher MFC performances in comparation with poly(*N*-isopropylacrylamide) hydrogel anode. In 2017, Szöllősi *et al.* formed hydrogel by immobilization of biocatalyst in alginate/polyaniline/titanium-dioxide/graphite composites and used it as bio-anode in MFC. Alginate as dopant and template was used for immobilization microorganism cells by entrapment method. Firstly,

aniline-alginate network was formed by ultra-sonication. After that, the composites were synthesized in presence of ammonium persulfate. Graphite powder and titanium-dioxide were added into hydrogel to improve the electrical conductivity. The alginate/polyaniline/titanium-dioxide/graphite composites with high electrical conductivity were successfully fabricated. This bio-anode demonstrated effectiveness in improving the power density in MFC.

2.2.3.2.4 Other applications

Biomedicine, controlled release or adsorbents are the other application of conducting polymer hydrogel. Bajpai *et al.* (2009) tested the biocompatibility of polyaniline/poly(vinyl alcohol) hydrogel with respect to blood coagulation. No cytotoxic effect was observed with growth of human skin fibroblasts in a polyaniline hydrogel based on bacterial cellulose (Shi *et al.*, 2014). The electroactive injectable degradable hydrogels could be considered as bioactive scaffolds for tissue regeneration because their non-toxic (Li *et al.*, 2014; Petrov *et al.*, 2016). In the controlled release application, Sharma *et al.* (2016) tested the releasing of amoxicillin trihydrate on polyaniline/poly(acrylic acid-*graft*-gum ghatti). Many drugs may interact with polyaniline as counter-ions or by other bonding interactions. Then, they can be released in suitable environment, for example under physiological conditions (Ansari *et al.*, 2018; Stejskal, 2017). Besides, polyaniline hydrogel was also used as an adsorbent. Yan *et al.* (2015) used polyaniline/phytic acid hydrogel to adsorb a cationic dye, methylene blue with the adsorption capacity being up to 71 mg/g. Moreover, polyaniline/poly(acrylic acid)/gum ghatti hydrogel was analyzed for moisture retention capacity in soil cultivation (Sharma *et al.*, 2014).

2.2.4 Bacterial cellulose

Bacterial cellulose (BC), an exopolysaccharide, was produced by different bacteria including Gram negative bacteria species such as *Acetobacter Azotobacter*, *Rhizobium*, *Agrobacterium*, *Pseudomonas*, *Salmonella*, *Alcaligenes*, as well as Gram-positive bacterial species such as *Sarcina ventriculi* (Wang *et al.*, 2019). *Gluconacetobacter xylinus* (formerly *Acetobacter xylinum*) is one of the most commonly used source for bacterial cellulose (Keshk *et al.*, 2006; Nguyen *et al.*, 2008). BC has an ultra-fine network of cellulose nanofibers with the diameter is 20 – 100 nm and has a chemical structure similar to the cellulose, where hydroxyl functional groups exist (Manoukian *et al.*, 2019).

2.2.4.1 Production

The production of bacterial cellulose could be carried out in solid-phase or submerged culture (El-Saied *et al.*, 2004). Stationary culture and agitated culture are two methods generally used (Watanabe *et al.*, 1998). In the static cultivation, the bacteria strain was produce a gelatinous bacterial cellulose membrane on the surface of the nutrition solution (Rani *et al.*, 2011), whereas the agitated/shaking culture method, the bacterial cellulose is accumulated as irregular masses such as granule, stellate, and fibrous strand (Wang *et al.*, 2019). There are some differences in the structure of bacterial cellulose between two produced methods. In the static culture method, the crystallinity and Iα content of cellulose were found higher than that in the agitated culture method. Additionally, the degree of polymerization of cellulose molecule in the agitated culture method was lower than in the other. The agitated culture method is applied for industrial production of bacterial cellulose (El-Saied *et al.*, 2004), while the static culture method is used for the biomedical and cosmeceutical applications with a proper shape (film, sheet or membrane) (Park *et al.*, 2009)

The condition of the culture environment such as nutrition, pH and oxygen supplied impacts the properties of BC (Pourramezan *et al.*, 2009; Zeng *et al.*, 2011). *Aerobacter*, *Alcaligenes* produced fibril structure BC with the flocculation in wastewater, *Acetobacter* produced ribbon structure BC, while *Gluconacetobacter* can produce BC with 3D network nanofiber **(Table 2.8)**.

Table 2.8. Effects of bacterial strain on structure and biological role of cellulose products (Wang *et al.*, 2019)

Genus	**Biological role**
Fibril structure	
Aerobacter	Flocculation in wastewater
Agrobacterium	Attachment to plants
Alcaligenes	Flocculation in wastewater
A. hansenii	Maintenance in aerobic bio-reactors for fermentation
Rhozobium	Attachment to plants
Ribbon structure	
Acetobacter	Maintenance of aerobic environment
Achromobacter	Flocculation in wastewater
3D network nanofiber	
Gluconacetobacter	Aerobic environment

The bacterium *Acetobacter xylinum* is reported to be one of good strain for production of BC (Park *et al.*, 2009). The main carbon source for this aerobic bacteria strain is glucose or sucrose and it can covert 108 glucose molecules into cellulose per hour (Park *et al.*, 2009; Wang *et al.*, 2019). Moreover, the other carbon source such as both 5- or 6-carbon monosaccharides, oligosaccharides, starch, alcohol, and organic acids are also reported to use for the biosynthesis of cellulose (Park *et al.*, 2009). In recent years, the use of agricultural- and industrial-based wastes as nutrient sources has been on focus because they are cheap substrates (Castro *et al.*, 2011; Li *et al.*, 2015; Revin *et al.*, 2018). Yeast extract, peptone, few amino acids are also as good nitrogen source for the growth and production of bacterial cellulose (El-Saied *et al.*, 2004).

The growth of bacteria strains has four phases such as lag, log, stationary and death phase. Generally, BC is produced in the log and stationary phases. The production of bacterial cellulose is described as follows: at the beginning, the cell number of bacteria is very low and BC film forms slowly. Then the microfibers are produced, and they intertwine and aggregate with each other forming the irregular matrix or flocculent structures. When the bacterial cell concentration increase, more and more BC films are secreted. Media with low pH can improve growth of bacteria, and the BC biosynthesis is stopped when pH value is outside the suitable range of pH 4 and pH 7 (Wang *et al.*, 2019).

2.2.4.2 Structural features and properties

Bacterial cellulose composed of β-1,4-D-glucopyranose units linked to each other by β-glycosidic bonds and so called exopolysaccharide (Lin *et al.*, 2014). BC has the same chemical structure as plant cellulose, but the degree of polymerization is about 2,000 to 6,000 for bacterial cellulose and 13,000 to 14,000 for plant. A continuous long unbranched polymer chain was formed in BC by the repeated glucose monomers. Several cellulose chains in BC are held together via strong intra- and intermolecular hydrogen bonds that form a sheet. In addition, the bacterial cellulose sheets are linked by hydrogen bonds forming the crystalline structure (Ullah *et al.*, 2019). Bacterial cellulose has two different crystalline structures, namely cellulose Iα and cellulose Iβ. Cellulose Iα is a triclinic unit cell consisting of one cellulose chain and dominant in bacterial cellulose, while Iβ is a monoclinic unit cell consisting of two cellulose chains and dominated in plant cellulose (Park *et al.*, 2009).

BC has the tensile strength, crystallinity and purity higher than plant cellulose **(Table 2.9)**. During biosynthesis in static culture condition, the bacteria utilized carbon source

polymerizing into single, linear β-1,4-glucan chains and then they are secreted to outside of the cells. The β-1,4-glucan chains are linked to each other leading to formation of subfibrils (consisting of 10–15 nascent β-1,4-glucan chains). A thick membrane was formed from these subfibrils when they are crystallized into microfibrils, in turn into bundles, and the latter into ribbons. The 3D structure membranes are formed consisting of an ultrafine network of cellulose nanofibers. Meanwhile, the 3D structure of bacterial cellulose results in a higher crystallinity (60-80%) and tremendous mechanical strength, whereas the plant cellulose lacks a 3D structure (Park *et al.*, 2009).

Table 2.9. Comparison of properties for bacterial and plant-based cellulose (Wang *et al.*, 2019)

Properties	Bacterial cellulose	Plant-based cellulose	References
Tensile strength (MPa)	20 – 300	25 – 200	Feng *et al.*, 2015; Gibson, 2012
Young's modulus (MPa)	Sheet: 20,000 Single fibre:130,000	2.5 – 0.170	Lynd *et al.*, 2002; Nishi *et al.*, 1990
Water holding capacity (%)	> 95	25 – 35	Rebelo *et al.*, 2018; Ul-Islam *et al.*, 2012
Size of fibers (nm)	20-100	micrometer scale	Genet *et al.*, 2007; Szymanska-Chargot *et al.*, 2011
Crystallinity (%)	74 – 96	40 – 85	Park *et al.*, 2010
Relative hydrophilicity (%)	40 – 50	20 – 30	Bishop, 2007
Purity (%)	> 99	< 80	Klemm *et al.*, 2005
Degree of polymerization	14000 – 16000	300 – 10000	Tahara *et al.*, 1997
Porosity (%)	> 85	< 75	Al-Shamary *et al.*, 2013
Total surface area (m^2/g)	> 150	< 10	Bismarck *et al.*, 2002; Ul-Islam *et al.*, 2012

Due to the large network of fibers, bacterial cellulose has a very large surface area. The bacterial cellulose has approximately 100 times smaller in the size of fibrils than plant cellulose. Additionally, BC has the ability to form hydrogen bonds and interact with water, thus bacterial cellulose can absorb water up to 200 times of its dry mass (Czaja *et al.*, 2006). In additions, Young's modulus of BC is definitely higher than plant cellulose. This issue can be explained that the ultrafine fibrils of BC have the strong interfibrillar binding and BC has a

higher crystallinity structure (Park *et al.*, 2009). The properties of bacterial cellulose are summarized in **Table 2.10**.

Table 2.10. Distinguishing features of microbial cellulose (El-Saied *et al.*, 2004)

Properties	**Description**
Purity	- Cellulose is the only biopolymer synthesized - Absence of lignin or hemicelluloses - Completely biodegradable and recyclable, a renewable resource
Great mechanical strength	- High strength crystalline cellulose I - Consistent dimensional stability - High tensile strength - Light weight - Remarkable durability
Extraordinary absorbency in the hydrated state	- Remarkable capacity to hold water - Selective porosity - High wet strength - High surface-to-volume carrier capacity
Direct membrane assembly during biosynthesis	- Intermediate steps of paper formation from pulp unnecessary - Intermediate steps of textile assembly from yarn unnecessary - Extremely thin, submicron, optical clear membranes can be assembled
Cellulose orientation during synthesis	- Dynamic fiber-forming capabilities - Uniaxially strengthened membranes
Direct modification of cellulose during assembly	- Delayed crystallization by introduction of dyes into culture medium - Control of physical properties of the cellulose during assembly (molecular weight and crystallinity)
Genetic modification of cellulose product	- Direct synthesis of cellulose derivatives (such as cellulose acetate, carboxy methyl cellulose, methyl cellulose, etc.) - Control of cellulose crystalline allomorph (cellulose I or cellulose II) - Control of molecular weight of cellulose

2.2.4.3 Conductive bacterial cellulose

BC has long been used as the raw material in many fields such as foods, paper industry, audio components and medical applications (El-Saied *et al.*, 2004). Structurally, BC are composed of interconnected 3D networks of nanofibers with high-molar-mass, hydrogen-bonded polymer chains in an extended-chain conformation (Kaewnopparat *et al.*, 2008; Kojima *et al.*, 1997). The principle benefits of using BC as a raw material include easy fabrication and its 3D structure, which is a key point for the conductivity performance of the

final composites (Ullah *et al.*, 2019). Moreover, BC can also incorporate polymerizable monomers into its network, interacting with the BC fiber chains. So, the characteristics of BC such as electrical conductivity, surface reactivity, mechanical and thermal resistance can be changed or improved (Shi *et al.*, 2012).

In the recent years, conductive bacterial cellulose blends, especially bacterial cellulose/polyaniline (BC/PANI) blends have been receiving attention from the scientists because of their electronic applications (Li *et al.*, 2012). Alonso *et al.* (2018) used BC as raw material and fabricated BC/PANI using different BC matrixes (drained, freeze-dried and regenerated) and different synthesis conditions (in situ and ex situ) to enhance the inherent properties of BC. Their results reported that the structure of BC/PANI was changed comparation with bare BC. The surface of BC/PANI have the presence of nitrogen, the amount of oxygen was decreased and along with an increase in the carbon due to the aromatic ring of PANI **(Figure 2.11)**.

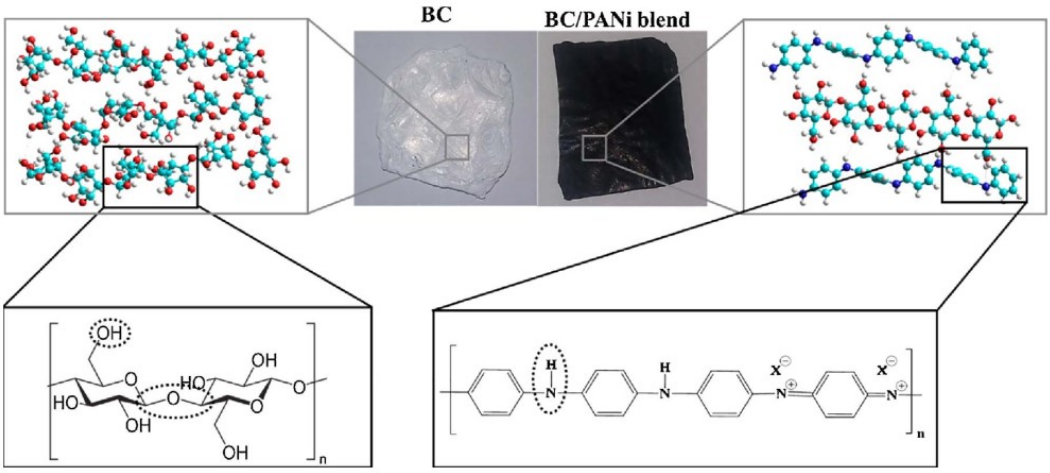

Figure 2.11. Schematic representation of the BC/PANI interaction with BC and respective functional groups (Alonso *et al.*, 2018)

In addition, the electrical conductivity of PANI can be enhanced by using additives such as carbon nanotubes (Oueiny *et al.*, 2014) graphene (Solonaru *et al.*, 2017) and metal salts (Ćirić-Marjanović, 2013). Yoon *et al.* (2006) prepared electrically conducting polymeric membranes by incorporating multiwalled carbon nanotubes (MWCNTs) into bacterial cellulose pellicles. It was found that the incorporation process is a useful method for dispersing MWCNTs in an ultrafine fibrous network structure and enhancing the electrical conductivity of the polymeric membranes. The conductivity of the MWCNTs-incorporated

cellulose pellicle was 1.4 × 10^{-1} S/cm. To enhance the electrical conductivity, Kim *et al.* (2019) fabricated the BC/PANI membrane with the addition Cu(II). The presence of copper salt improved the electrical conductivity of BC PANI to a level about 3.8 times higher than that of BC-PANI produced without metal salt. **Figure 2.12** presented the SEM images of the surface of bare BC, BC/PANI and the surface of MWCNTs-incorporated BC. MWCNTs were successfully embedded in the BC network **(Figure 2.12c)** and Cu(II) were also incorporated in BC/PANI membrane **(Figure 2.12e)**.

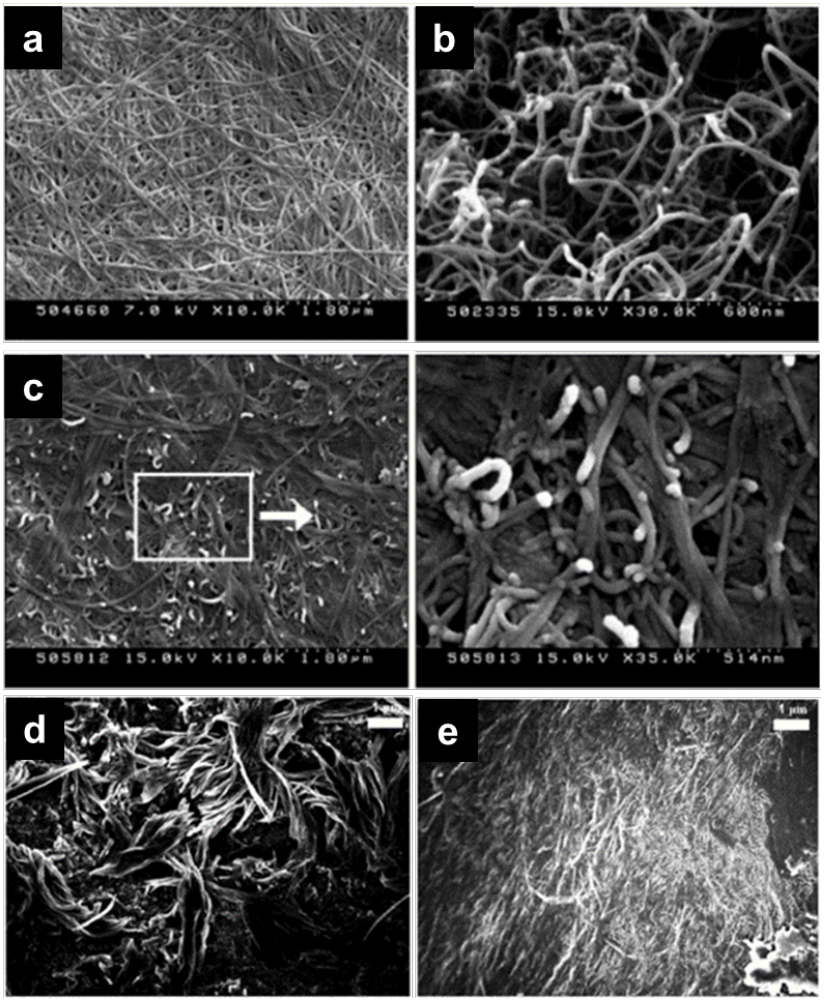

Figure 2.12. SEM images of (a) purified bacterial cellulose pellicle; (b) purified MWCNTs; (c) surface of the MWCNTs-incorporated bacterial cellulose pellicle; (d) surface of the BC/PANI; (e) surface of BC/PANI/Cu (Kim *et al.*; Yoon *et al.*, 2006)

3 MATERIALS AND METHODS

3.1 Chemicals and reagents

Riboflavin, yeast extract, marine agar, sodium chloride and ammonium persulfate were purchased from Reanal (Budapest, Hungary). Sodium hydroxide, hydrochloric acid, iron citrate and aniline were purchased from Merck (Darmstadt, Germany); tryptone was obtained from Oxoid Limited (Basingstoke, United Kingdom); Na-alginate was from Cargill (Hungary); titanium dioxide was from VWR (Hungary); graphite powder was from Pannoncolor (Hungary); cellulase enzyme was from Sigma-Aldrich (Hungary) and Bio-Rad Protein Assay Kit was from Bio-Rad (USA).

3.2 Microorganisms

Shewanella xiamenensis DSMZ 22215 was purchased from Deutsche Sammlung von Mikroorganizmen und Zellkulturen (DSMZ), Braunschweig, Germany.

Acetobacter xylinum (ATCC 23768) was from Institute of Biotechnology and Food technology, Industrial University of Ho Chi Minh city, Vietnam.

3.3 Media and preparation

3.3.1 Marina agar

Pepton	5 g
Yeast extract	1 g
Fe(III)-citrate	0.1 g
NaCl	19.4 g
$MgCl_2$	5.9 g
Na_2SO_4	3.24 g
$CaCl_2$	1.8 g
KCl	0.55 g
$NaHCO_3$	0.16 g
KBr	0.08 g
$SrCl_2$	34 mg
H_3BO_3	22 mg
Na-silicate	4 mg

NaF	2.4 mg
$(NH_4)_2NO_3$	1.6 mg
Na_2HPO_4	8 mg
Agar	15 g
Distilled water	1000 mL

The ingredients were dissolved in distilled water, adjusted pH 7 and sterilized at 121 °C for 15 minutes.

3.3.2 Luria-Bertani (LB)

Trypton	10 g
Yeast extract	5 g
NaCl	10 g
Distilled water	1000 mL

The ingredients were dissolved in distilled water, adjusted pH 7 and sterilized at 121 °C for 15 minutes.

3.3.3 Growth medium

The modified LB was used to carry out the experiment as following:

Trypton	10 g
Yeast extract	5 g
NaCl	10 g
Glucose	1 g
Distilled water	1000 mL

The ingredients were dissolved in distilled water and sterilized at 121 °C for 15 minutes.

3.4 Experimental processes and analytical parameters

The summarization of experimental processes and analytical parameters was illustrated in **Figure 3.1**. The scheme of fabrication of bio-anode was described in detail in **Figure 3.2** and **Figure 3.4.**

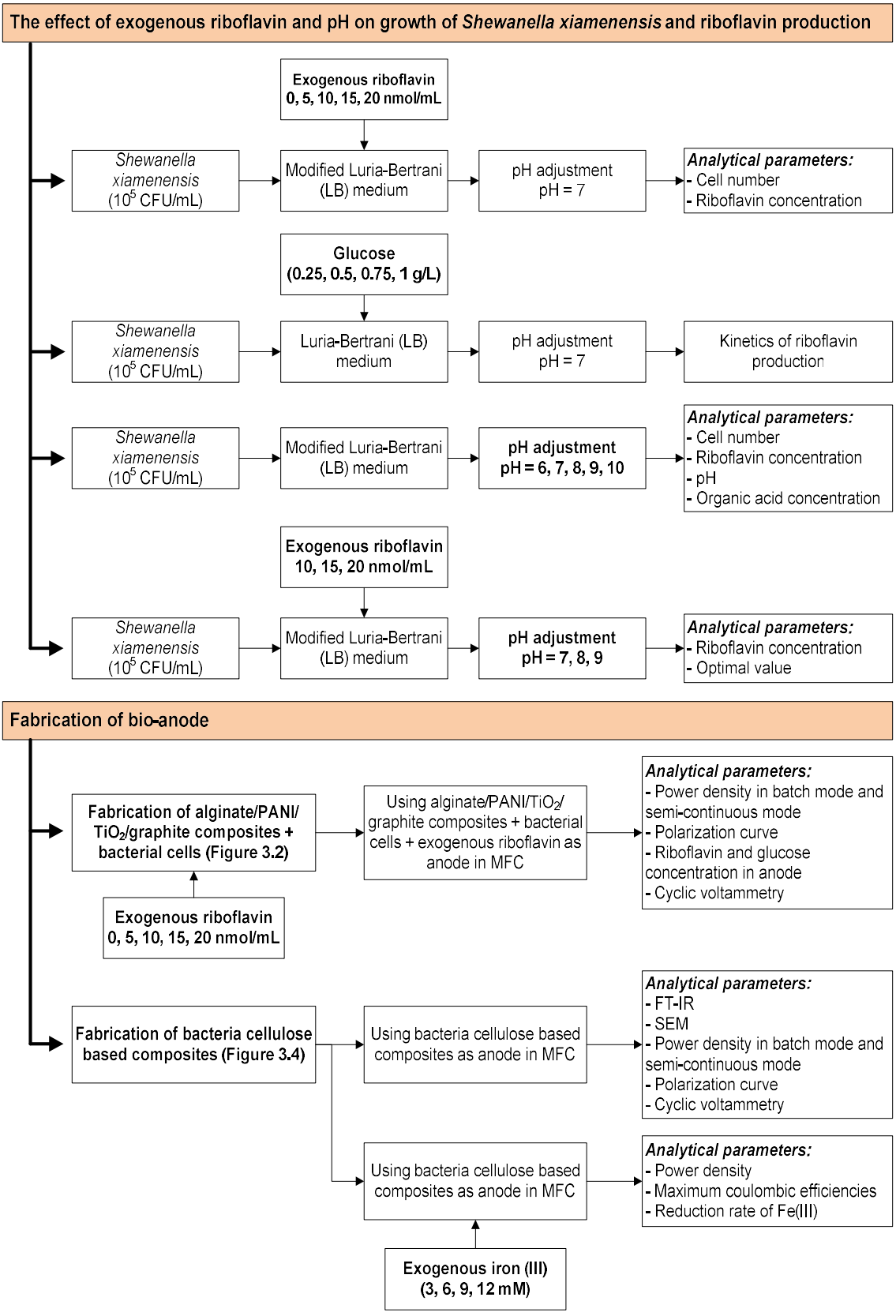

Figure 3.1. Experimental processes and analytical parameters

3.5 Culturing methods

3.5.1 Preculturing

The culture of *Shewanella xiamenensis* DSMZ 22215 maintained in the Marine agar was used for preculturing purpose. Preculturing was performed in an Erlenmeyer flask (working volume 150 mL) with incubation temperature 30 °C and shaking speed 180 rpm for 24 hours in an incubator shaker (Szöllősi *et al.*, 2015b). The *S. xiamenensis* cells were collected by centrifuge at 10,000 rpm.

3.5.2 Effect of exogenous riboflavin on growth of *S. xiamenensis* and riboflavin production

Systematic and judicious experiment was performed with Erlenmeyer flasks (working volume 150 mL) to understand the microbial growth, concentrations of extracellular riboflavin, pH in microbial broth with time progress. Batch mode experiments were performed with modified LB medium supplemented with different concentrations of riboflavin, ranging from 0 – 20 nmol/mL to understand the system dynamics. Before experiment, modified LB medium was autoclaved at temperature 120 °C and 15 psi for 20 minutes, followed by addition of riboflavin into the medium in aseptic condition due to its sensitivity towards high temperature. Initial pH of the medium 7.0 was adjusted by the 0.1 M HCl or NaOH. For each experiment, initial cells number was maintained to 10^5 CFU/mL. Programmed incubation temperature 30 °C under anaerobic condition and shaking speed 200 rpm for 120 hours was considered for this purpose. At every 24h intervals, 10 mL of samples from each Erlenmeyer flasks were collected in aseptic way and cells concentration was measured immediately. Subsequently, collected microbial broth was centrifuged with 12,000 rpm for 10 minutes at temperature 20 °C. Supernatant was collected, and concentrations of extracellular riboflavin, pH in microbial broth were measured.

3.5.3 Kinetics of growth and riboflavin production of *S. xiamenensis*

Generally, the growth rate of microorganism at the certain substrate concentration is described by **Eq. 3.1**.

$$v = \frac{dX}{dt} = \mu X \qquad \textbf{(Eq. 3.1)}$$

where:

v is growth rate (g/h)

μ is the specific growth rate (1/h)

X is biomass (g)

Media with different glucose concentration (from 0.25 g/L to 1 g/L) were prepared and then growth of *S. xiamenensis* was investigated. The kinetic parameters were determined by Monod model **(Eq. 3.2)**.

$$\mu = \frac{\mu_{max}.S}{K_S + S} \qquad \textbf{(Eq. 3.2)}$$

where:

μ is the specific growth rate (1/h)

μ_{max} is the maximum specific growth rate (1/h)

K_S is the saturation constant (g/L)

S is substrate concentration (g/L)

The relationship of cell growth to product formation was considered by Luedeking and Piret (1959). In our research, Luedeking and Piret model was used to illustrate the kinetics of riboflavin production of *S. xiamenensis* following equation **Eq. 3.3**.

$$\frac{dP}{dt} = \alpha \frac{dX}{dt} + \beta X \qquad \textbf{(Eq. 3.3)}$$

where:

α is growth-associated product formation coefficient

β is non-growth-associated product formation coefficient

P is product concentration (g/L)

X is biomass (g/L).

The equation **Eq. 3.3** can be expressed as:

$$\frac{1}{X}\left(\frac{dP}{dt}\right) = \alpha\left(\frac{1}{X}\frac{dX}{dt}\right) + \beta \Rightarrow \frac{1}{X}\left(\frac{dP}{dt}\right) = \alpha\mu + \beta \Rightarrow q_P = \alpha\mu + \beta \qquad \textbf{(Eq. 3.4)}$$

where:

q_P is the specific rate of product formation (1/h)

μ is the specific growth rate (1/h)

α is growth-associated product formation coefficient

β is non-growth-associated product formation coefficient

The α and β were calculated using regression analysis of experimental data. Both correlation coefficients (R^2) and t-probe of each estimated constants were checked for statistical significances.

3.5.4 Effect of pH on growth of *S. xiamenensis* and riboflavin production

The method of this experiment was following **3.5.2**. However, *S. xiamenensis* was growth in modified LB medium with different initial pH without exogenous riboflavin. For each experiment, initial cells number was maintained to 10^5 CFU/mL and initial pH of the medium was ranged from 6 – 10, adjusted by the 0.1 M HCl or NaOH. Cells numbers, riboflavin concentration, pH was measure after 24 hours intervals.

3.5.5 Optimization of riboflavin production

Central Composite Design (CCD) was used to investigate the effects of two independent variables such as exogenous riboflavin (X_1) and initial pH (X_2). Riboflavin production (Y) was measured at 72^{nd} hours of operation. The ranges of variables were concentration of exogenous riboflavin (10 – 20 nmol/mL) and initial pH (7.0 – 9.0). The second-order polynomial was calculated with a statistical package (Modde 5.0 software) to estimate the response of the dependent variable. The second-order polynomial model used in the response surface analysis was as follows:

$$Y = a_0 + a_1X_1 + a_2X_2 + a_{11}X_1^2 + a_{22}X_2^2 + a_{12}X_1X_2 \qquad \textbf{(Eq. 3.5)}$$

where Y is the response variable; X_1 and X_2 are the independent variables; a_0 is the interruption coefficient; a_1 and a_2 are the coefficients of the linear effects; a_{11} and a_{22} are the coefficients of the quadratic effects; and a_{12} is the coefficient of the interaction effect.

The central composite design consisting of 11 experimental points **(Table 4.4)**. The fit of the models was evaluated by the determination coefficients (R^2) and adjusted R^2 (R^2-adj).

3.6 Fabrication of hydrogel bio-anode composites

3.6.1 Fabrication of hydrogel composites with the riboflavin and bacterial cells

A hydrogel composites containing gel-entrapped bacteria in alginate/polyaniline/TiO_2/graphite composites was prepared as previously described by Szöllősi *et al.* (2017). First, composites coated hydrogels were fabricated. Na-alginate 0.1g

was dissolved in 10 mL distilled water and then aniline 2 mg were added to the mixture and mixed rigorously. This solution was mixed rigorously with ultra-sonication (Clifton MU-8 sonicator, 40 kHz, 30 W) for 2 hours. In the next step, the composites were synthesized in the 2nd ultra-sonication (40 kHz, 30 W) condition for 2 hours at in ice. TiO_2 (in range of 0.1 g) and 0.1 g ammonium persulfate combined with aniline-alginate network gel (formed in the first ultra-sonication). After ultra-sonication, 5 mg graphite powder was mixed with the solution. At the end of this process, before dropping down the mixed solution into Calcium chloride, bacteria cells (*S. xiamenensis*) at 10^7 CFU/mL was added with graphite powder and riboflavin with different concentration from 5 to 20 nmol/mL **(Figure 3.2)**. Composites coated hydrogel particles was formed with 0.3 cm in diameter.

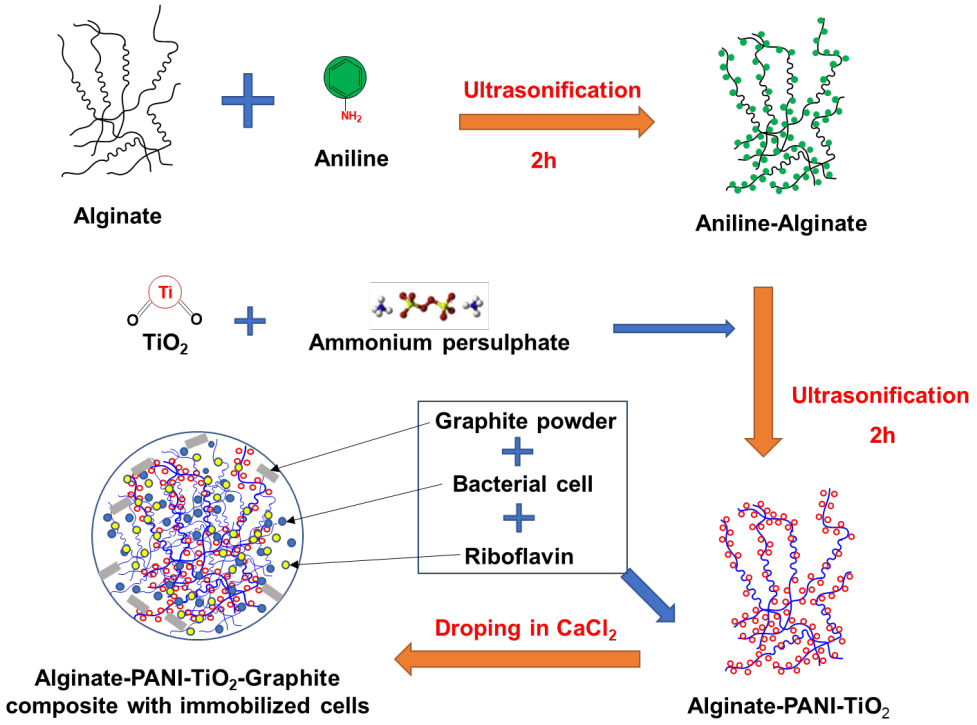

Figure 3.2. Scheme of fabrication of alginate/PANI/TiO_2/graphite composites with immobilized cells particles and riboflavin

3.6.2 Forming hydrogel bio-anode electrode with composites gels

The hydrogel gel composites with the immobilization of *S. xiamenensis* cells and riboflavin was used to create hydrogel bio-anode. The composites gel was contained in a bag made of graphite cloth (University of Reading, Department of Microbiology, UK). The size of the bag depends on the size of the MFCs. In this study, the size of the bag was 2.5 × 3.5 × 0.7 cm. The joints of bag were sewn with copper wire. The bag was filled approximately 50%

with hydrogel composite. The upper part of the bag was also connected to the conductive copper wire. This conductive cooper wire will be responsible for transmitting electrons through cathode electrode. Graphite cloth cover ensures better transmission and capture of electrons.

3.6.3 Construction batch and semi-continuous batch of MFC

Dual-chamber MFCs was prepared according to description by Szöllősi *et al.* (2015b). Working volume of each chamber was 24 mL and they were separated by the Nafion 117 proton-exchange membrane. The anode chamber was filled with bag containing hydrogel composites with immobilization of *S. xiamenensis* cells and riboflavin. The cathode chamber was filled with 0.1 M of potassium-hexaferrocyanate and 0.5 M of Sorensen phosphate buffer (pH = 7) and connected with a pump to provide the air. Graphite sheets (Department of Microbiology, University of Reading, UK) with surface area 8 cm^2 as cathode was placed. The electrodes of the MFCs were connected with an external resistance (500 Ω) and parallel with a digital multimeter **(Figure 3.3)**. Voltage output value was measure and power density was calculated during operation of systems. Batch and semi-continuous operation modes used the same type of MFCs.

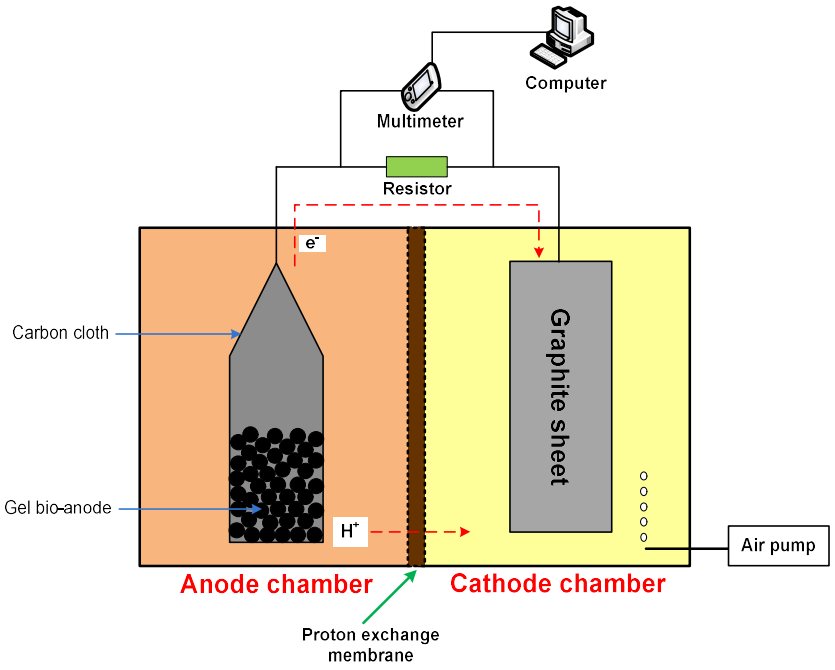

Figure 3.3. Schematic construction of dual-chamber MFCs containing hydrogel bio-anode

Anode chamber was filled with modified LB medium (1g/L glucose, 5 g/L yeast extract, 10 g/L NaCl and 1 g/L tryptone). In the semi-continuous batch, modified LB medium was removed when the voltage came down to low level and fresh medium was fed.

In the control experiment, anode chamber with the hydrogel bio-anode without riboflavin was used.

3.7 Fabrication of electrically conducting composites

3.7.1 Preparation of bacterial cellulose hydrogel

Acetobacter xylinum (ATCC 23768) was used to produce the bacterial cellulose. The bacteria were cultured on SH medium included 2% (w/v) glucose, 0.5% (w/v) peptone, 0.5% (w/v) yeast extract, 0.27% (w/v) Na_2HPO_4, 0.15% (w/v) citric acid (Kimura *et al.*, 2001). These culture media were sterilized at 120 $^{\circ}$C in an autoclave for 2 hours. A single *A. xylinum* colony on SH agar medium was transferred into liquid SH medium. After 7 days of cultivation at 28°C, the cellulose sheets formed on the surface of the culture broth. The cellulose sheets with 0.5 cm thickness will be removed and washed with deionized water, sodium dodecyl sulfate 2% and purified in NaOH 0.1N (Fijałkowski *et al.*, 2015). They will be cut into 2 × 3 cm pieces and sterilized in an autoclave at 121 $^{\circ}$C for 15 min before used for fabrication electrically conducting composites and cells immobilization.

3.7.2 Preparation of electrically conducting BC/PANI and BC/PANI/TiO_2 composites

BC/PANI composites were prepared in situ aniline oxidative polymerization by using ammonium persulfate (APS) called BC/PANI/APS or iron (III) chloride hexahydrate ($FeCl_3.6H_2O$) called BC/PANI/$FeCl_3.6H_2O$ as oxidant. BC/PANI composites were prepare according to description by (Müller *et al.*, 2012; Wang *et al.*, 2012a) with some modifications. Briefly, BC hydrogel membranes with 2 × 3 × 0.5 cm were cut and immersed in distilled water (1:10 w/v) and then aniline was added. Ultra-sonication (Clifton MU-8 sonicator, 40 kHz, 30 W) technique was used for 2 hours, hydrogen bonding was formed allowing the monomer to assemble onto the surface of BC. In the next step, the oxidant (ammonium persulfate or iron (III) chloride hexahydrate) and was mixed. The BC was synthesized in the 2nd cycle of ultra-sonication (40 kHz, 30 W) for 2 hours at in ice. After polymerization, the colour of the solution changed to dark green from ivory. In the case of fabrication of electrically conducting BC/PANI/TiO_2 composites, TiO_2 was mixed

simultaneously with oxidants. Bare BC without aniline oxidative polymerization was used as control.

3.7.3 Immobilization of bacterial cells into bare BC, BC/PANI and BC/PANI/TiO_2

The *S. xiamenensis* cells in LB broth medium after 24 hours at 30 °C in incubator shaker 180 rpm were separated using the centrifugal method and suspended in isotonic phosphate buffered saline (PBS, Sigma-Aldrich) to obtain cell-suspension with 10^9 CFU/mL cell concentration. Bare BC, BC/PANI and BC/PANI/TiO_2 composite membranes were incubated in *S. xiamenensis* suspension at 30 °C and 200 rpm for 12 – 96 hours. After that, composite membranes were washed 3 times with PBS to remove free cells (Fijałkowski *et al.*, 2015). **Figure 3.4** illustrated the process of fabrication of electrically conducting bacterial cellulose/polyaniline/titanium-dioxide composites with the immobilization of *S. xiamenensis* cells.

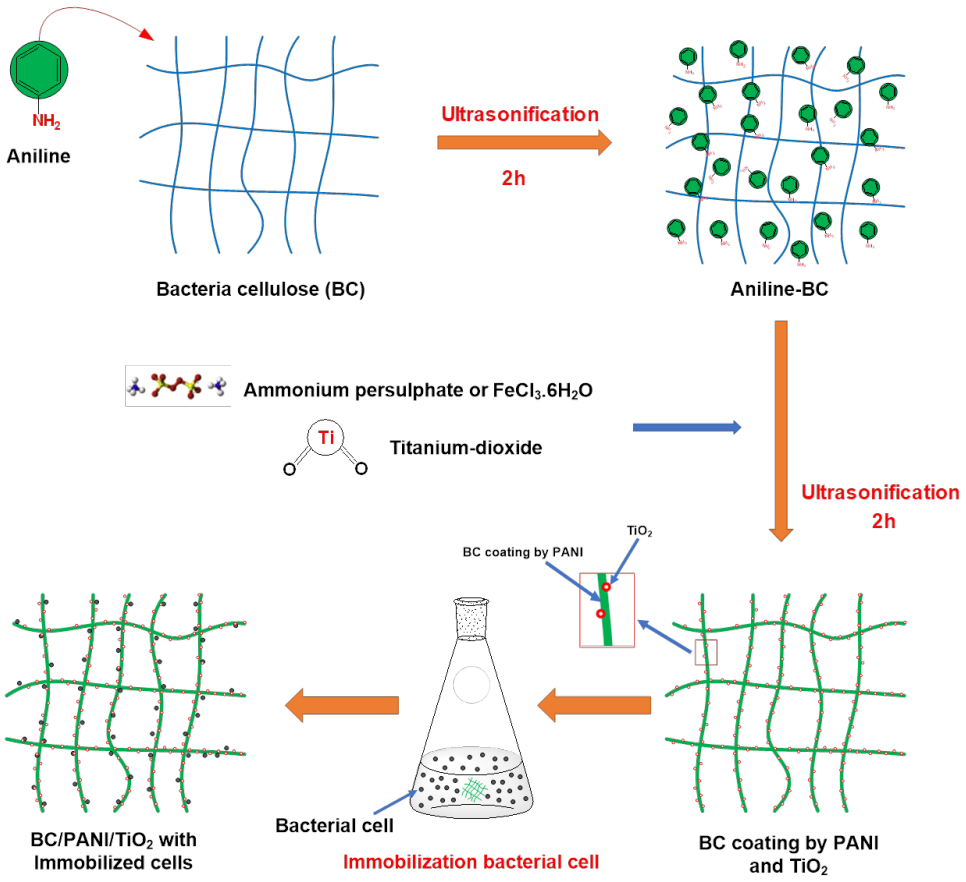

Figure 3.4. Scheme of fabrication of BC/PANI/TiO_2 and immobilized cells particles

3.7.4 Construction batch and semi-continuous batch of MFC

Dual-chamber MFC system was also used for this experiment with similar volume of anode and cathode chamber (24 mL) and they were separated by the Nafion 117 proton-exchange membrane. The cathode chamber was filled with 0.1 M of potassium-hexaferrocyanate and 0.5 M of Sorensen phosphate buffer (pH = 7) and connected with a pump to provide the air. Bare BC, BC/PANI and BC/PANI/TiO_2 with immobilized bacterial cells acts as an anode electrode and anode chamber was filled with modified LB medium (1g/L glucose, 5 g/L yeast extract, 10 g/L NaCl and 1 g/L tryptone). Graphite sheets with surface area 8 cm^2 as cathode were placed in the respective chambers. The electrodes of the MFCs were connected with an external resistance (500 Ω) and parallel with a digital multimeter (**Figure 3.5**). Voltage output value was measure and power density was calculated during operation of systems. Batch and semi-continuous operation modes used the same type of MFCs.

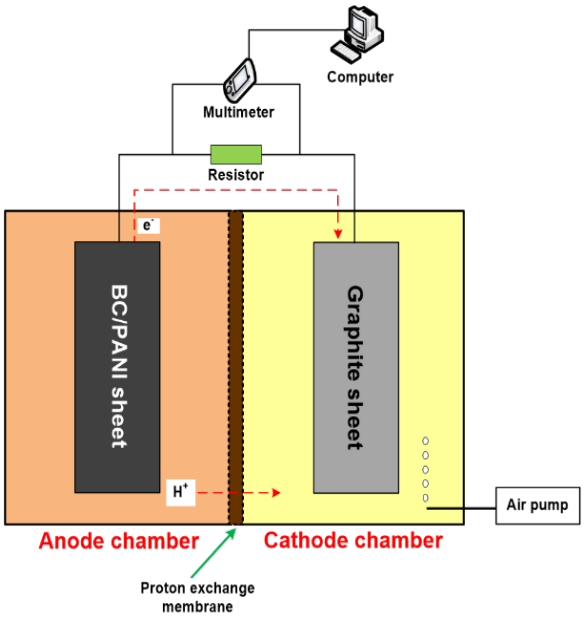

Figure 3.5. Schematic construction of dual-chamber MFCs using BC/PANI as anode

3.7.5 Effect of iron ferric on the performance of MFCs

Dual-chamber MFC system was applied. BC/PANI/TiO_2/APS with immobilized *S. xiamenensis* cells was used as an anode electrode. The cathode chamber was filled with 0.1 M of potassium-hexaferrocyanate and 0.5 M of Sorensen phosphate buffer (pH = 7.0). Anode

chamber was filled with modified LB medium (1g/L glucose, 5 g/L yeast extract, 10 g/L NaCl and 1 g/L tryptone) and different Fe(III) concentration (from Fe(III)-citrate) ranging from 3 mM to 12 mM. The electrodes of the MFCs were connected with an external resistance (500 Ω) and parallel with a digital multimeter. Voltage output value was measure and power density was calculated during operation of systems.

3.8 Analytical methods

3.8.1 Determination of cells number

The cells numbers of microbes in the growth medium was determined by plate count technique and optical density (OD600nm) using UV-visible spectrophotometer at 600 nm wavelength (Fijałkowski *et al.*, 2015).

Strong correlation between absorbance (optical density OD600nm) and CFU/mL was found **(Figure 3.6).** In the growth phase, the samples of bacterial culture in regular interval were taken and the optical density of samples was measured. Plate count technique was used in triplicate for each dilution to determine the cell density.

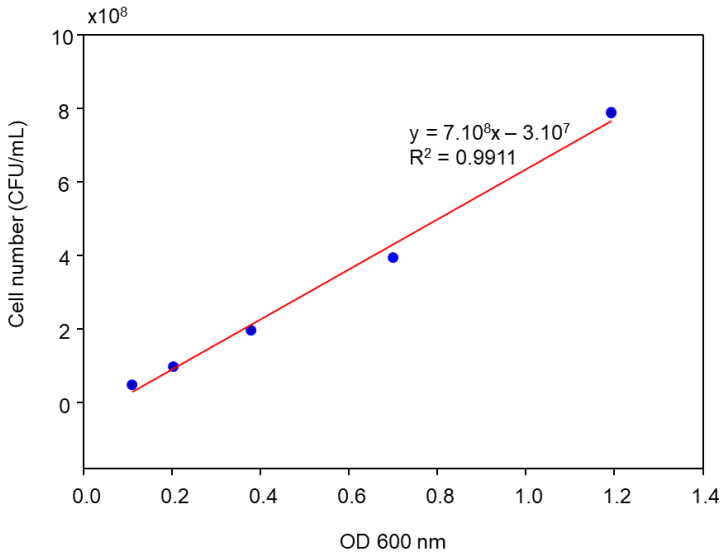

Figure 3.6. Standard curve of OD600 nm versus viable cells count

3.8.2 Measurement of pH

Constant volume of microbial broth (10 mL) was collected aseptically from each Erlenmeyer flask at every 24 hours intervals. The pH of sample was measured by digital pH meter.

3.8.3 Determination of riboflavin concentration

The riboflavin concentration in solution was measured by a high-performance liquid chromatography (HPLC) method (Marsili *et al.*, 2008; Yong *et al.*, 2013). In brief, 2 mL of culture broth was centrifuged with 15,000 rpm for 10 min at temperature 20 °C and supernatant was filtrate with 0.22 µm microfiltration membrane. The HPLC system (Surveyor, Thermo Scientific, San Jose, USA) used a column of Hi-Plex Ca 7.7 x 300mm (Agilent, Santa Clara, USA) with PDA detector to detect riboflavin. The mobile phase was 40% grade methanol and 60% distilled water, the flow rate for elution was 0.6 mL/min at room temperature, injected volume was 5 µl. Riboflavin for the standard was HPLC grade of purity and used without further purification.

3.8.4 Determination of reducing sugars and organic acids

Samples were centrifuged at 15,000 rpm for 10 minutes before analysis. Sugars (glucose, galactose, saccharose, maltose etc.) and organic acids (propionic, acetic, lactic, succinic, malic and citric acids) were detected by a HPLC system (Surveyor, Thermo Scientific, San Jose, USA) with a column of Hi-Plex H 7.7 x 300mm (Agilent, Santa Clara, USA). The mobile phase was 5 mM H_2SO_4 solution, the flow rate for elution was 0.6 mL/min at 45 °C, injected volume was 10 µl. The temperature of the column was maintained at 85 °C, the measurement time was 25 min at constant flow rate. The sugars and organic acids were detected by RI and PDA detectors, respectively. All chemicals for the standards were HPLC grade of purity and used without further purification.

3.8.5 Preparation of polarization curve

Polarization curve of MFC was prepared once the MFC get the stabilized voltage. Various external resistances (from 0 Ω to 1 MΩ) were connected across the MFC. The voltage of MFC for each external resistance was recorded by digital multimeter VC-820 (VoltCraft, Germany) until the voltage was stable. Current density and power density were

calculated and the relationship between voltage and current density, power density will be plotted.

3.8.6 Preparation of cyclic voltammetry

Electrochemical characterization of MFCs was performed by cyclic voltammetry (CV) techniques. Cyclic voltammetry (CV) was conducted using the open source potentiostat (IO Rodeo, USA) with saturated calomel electrode (SCE) and platin wire as the reference electrode and counter electrode, respectively **(Figure 3.7)**. The scan rate was 10 mV/s and the potential window was range from -1 to 1 V. Cyclic voltammetry was measured in the presence of substrate. It was repeated 2 times and 1 cycle for each measurement.

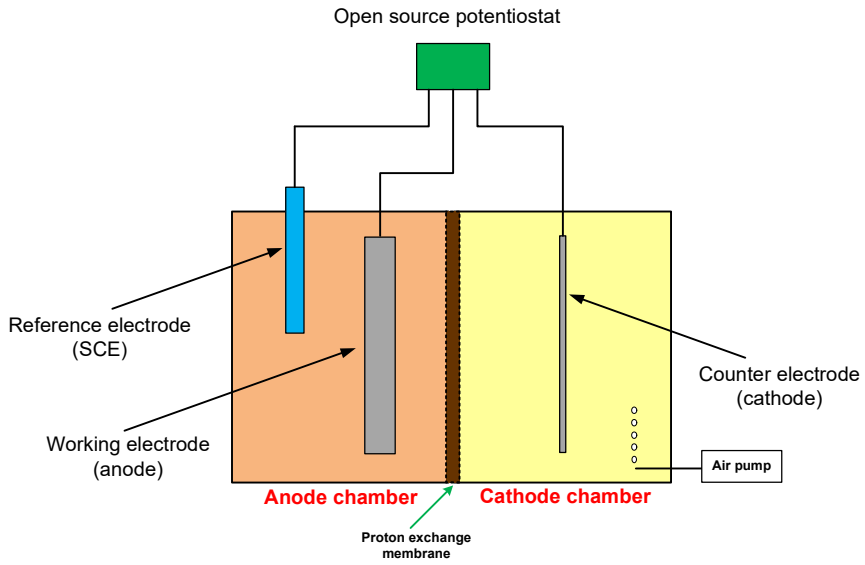

Figure 3.7. The scheme of CV experimental arrangement

3.8.7 Characterization of bare BC, BC/PANI and BC/PANI/TiO_2

3.8.7.1 Measurement of electrical conductivity

The conductivity of BC/PANI, BC/PANI/TiO_2 was measured with a conventional four-point probe technique. According to the four-point method, electrical resistance and electrical current were measured by a digital multimeter VC-830 (VoltCraft, Germany).

3.8.7.2 FT-IR

The infrared spectra of bare BC, BC/PANI and BC/PANI/TiO_2 composite membranes were obtained on a JASCO-4700 infrared spectrometer using KBr pellets. The wavelength range is 4000 to 400 cm^{-1} with a resolution of 4 cm^{-1} at room temperature.

3.8.7.3 Scanning electrode microscope (SEM)

Scanning electrode microscope (SEM, JSM-6480LV-JED 2300, Jeol, Japan) was used to analyze the morphology and structure of surface of bare BC, BC/PANI and BC/PANI/TiO_2.

3.8.7.4 Determination of the number of immobilized S. xiamenensis cells

The number of immobilized *S. xiamenensis* cells in bare BC, BC/PANI and BC/PANI/TiO_2 were determined by plate count method on Marine agar. After immobilization of *S. xiamenensis* cells, bare BC and synthesized BC were washed 3 times with PBS and digested with the cellulase enzyme. The grown of colonies were counted after incubation for 24 hours and the number of Colony Forming Units (CFU) per 1 gram of cellulose was determined (Fijałkowski *et al.*, 2015).

3.8.8 Determination of iron(III)-reduction

Iron(III)-reduction was determined following the description in report of Szöllősi *et al*. (2015b). The samples are adjusted pH 2 with sulfuric acid. Ammonium-thiocyanate (NH_4SCN) 50g/L was added into samples. After dilution 200 times and rigorous mixing, the absorbance was measured in 460 nm by a spectrophotometer (Szöllősi *et al.*, 2015b).

3.9 Calculation of current density, power density and coulombic efficiency

The voltage was continuously measure in the external resistance (500 Ω). Current was calculated according to the Ohm's law

$$I = \frac{V}{R} \qquad \textbf{(Eq. 3.6)}$$

where,

V is the voltage (V)

R is the external resistance (Ω)

The power is calculated based on the electric current $P = I.V$. Power density is obtained according to

$$P_d = \frac{I.V}{d} \qquad \textbf{(Eq. 3.7)}$$

where d is the volume of the hydrogel bio-anode composite (Logan *et al.*, 2006; Szöllősi *et al.*, 2017).

Coulombic efficiency (CE) is calculated as

$$CE = \frac{8\int_0^{tb} Idt}{FV_{MFC}\Delta COD} \qquad \text{(Ghasemi } et\ al.\text{, 2020)} \qquad \textbf{(Eq. 3.8)}$$

where,

I is current

F = Faraday's constant

V_{MFC} is the volume of the anode chamber

COD is the chemical oxygen demand

4 RESULTS AND DISCUSSION

4.1 Effect of exogenous riboflavin and initial pH on growth of *S. xiamenensis* and riboflavin production

4.1.1 Effect of exogenous riboflavin

In this experimental set, the effect of exogenous riboflavin on growth and production of riboflavin by *S. xiamenensis* was focused. Series of growth media supplemented with different amounts of exogenous riboflavin (from 0 nmol/mL to 20 nmol/mL) was used. Cell count and riboflavin concentration were monitored in time interval during process.

The cells number of bacteria grew rapidly after 24 hours, increased slowly after 72 hours and then stabilized **(Figure 4.1)**. The maximum cell number was 3.3×10^8 CFU/mL in the sample with initial exogenous riboflavin 20 nmol/mL after 24 hours of fermentation. At 72^{nd} hour of operation **(Figure 4.2)**, the cells number of bacteria in the samples with exogenous riboflavin concentration 15; 20 nmol/mL were around 1.3-fold higher than in the sample with exogenous riboflavin concentration 5 nmol/mL. According to statistical analysis of one-way ANOVA **(Table 4.1)** and Tukey's test ($p<0.05$), there was significant difference in cell number between samples with initial exogenous riboflavin 15; 20 nmol/mL and samples with 0; 5 nmol/mL.

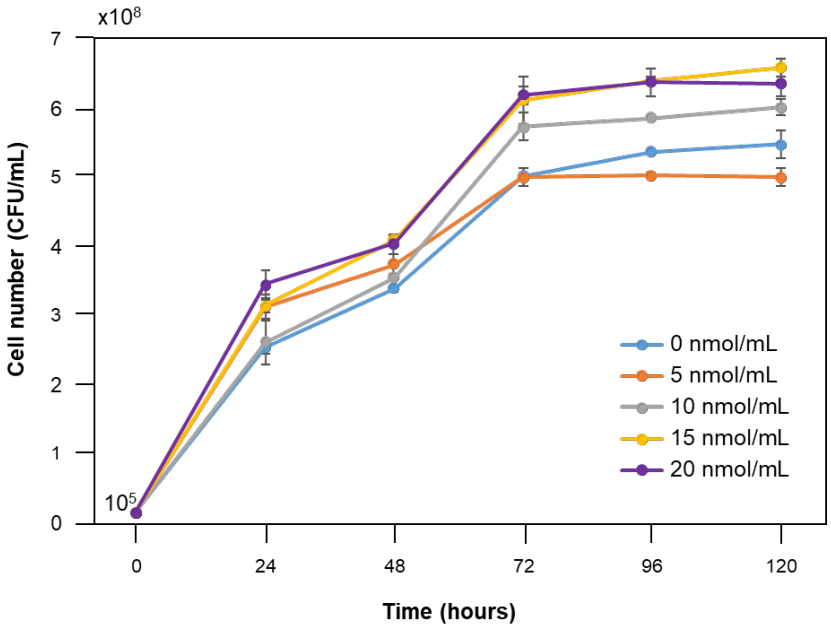

Figure 4.1. The growth of *S. xiamenensis* in LB fermentation broth supplemented with different concentration of exogenous riboflavin

Table 4.1. One-way ANOVA of cell count and exogenous riboflavin concentration

Sources of variation	Degrees of freedom	Sum of squares	Mean square	F	p-value
Between groups	4	4.291	1.073	1141.110	2.9×10^{-13}
Within groups	10	0.009	0.001		
Total	14	4.300			

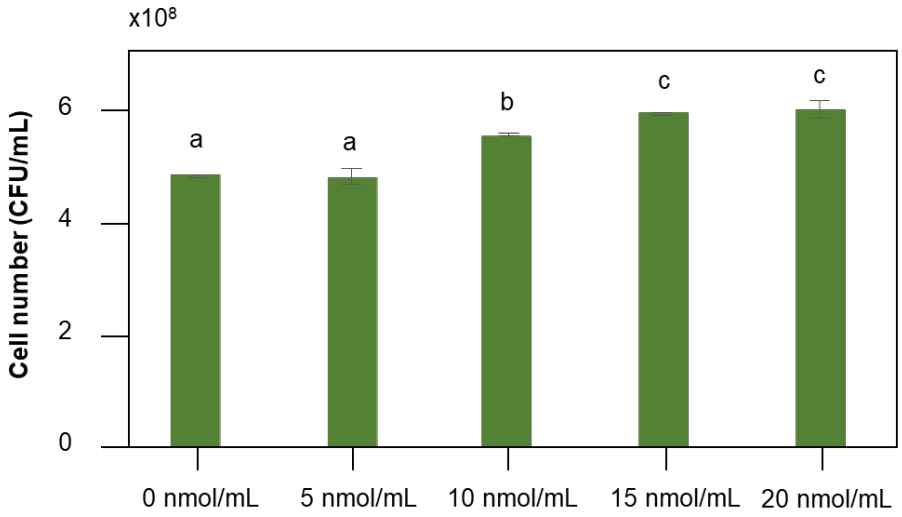

Figure 4.2. Cell number of *S. xiamenensis* in LB fermentation broth with different exogenous riboflavin at 72nd hour

[a, b, c] significant difference according to the Tukey's test ($p<0.05$)

Generally, microorganisms may have a capability to synthetize riboflavin. In my research, riboflavin production ability of *S. xiamenensis* was investigated in anaerobic condition with different initial exogenous riboflavin, and the results ware illustrated in **Figure 4.3**. The riboflavin concentration increased steadily and reached a peak after 72 hours operation, then decreased. Self-production of riboflavin by *S. xiamenensis* is apparent in sample without exogenous riboflavin. In this sample, riboflavin concentration increased after 24 hours operation (2.74 ± 0.7 nmol/mL vs 0.91 ± 0.04 nmol/mL at the beginning of operation). It continued to increase and reached the peak after 72 hours (5.51 ± 0.81 nmol/mL).

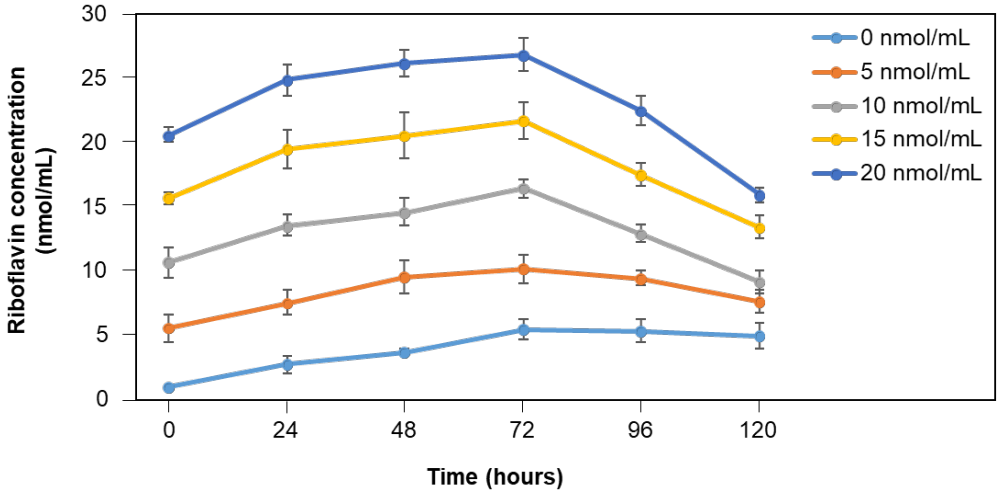

Figure 4.3. Riboflavin concentration in LB fermentation broth with different exogenous riboflavin

Figure 4.4 showed the riboflavin concentration in all samples produced after 72 hours of operation. In the samples with initial exogenous riboflavin 5; 10; 15; 20 nmol/mL, the riboflavin concentration accreted 4.62 ± 0.81; 5.73 ± 0.72; 6.11 ± 0.75; 6.17 ± 0.68 nmol/mL respectively, while the accreted value of sample without exogenous riboflavin reached 4.54 ± 0.8 nmol/mL. In these results, the higher initial exogenous riboflavin concentration present, the higher riboflavin production obtained. There were significant differences on riboflavin production between initial exogenous riboflavin 10 nmol/mL and 15 nmol/mL. However, statistical analysis of one-way ANOVA **(Table 4.2)** and Tukey's test revealed that there was no significant difference in riboflavin production among samples with initial exogenous riboflavin 15 nmol/mL and 20 nmol/mL.

Table 4.2. One-way ANOVA of riboflavin and initital exogenous riboflavin concentration

Sources of variation	Degrees of freedom	Sum of squares	Mean square	F	p-value
Between groups	4	7.722	1.931	1608.853	5.4×10^{-14}
Within groups	10	0.012	0.001		
Total	14	7.734			

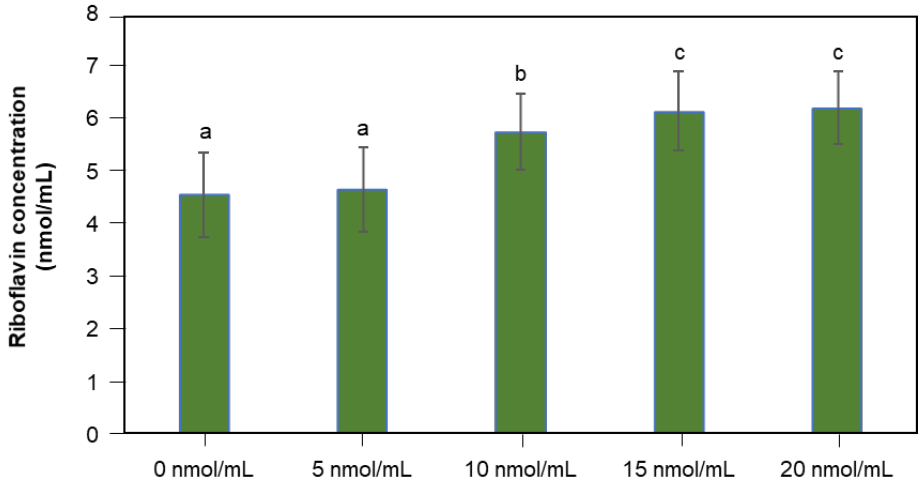

Figure 4.4. Riboflavin concentration was produced by *S. xiamenensis* in LB fermentation broth with different exogenous riboflavin at 72nd hour

[a, b, c] significant difference according to the Tukey's test ($p<0.05$)

Several microorganisms were reported to produce riboflavin. *Clostridium acetobutylicum* was well-known one of the earliest organisms used to produce riboflavin (Lim *et al.*, 2001). *Bacillus subtilis* in the fermentation broth with glucose as carbon source can produce 0.08 g/L riboflavin after 0.3 hours (Sauer *et al.*, 1996). *Candida guilliermondii* in liquid brewery waste with the presence of biotin produced 0.2 g/L riboflavin after 72 hours. In addition, after 8 days of fermentation using soybean as carbon source with the supplement of glycine, *Ashbya gossypii* produced 5.5 g/L riboflavin (Lim *et al.*, 2001). Besides, *Aspergillus terreus*, *Candida flareri, Eremothecium ashbyii* were reported to be able to produce riboflavin from 1.0 g/L to 3.3 g/L (Kalingan *et al.*, 1997; Levine *et al.*, 1949; Sabry *et al.*, 1994).

The kinetics of riboflavin production by *S. xiamenensis* in the sample without exogenous riboflavin was studied. Glucose with different concentration (from 0.25 g/L to 1 g/L) was used to analyze the growth of bacteria and riboflavin production. The built model is presented in **Figure 4.5**. Maximum specific cell growth rate (μ_{max}) of model was determined as 0.079 1/h with Monod constant (K_S) was 0.15 g/L. The ratio of the amount of biomass produced to the amount of glucose consume (Y_{XS} biomass yield) was 0.001 g biomass/g glucose. Additionally, the ratio of the amount of riboflavin produced to the amount of glucose consume (Y_{PS} riboflavin yield) was 0.003 g riboflavin/g glucose. Some researchers also reported the kinetic of riboflavin production. Lehmann *et al.* (2009) studied the formation of riboflavin of *Bacillus subtilis* with the presence of 0.102 mM GTP cyclohydrolase II (*rib*A) and maximum specific growth rate was 0.035 1/s, Kis *et al.* (1995) showed that the maximum

specific growth rate was 0.32 1/s with the presence of 0.102 mM riboflavin synthase (*rib*B). In addition, Tamer *et al.* (1988) described the kinetics of riboflavin production by *Saccharomyces cerevisiae* and *Saccharomyces carlsbergensis* in synthetic media. In the case of *S. carlsbergensis*, the specific cell growth rate was 0.30 1/h under anaerobic conditions and the amount of riboflavin to the amount of biomass was determined as 1.04×10^{-5} g/g. The specific cell growth rate of *S. cerevisiae* in wort with 2 mg/L of biotin supplement under anaerobic condition was 0.19 1/h. In both cases, the ratio of the amount of substrate to the amount of biomass was 2.6 g/g.

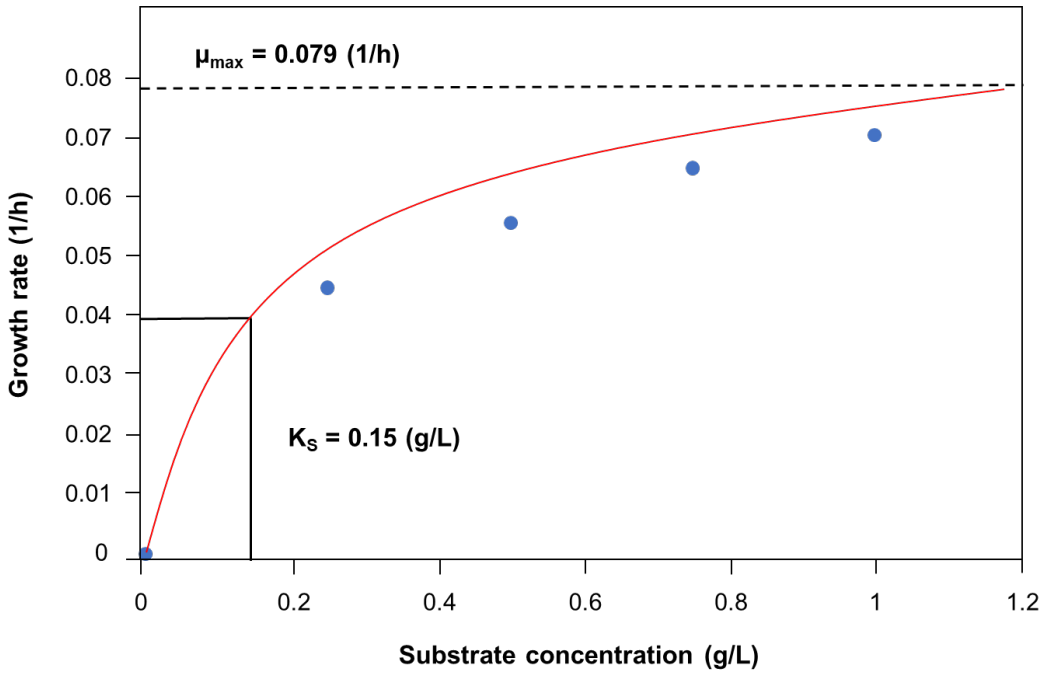

Figure 4.5. Modeling of growth rate related to substrate concentration

The method of Luedeking and Piret was used for evaluation of growth-associated (α) and non-growth-associated (β) product formation coefficients during riboflavin production (Mullai *et al.*, 2013; Szöllősi *et al.*, 2015a). **Figure 4.6** illustrated the relationship of specific growth rate versus specific product formation rate of *S. xiamenensis*. Value of specific production rate was plotted against specific growth rate and the equation obtained was $y = 3.3277x + 0.002$ with regression coefficient (R^2) of 0.98. The growth-associated (α) was determined as 3.3277 and significantly greater than zero that indicates riboflavin is purely a growth associated product. The biomass-associated (β) was 0.002 and also significantly

greater than zero. Based on these results, it can be concluded that the production of riboflavin is affected by both growth of bacteria and amount of biomass. This result is in agreement with one published by Szöllősi *et al*. (2015) when they studied the Fe^{3+}-reduction of *Geobacter toluenoxydans*.

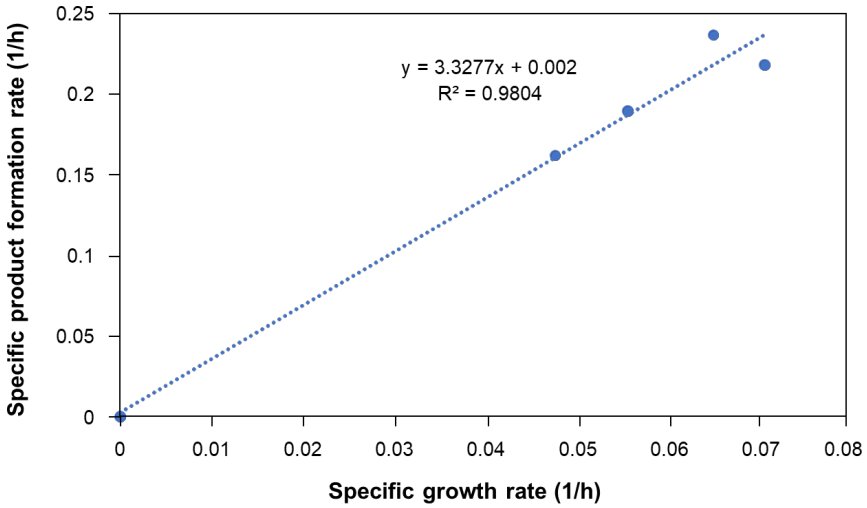

Figure 4.6. Connection between specific growth rate and specific product formation rate

4.1.2 Effect of pH on growth of *S. xiamenensis* and riboflavin production

Riboflavin production by *S. xiamenensis* at different initial pHs of medium is showed in **Figure 4.7**. Overall, riboflavin production of all pH levels increased after 24 hours of operation, then reached peaks after 72 hours.

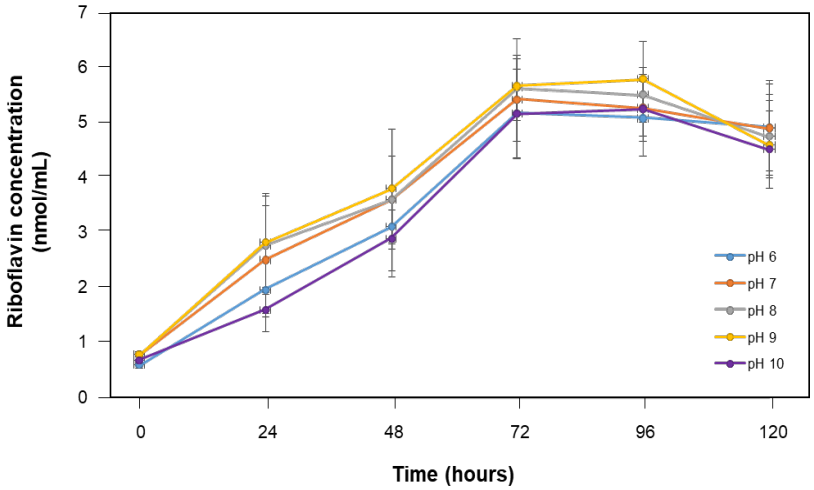

Figure 4.7. Riboflavin concentration in fermentation broth with different initial pH

Figure 4.8 showed the riboflavin concentration produced by *S. xiamenensis* at varying pH levels after 72 hours of operation. According to statistical analysis of one-way ANOVA **(Table 4.3)** and Tukey's test ($p<0.05$), there were significant differences in riboflavin production among pH 6, pH 7, pH 10 and pH 8, pH 9. Between pH 6, pH 7 and pH 10, there were no significant differences on riboflavin production by *S. xiamenensis*. The riboflavin production of pH 6, pH 7 and pH 10 was lower than that of other pH. With the alkaline pH, there was an increase in riboflavin production. The riboflavin production at pH 9 was the highest (4.89 ± 0.51 nmol/mL), followed by pH 8 (4.85 ± 0.72 nmol/mL) and pH 7 (4.54 ± 0.54 nmol/mL). Yong *et al.* (2013a) investigated the effect of pH on riboflavin biosynthesis of *Shewanella oneidesis* MR-1. They reported that the riboflavin concentration at pH 9 was highest with 367 nM level, and the riboflavin concentration at pH 6, pH 7, pH 8 and pH 10 were lower values. Kolonne *et al*. (1994) and Yamane *et al*. (1995) indicated the synthesis of riboflavin was strongly affected by pH, because pH plays an important rule on the conformation of key enzymes (Singh *et al.*, 2011).

Table 4.3. One-way ANOVA of pH and riboflavin concentration

Sources of variation	Degrees of freedom	Sum of squares	Mean square	F	p-value
Between groups	4	1.039	0.260	6495.250	5.1×10^{-17}
Within groups	10	4×10^{-4}	4×10^{-5}		
Total	14	1.039			

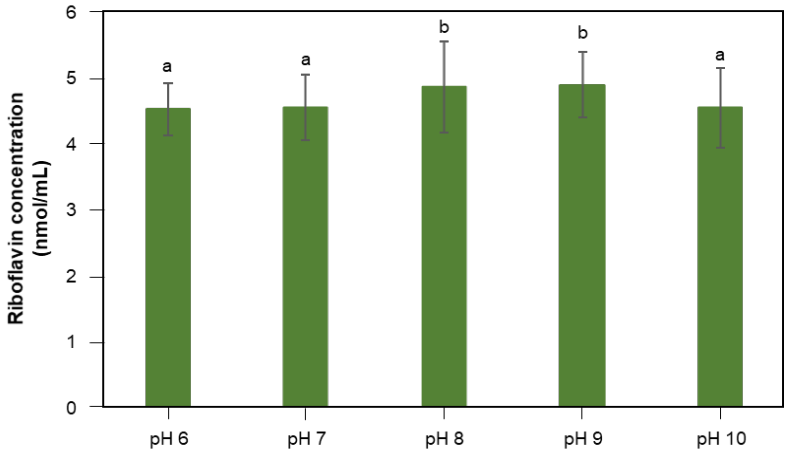

Figure 4.8. Riboflavin concentration produced by *S. xiamenensis* in LB fermentation broth with different initial pH value at 72nd hour

[a, b, c] significant difference according to the Tukey's test ($p<0.05$)

The *S. xiamenensis* cells growth with initial pH from 7 to 9 were similar, while they grew slowly at pH 6 and pH 10 after 24 hours of operation **(Figure 4.9)**. At 72nd hour, the maximum of cell concentration (5.78 × 10^8 CFU/mL) peaked in the sample with initial pH 9 meaning 1.3-fold and 1.6-fold higher than in the samples with initial pH 6 (4.43 × 10^8 CFU/mL) and pH 10 (3.58 × 10^8 CFU/mL), respectively.

In the sample with initial pH 10, the pH value decreased rapidly after 24 and 48 hours to achieve around pH 8. Therefore, bacteria grew quite slowly in this period. This trend was similar to pH 9. However, the sample with initial pH 9 achieved around pH 8 after 24 hours. On the contrary, the pH value increased after 24 and 48 hours to get around pH 8 in the sample with initial pH 6. Overall, *S. xiamenensis* adjusted pH value in the fermentation broth to suit their growth.

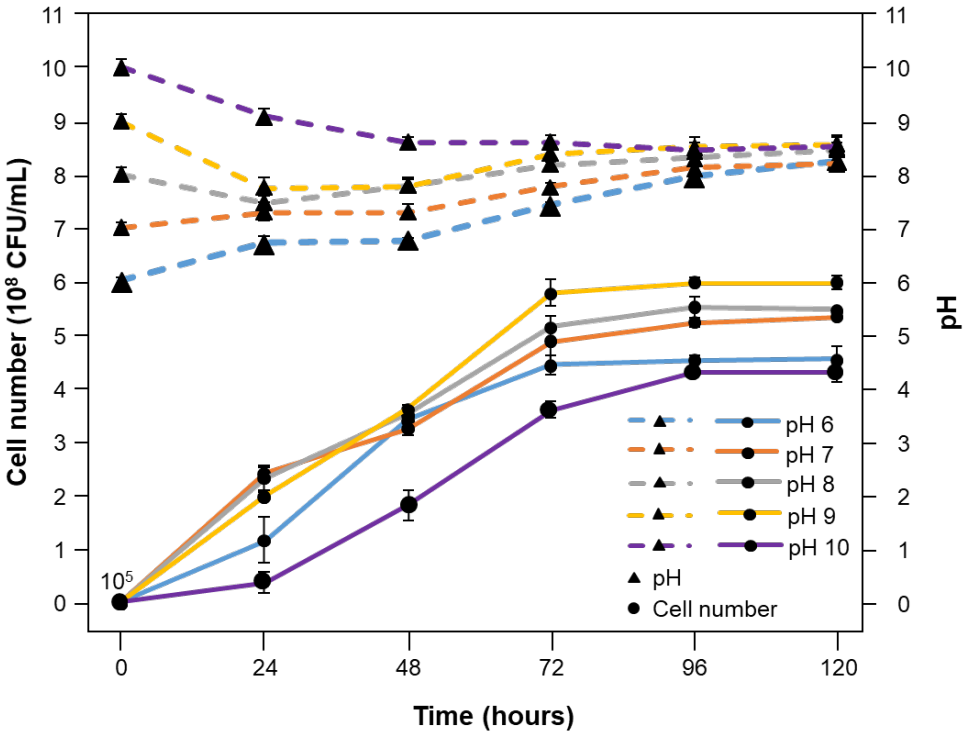

Figure 4.9. Change of pH and growth of *S. xiamenensis* in fermentation broth with different initial pH

The pH adjustment of *S. xiamenensis* produced organic acids such as propionic, acetic, succinic, malic, citric, lactic **(Figure 4.10)**. In samples with initial pH 6, propionic acid concentration was 23.08 mmol/L in comparation with 13.51, 12.87, 6.72, 3.05 and 0.62 mmol/L of propionic, acetic, lactic, succinic, malic, citric acid, respectively after 24 hours of fermentation. At 120th hour, the amount of organic acid decreased (propionic acid

concentration was 14.84 mmol/L in comparation with 1.83, 2.71 and 1.27 mmol/L of propionic, acetic, succinic, malic acid, respectively) and pH values of these samples increased from 6.76 to 8.24. In contrast, the amount of organic acid of samples with initial pH 10 increased from 24th hour to 96th hour of fermentation (for example, propionic acid concentration increased from 1.48 mmol/L to 10.39 mmol/L) and pH values decreased from 9.08 to 8.44. In the other samples from 24th hour to 120th hour, the total amount of organic acid decreased (for example, propionic acid concentration was from 37.79, 28.34, 24.97 mmol/L to 13.22, 11.21, 6.88 mmol/L in samples with initial pH 7, pH 8, pH 9, respectively), and pH value increased (from 7.29, 7.46, 7.74 to 8.20, 8.46, 8.58 in samples with initial pH 7, pH 8, pH 9, respectively). Citric and lactic acid presented only in samples with initial pH 6 after 24 and 48 hours of fermentation.

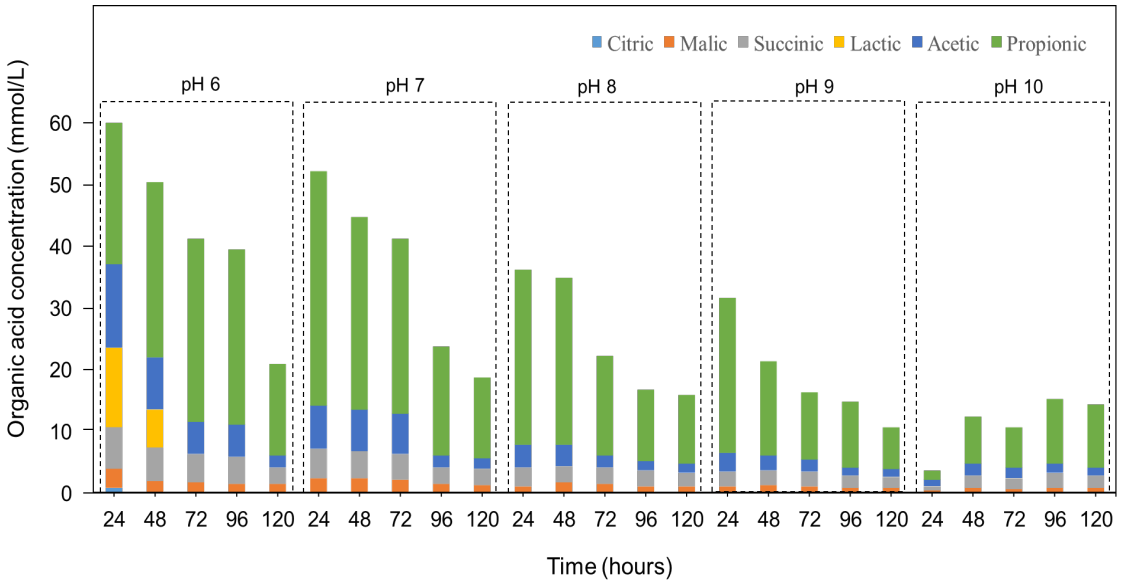

Figure 4.10. Organic acid concentration in fermentation broth with different initial pH

4.1.3 Optimisation of exogenous riboflavin and initial pH for enhancement of riboflavin production

Effects of exogenous riboflavin (X_1) and initial pH (X_2) on riboflavin production (Y) of *S. xiamenensis* was investigated using Response Surface Methods (RSM). The Central Composite Design (CCD) and results were showed in **Table 4.4**. The experimental set consisting of 11 runs was carried out using different combinations of the two independent variables. The riboflavin production was measured at 72nd hour of fermentation.

Table 4.4. Experimental design and results of riboflavin production

Run No.	X_1	X_2	Y
1	10	7	5.73
2	10	9	6.05
3	20	7	6.10
4	20	9	6.21
5	15	7	6.11
6	15	9	6.23
7	10	8	5.91
8	20	8	6.10
9	15	8	6.35
10	15	8	6.34
11	15	8	6.31

X_1: exogenous riboflavin (nmol/mL), X_2: initial pH, Y: riboflavin production (nmol/mL)

Second order polynomial model was applied to evaluate experimental data and regression analysis was used. The p-value was 0.007 (p-value < 0.05) indicating the fit of the regression model at high significant level. The coefficient of determination (R^2) was 0.926 meaning that 92.6% of the variability in the response could be explained by the model **(Table 4.5)**.

Table 4.5. ANOVA for the factorial design (R^2 = 0.926)

Sources of variation	Degrees of freedom	Sum of squares	Mean square	F	p-value
Regression	5	0.331	0.066	12.573	0.007
Residual	5	0.026	0.005		
Total Corrected	10	0.358	0.036		

The exogenous riboflavin and initial pH significantly affected the change of riboflavin production (p-value < 0.05), while the interaction of these independent variables was not significant **(Table 4.6)**.

Table 4.6. Regression analysis of model

Factors	Coefficient	Standard error	p-value	Conf. int (±)
Constant	6.295	0.037	1.38×10^{-10}	0.096
X_1	0.092	0.029	0.027	0.076
X_2	0.120	0.029	0.009	0.076
X_1^2	-0.068	0.045	**0.196**	0.117
X_2^2	-0.233	0.045	0.004	0.117
$X_1.X_2$	-0.053	0.036	**0.208**	0.093

According to results of regression analysis, the following second-order polynomial model (**Eq. 4.1**) was suggested to describe riboflavin production by *S. xiamenensis*.

$$Y = 6.295 + 0.092X_1 + 0.12X_2 - 0.233X_2^2 \qquad \textbf{(Eq. 4.1)}$$

where Y is riboflavin production (nmol/mL), X_1 is exogenous riboflavin concentration (nmol/mL) and X_2 is initial pH value

Response surface of riboflavin production was drawn based on the regressed model (**Figure 4.11)**. The optimal exogenous riboflavin and pH were determined to be 18 nmol/mL and pH 8.2, respectively. At these conditions, the predicted riboflavin production value was 6.33 nmol/L and was validated experimentally. Three experimental sets were designed and carried out at the optimal conditions. The concentration of riboflavin was determined to be 6.26 ± 0.29 nmol/mL that was very closed to the predicted value (6.33 nmol/mL).

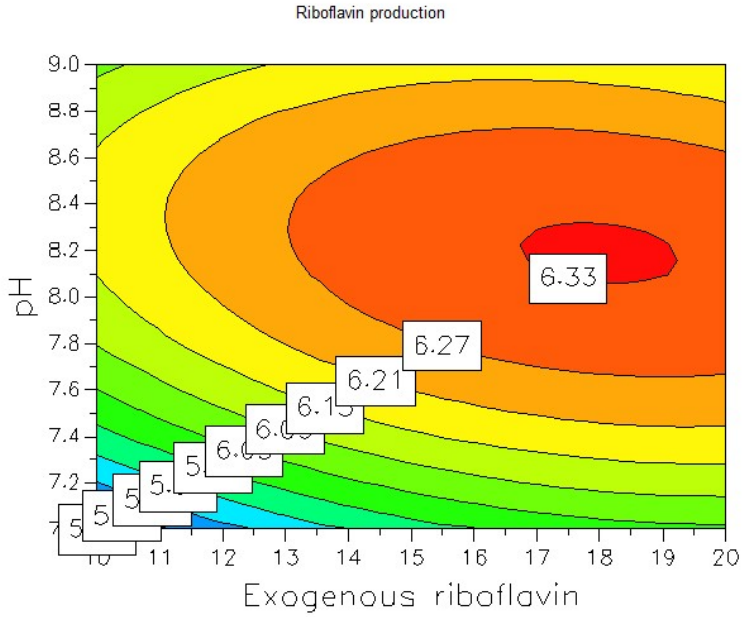

Figure 4.11. Response surface of riboflavin production in the optimal conditions

Overall, the optimal condition values were obtained as follow: initial pH 8.2; exogenous riboflavin 18 nmol/mL; operation time 72 hours; initial bacterial cells number 10^5 CFU/mL and LB fermented broth was used for the growth of bacteria.

4.2 Engineering of hydrogel composites-based bio-anode

4.2.1 Effect of riboflavin concentration on performance of MFC

MFC1, MFC2, MFC3, MFC4 and MFC5 were set-up with hydrogel composite bio-anode included 0, 5, 10, 15 and 20 nmol/mL riboflavin, respectively. Riboflavin identified as the electron shuttle of *Shewanella* sp. (Yong *et al.*, 2013) and played a role as a soluble redox shuttle transferring electrons from the cells surface to the external acceptors. The absence of riboflavin from biofilms reduced the rate of electron transport to electrode around 70% (Marsili *et al.*, 2008). The presence of riboflavin accelerates such process. The power density of different MFC with hydrogel composite bio-anode was illustrated in **Figure 4.12**.

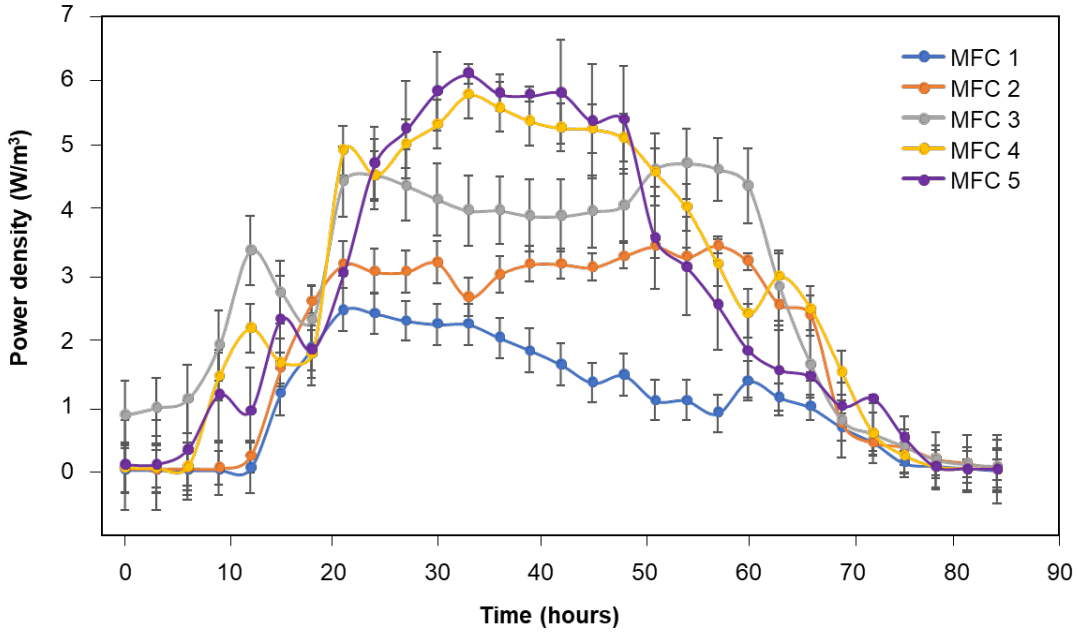

Figure 4.12. Power density of MFCs with different bio-anodes in batch mode

From initiation to around 21st hour, the power density of MFC1, MFC2 and MFC3 increased constantly due to intensive metabolic activity of the immobilized bacterial cells. The power density speedily increased in MFCs with higher riboflavin concentration (MFC4 and MFC5) in compared with control system MFC1. In the case of MFC5, the maximum power density was 6.06 ± 0.15 W/m^3 at 36th hour, and it was 2.7-fold higher than one (2.23 ± 0.31 W/m^3) in the case of MFC1. There was not a significant effect on power density when increasing riboflavin concentration from 15 nmol/mL to 20 nmol/mL. In the end of period (from around 50th hour), the power density of MFC4, MFC5 was decreased rapidly.

Meanwhile, the decrease in power density of MFC2 and MFC3 was also observed from 63rd hour. It can be explained by the run out of glucose the main carbon source in the anodic chamber. The change of glucose concentration in MFCs was illustrated in **Figure 4.14**

Wang *et al*. (2017b) showed that the presence of riboflavin in graphene/riboflavin composite electrode as the anode with the power density output 5.3-fold higher than bare graphite paper electrode. Flavin mononucleotide can improve electro-catalytic performance of MFC on the anode surface and enhances current production (Lee *et al.*, 2015).

4.2.2 Characterization of hydrogel bio-anode

4.2.2.1 Polarization curve

The performance of MFC is usually estimated by polarization curve (Pandit *et al.*, 2014). The polarization curves of MFCs with different riboflavin concentration were calculated and drawn in **Figure 4.13**. The open-circuit voltage of MFC5 (0.33 V) was 1.94-fold higher than MFC1 (0.17 V). The MFC1 produced a maximum power density of 2.4 W/m^3, while MFC5 got a peak at 5.82 W/m^3.

In general, the decreasing external load increased the current density and decreased the cell voltage (Nien *et al.*, 2011). A perfect polarization curve should show the power density rising to a peak point before dropping as the current continues to increase (Ieropoulos *et al.*, 2010). However, the power overshoot was observed. Here, this phenomenon was occurred in MFC1 and MFC2 at high electrical current (52 A/m^3 and 62 A/m^3, respectively). It was reported that cells voltage and electrical current reduced when reduced external resistor (Pandit *et al.*, 2014). According to Ieropoulos *et al.* (2010), electrical and ionic depletion is a result of the power overshoot phenomenon. At the lower external load, the demand of electrons (due to the more conductive external path) exceeds the microbial rate that they can be supplied at, the anolyte becomes depleted of electron and ions. However, increasing riboflavin concentration in hydrogel composite bio-anode from 10 nmol/mL to 20 nmol/mL, the overshoot was absent.

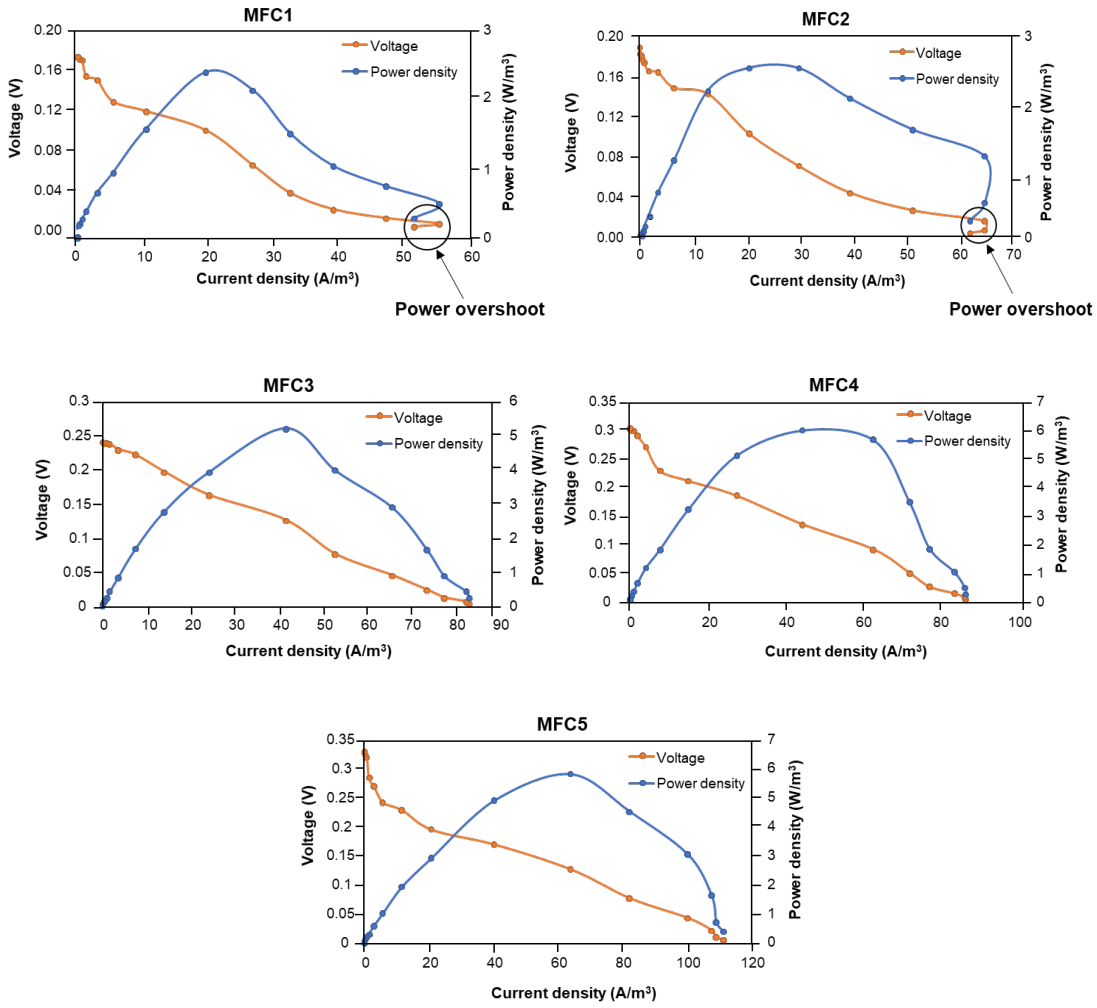

Figure 4.13. Effect of immobilized riboflavin concentration on electric performance of MFC

4.2.2.2 Changes of riboflavin and glucose concentration

The riboflavin production increased with the present of immobilized exogenous riboflavin in bio-anode **(Figure 4.14)**. The riboflavin production with initial 20 nmol/mL exogenous riboflavin get up to 46% higher than other without exogenous riboflavin after 72 hours (6.24 ± 0.07 vs 4.25 ± 0.38 nmol/ml). After 24 hours, glucose concentration of MFC1, MFC2 decreased around 30 - 31% in comparison with 35 - 36% in MFC3, MFC4, MFC5. At 85th hour, the glucose concentration was determined to be only 4% (MFC4, MFC5) and 6% (MFC1, MFC2, MFC3) and the power density of MFC system was quite low (0.11 – 0.19 W/m^3).

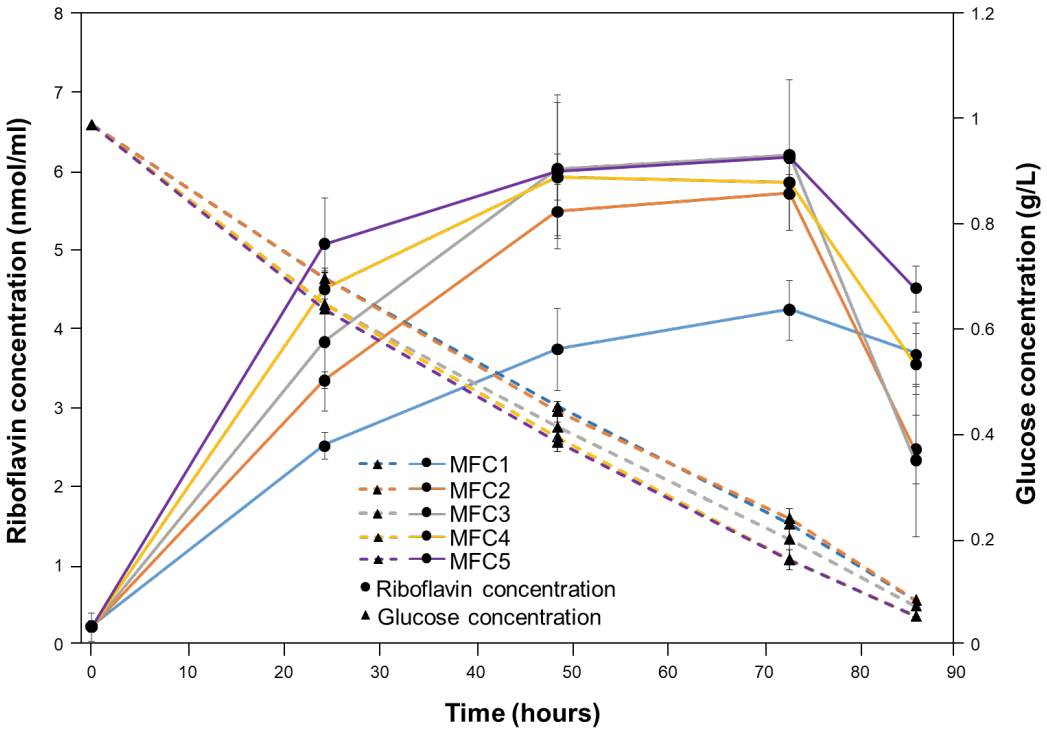

Figure 4.14. Changes of riboflavin and glucose concentration in anode chamber of MFCs with different bio-anode

4.2.2.3 Cyclic voltammetry (CV) of MFCs

Cyclic voltammetry (CV) is extensively used to consider the extracellular electron transfer processes in MFCs. This method was used to study the catalytic and capacitive behavior of different bio-electrodes (Pandit *et al.*, 2014). The redox peaks were found for the systems of bio-anode with riboflavin from 5 to 20 nmol/mL **(Figure 4.15)**. The oxidation and reduction peaks of all systems with bio-anode composite with riboflavin were -0.4V and -0.7 V, respectively. Besides, the area of the CV curves of bio-anode composite with riboflavin was larger than the system with lower riboflavin. The redox peaks of bio-anode with 20 nmol/mL exogenous riboflavin were 0.05 A/m^3 and 0.26 A/m^3, while in the case of 5 nmol/mL riboflavin were 0.07 A/m^3 and 0.19 A/m^3. Wang *et al*. (2017a) mentioned the same result. They fabricated riboflavin immobilized graphene composites and used it as anode in MFC with *S. oneidensis* MR-1 as well assessing the electrochemical activity of this anode material by condution of CV analyses. Their result showed that no obvious redox peaks in the CV curves of the bare graphene was observed, while the CV of graphene/riboflavin got a redox peak at about -0.4V. Wu *et al*. (2016) detected riboflavin in the supernatant of *Pachysolen tannophilus* culture, and they reported the redox peaks around -0.4V. This result

affirmed that c-type cytochromes were involved in the electron transfer process (Zhang *et al.*, 2017). Okamoto *et al*. (2012) investigated the role of c-type cytochrome in electron conduction across biofilm of *S. oneidensis* MR-1. To determine the transportation of respiratory electrons generated by microbial metabolism to distant electrodes via the redox cycling of c-type cytochrome, cyclic voltammetry was used to scan multilayer biofilms with the presence and the absence of lactate. With the presence of lactate, a redox peak was observed, and the columbic area of anodic current was 4-fold larger than that of the cathodic current. In the absence of lactate, the CV showed the lower columbic areas. Their result demonstrated that the electron conduction property of multilayer biofilms of *S. oneidensis* MR-1 was mediated by the redox cycling of outer-membrane c-type cytochrome.

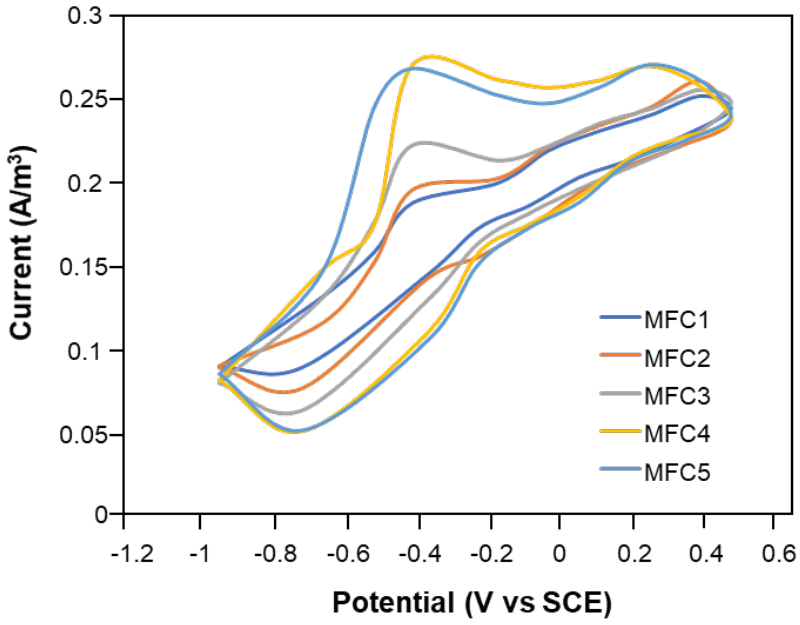

Figure 4.15. Cyclic voltammograms in MFCs with different bio-anodes

4.2.3 Set-up semi-continuous MFCs

Semi-continuous MFCs were set-up after the power density of MFCs decreased to the low value (around 0.11 – 0.19 W/m^3 at 85th hour of every stage) to consider the effectiveness of hydrogel bio-anode with the immobilization of riboflavin and *S. xiamenensis*. The anode champers of MFCs were fed fresh substrate.

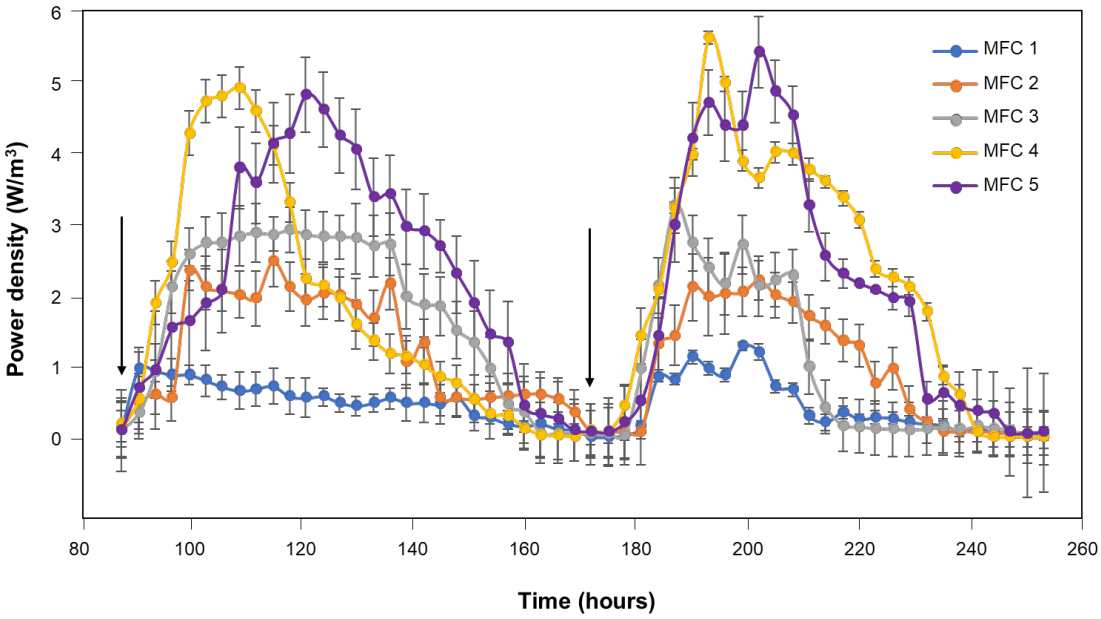

Figure 4.16. Power density of MFCs with different bio-anode in semi-continuous batch ("↓" indicate the new feeding cycle)

The power density of MFC4 reached the maximum value (4.93 ± 0.29 W/m^3) compared with 0.65 ± 0.25 W/m^3 in MFC1 after 21 hours of the second cycle **(Figure 4.16)**. However, the maximum values of MFCs in the second and third cycle were lower than in the first cycle. The maximum power density in the third cycle peaked at 5.64 ± 0.09 W/m^3 in MFC4. This result indicated that the MFCs still maintains the ability to produce electricity if the nutrients are available. The cycle time of MFCs takes about 80-85 hours from the feeding fresh medium to the run out of glucose.

4.3 Engineering of bacterial cellulose-based bio-anode

4.3.1 Fabrication of bacterial cellulose based composites and bio-anode

4.3.1.1 Effect of aniline concentration

In this experimental set, ammonium persulfate (APS) or iron (III) chloride hexahydrate ($FeCl_3.6H_2O$) were used as oxidants. The concentration of aniline ranged from 0.1 mol/L to 0.25 mol/L. The molar ratio of ammonium persulfate (or iron (III) chloride hexahydrate) to aniline was kept stable at 1:1.

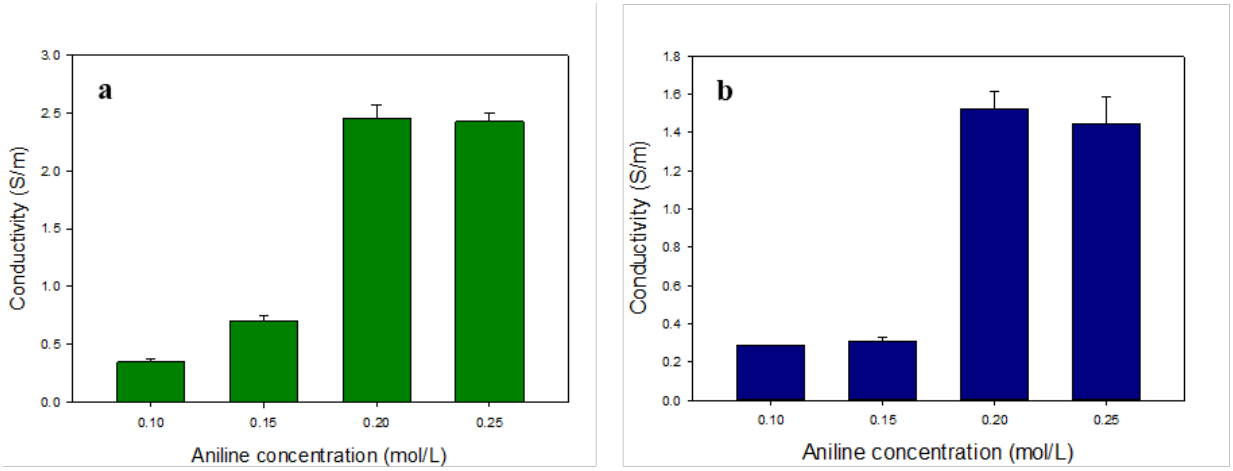

Figure 4.17. Effect of aniline concentration on the conductivity of BC/PANI composites (a) BC/PANI/APS; (b) BC/PANI/$FeCl_3.6H_2O$

As a result **(Figure 4.17)**, the electrical conductivity of BC/PANI increased when the aniline concentration increased. Meanwhile, use of APS as oxidant, the maximum electrical conductivity of BC/PANI was 2.47 ± 0.11 S/m at 0.2 mol/L aniline concentration, where in the case of $FeCl_3.6H_2O$ as oxidant, the maximum electrical conductivity of BC/PANI peaked 1.52 ± 0.09 S/m at the similar aniline concentration. Statistical analysis of one-way ANOVA revealed that there were no significant differences in electrical conductivity when aniline concentration increased from 0.2 mol/L to 0.25 mol/L in both of samples.

4.3.1.2 Effect of molar ratio of oxidant to aniline

The aniline concentration using in this experiment was 0.2 mol/L. The molar ratio of oxidant (APS or $FeCl_3.6H_2O$) to aniline ranged from 0.5:1 to 2:1 with 0.5:1 stepwise.

In the case of using APS as oxidant, the maximum electrical conductivity of BC/PANI/APS was 2.54 ± 0.17 S/m at 1.5:1 of molar ratio of APS to aniline (**Figure 4.18)**. At ratio 1:1, the electrical conductivity was 2.46 ± 0.12 S/m. There was no significant difference in electrical conductivity when the molar ratio of APS to aniline increased from 1.5:1 to 2.0:1. In the case of using $FeCl_3.6H_2O$ as oxidant, the electrical conductivity peaked at 2.0:1 of molar ratio of $FeCl_3.6H_2O$ to aniline (2.13 ± 0.2 S/m). However, there was no significant difference in electrical conductivity when the molar ratio of $FeCl_3.6H_2O$ to aniline ranged between 1.5:1 and 2.0:1.

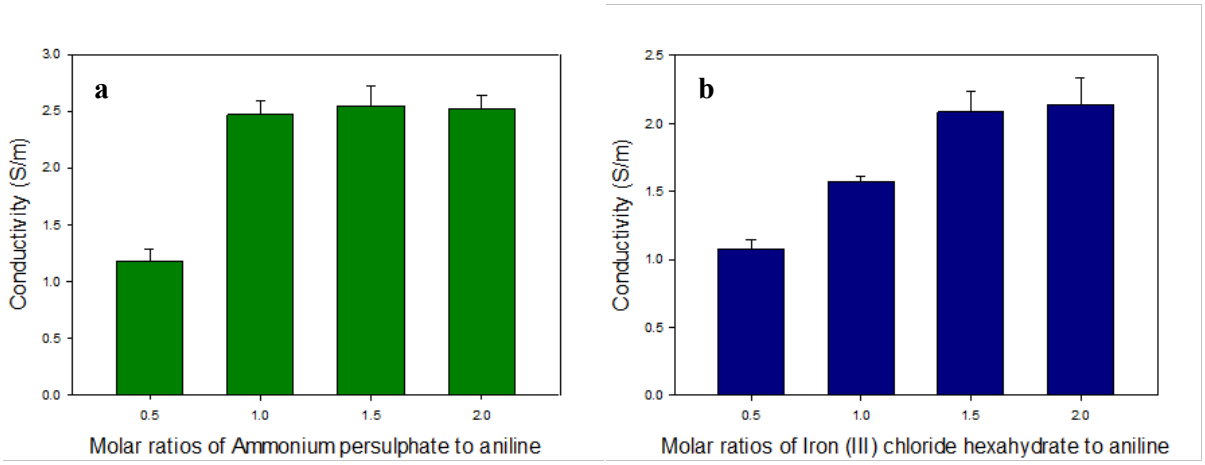

Figure 4.18. Effect of molar ratios of oxidant to aniline on the conductivity of BC/PANI composites (a) BC/PANI/APS/; (b) BC/PANI/$FeCl_3.6H_2O$

The aniline concentration as well as molar ration of oxidant agents to aniline were optimized for maximal electrical conductivity of BC/PANI preparations using response surface method **(Figure 4.19)**. The electrical conductivity of BC/PANI composites was strongly dependent on aniline concentration and the molar ratio of oxidant to aniline.

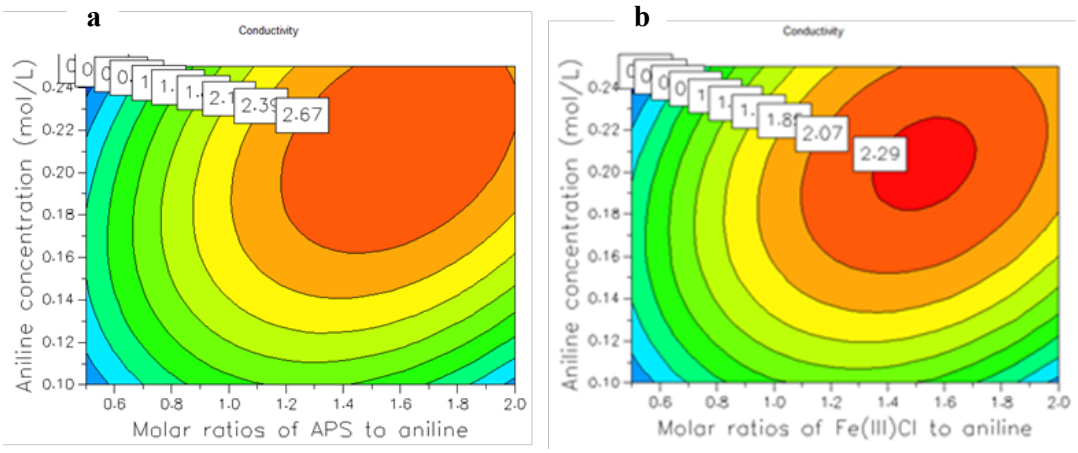

Figure 4.19. Response surface of electrical conductivity of BC/PANI with aniline concentration and molar ratio of oxidant to aniline
(a) BC/PANI/APS; (b) BC/PANI/$FeCl_3.6H_2O$

Based on the results, the maximum conductivity of BC/PANI composites could be obtained as follow: 0.2 mol/L aniline, 1.2:1 of molar ratio of ammonium persulfate to aniline or 1.5:1 of molar ratio of $FeCl_3.6H_2O$ to aniline, 0 – 5 $^{\circ}$C reaction temperature, and 2 hours and 12 hours polymerization time. The conductivity of BC/PANI/APS composites obtained

2.62 ± 0.15 S/m and 2.21 ± 0.11 S/m with BC/PANI/$FeCl_3.6H_2O$ composites (predicted values were 2.67 S/m and 2.29 S/m, respectively). Wang *et al*. (2012a) fabricated bacterial cellulose nanofiber-supported polyaniline nanocomposites with flake-shaped morphology and used it as supercapacitor electrodes. In their report, ammonium persulfate was used as oxidant and aniline was as monomer for polymerization process in a mixed solvent of dimethylformamide (DMF) and distilled water. They reported that the electrical conductivity of bacterial cellulose/polyaniline nanocomposites was strongly dependent upon reaction conditions. The electrical conductivity of BC/PANI nanocomposite films obtained 5.1 S/cm with mass ration of BC/aniline as 1:10, molar ratio of ammonium persulfate/aniline as 1:1, molar ratio of HCl/aniline as 1.2:1, volume ratio of DMF/H_2O as 1:2, reaction temperature as 0 – 10 $^{\circ}$C, and reaction time longer than 4 hours. In other research, Müller *et al.* (2012) prepared BC/PANI using $FeCl_3.6H_2O$ as oxidant. The reaction were performed in the present or absence of HCl aqueous solution. They showed that the polymerization process denpended on molar ratio of $FeCl_3$/aniline and reaction time. BC/PANI composites prepared with HCl solution exhibited higher electrical conductivity (0.9 S/cm) than BC/PANI without HCl.

4.3.1.3 Effect of titanium-dioxide

The maximum electrical conductivities of BC/PANI/APS with 0.3 mol/L TiO_2 and BC/PANI/$FeCl_3.6H_2O$ with 0.2 mol/L TiO_2were 3.71 ± 0.2 S/m and 2.9 S/m, respectively **(Figure 4.20)**. The coating TiO_2 greatly improved electrical conductivity of BC/PANI. The electrical conductivity of BC/PANI/APS coating TiO_2 was 1.4-fold higher than sample without coating TiO_2, and 1.2-fold higher in case of BC/PANI/$FeCl_3.6H_2O$.

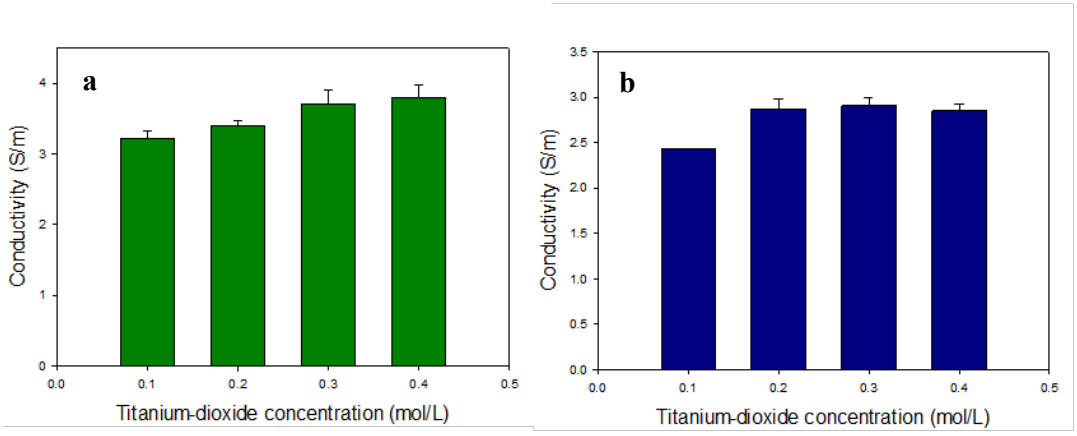

Figure 4.20. Effect of titanium-dioxide concentration in fabrication of BC/PANI/TiO_2 composites process on its conductivity (a) BC/PANI/APS; (b) BC/PANI/$FeCl_3.6H_2O$

4.3.1.4 Chemical structure and surface characteristics

The infrared spectra of bare BC and synthesized BC composites were determined by FT-IR **(Figure 4.21)**.

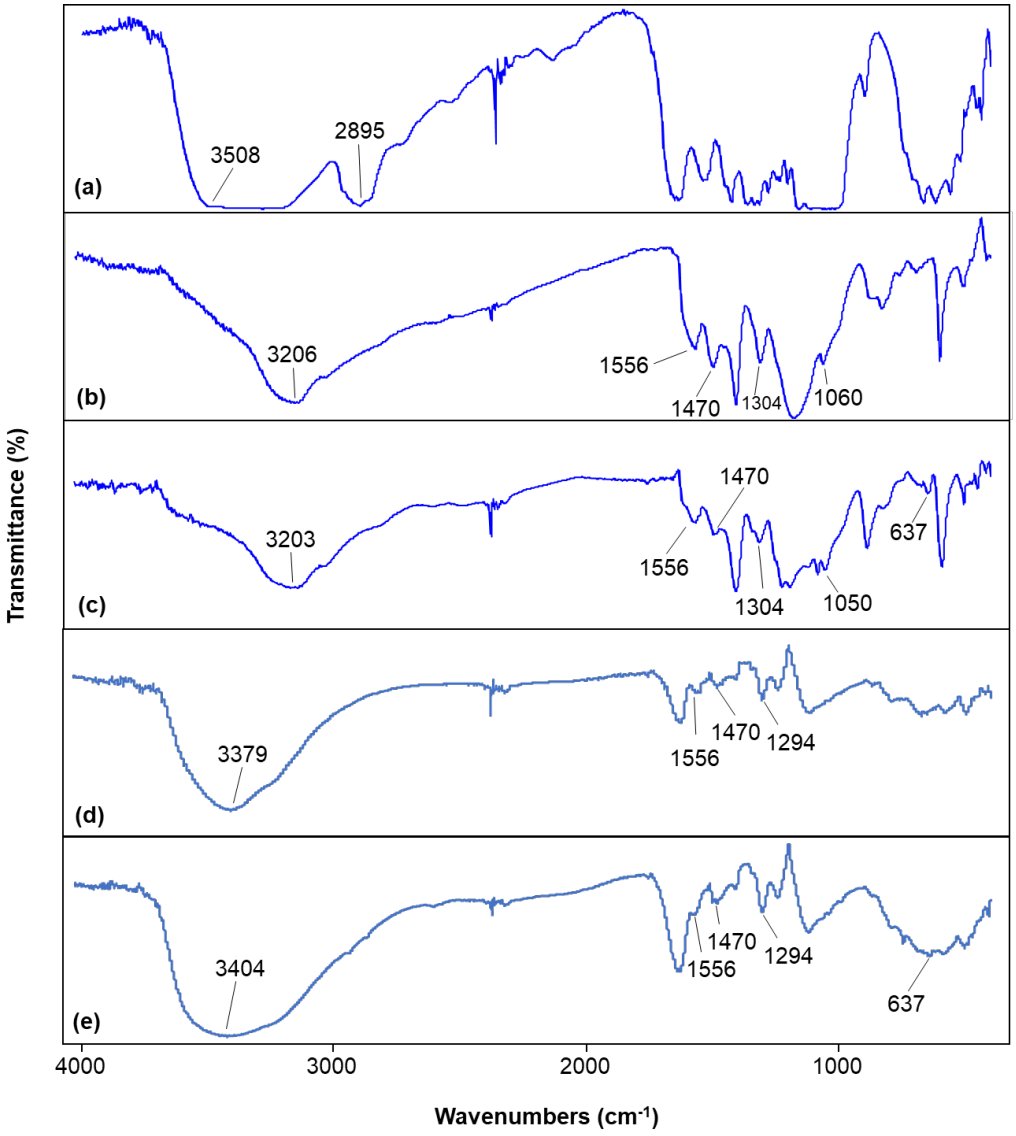

Figure 4.21. FT-IR spectra of (a) bare BC; (b) BC/PANI/APS; (c) BC/PANI/TiO_2/APS; (d) BC/PANI/$FeCl_3.6H_2O$; (e) BC/PANI/TiO_2/$FeCl_3.6H_2O$

The FT-IR spectrum of bare BC showed broad adsorption band in the region of 3200 - 3550 cm^{-1}, which is assigned to hydrogen bond for -OH (Jahan *et al.*, 2011; Sun *et al.*, 2002; Wan *et al.*, 2019; Wang *et al.*, 2012a). The peak at 2895 cm^{-1} showed the aliphatic C-H stretching vibration. In the case of BC/PANI composite, the stretching vibration of quinoid

and benzenoid rings structure was at peak 1556 and 1470 cm^{-1}, respectively. C-O-C stretching vibrations of the pyranose skeletal ring were at range of 1060-1030 cm^{-1} (Wang *et al.*, 2012a). In addition, the bands at 1294 and 1304 cm^{-1} correspond to the C-N in-plane ring bending modes (Han *et al.*, 2019; Khodamoradi *et al.*, 2019).

The FT-IR spectra of BC/PANI/TiO_2 composites showed the absorption band at 637 cm^{-1}. This point demonstrated the interaction was formed between TiO_2 and hydroxyl group of cellulose (Afsharpour *et al.*, 2011). This result showed that the BC was sufficiently coated by PANI and TiO_2.

The surface characteristics of BC, BC/PANI and BC/PANI/TiO_2 were evaluated by Scanning Electron Microscopy (SEM). **Figure 4.22** showed the SEM image of bare BC and BC/PANI at ×1000 magnification.

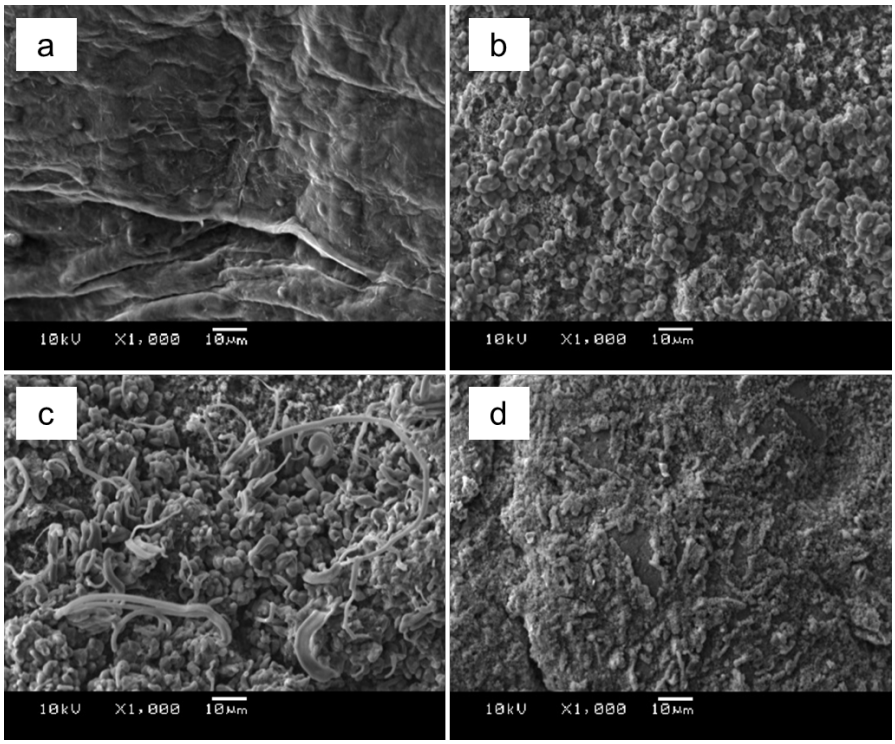

Figure 4.22. SEM images of (a) Bare BC, (b) BC/PANI/APS, (c) BC/PANI/TiO_2/APS, (d) BC/PANI/TiO_2/$FeCl_3.6H_2O$

The morphologies are particularly different between bare BC and BC/PANI. In the case of bare BC, a smooth surface with featureless morphology was observed **(Figure 4.22a)**. In comparison, the surface of BC/PANI was rough and covered with materials **(Figure 4.22b-d)**. The surface structure of BC/PANI/TiO_2 showed the particles entangled with cellulose and

PANI particles, present a much denser structure **(Figure 4.22c, d)**. This result was showed that the BC coating adhered to the cellulose and formed a continuous conducting network for the high electrical conductivity (Lv *et al.*, 2016; Müller *et al.*, 2012; Wang *et al.*, 2012a).

4.3.1.5 Fabrication of bacterial cellulose based bio-anode

S. xiamenensis cells were immobilized in BC, BC/PANI and BC/PANI/TiO_2 composites**.** In the case of bare BC, the cell number increased until 36 hours whereupon a stable value was observed for further 36 hours (1.2×10^6 CFU/g). After 48 hours of immobilization microorganisms on BC/PANI and BC/PANI/TiO_2 electrodes had reached their maximum cell numbers and were stable for further 24 hours (**Figure 4.23)**. The maximum cells number of BC/PANI/TiO_2 using ammonium persulphate and $FeCl_3.6H_2O$ as oxidant were 1.2×10^6 CFU/g and 1.1×10^6 CFU/g, respectively. When the immobilization process completed, the BC, BC/PANI, BC/PANI/TiO_2 were covered by sodium alginate film. The ability to immobilize microorganisms into bare BC was also described (Fijałkowski *et al.*, 2015).

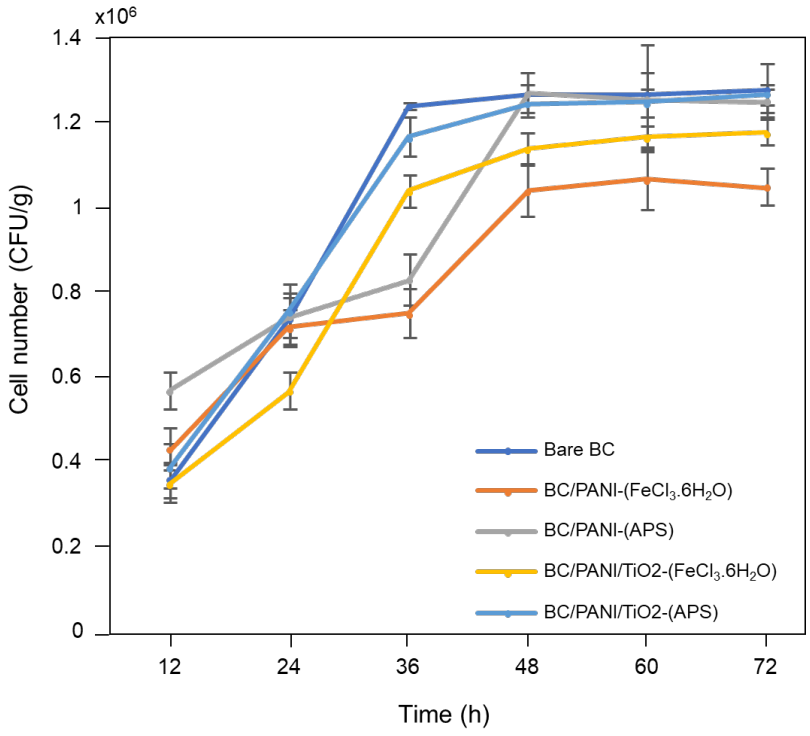

Figure 4.23. The number of immobilized *S. xiamenensis* cells (CFU/g BC) in bare BC, BC/PANI and BC/PANI/TiO_2 by adsorption-incubation method

4.3.2 Performance of bacterial cellulose based bio-anode in MFC systems

4.3.2.1 Electrical performance

Five types of bioanodes namely bare BC, BC/PANI/$FeCl_3.6H_2O$, BC/PANI/APS, BC/PANI/TiO_2/$FeCl_3.6H_2O$ and BC/PANI/TiO_2/APS with the immobilization *S. xiamenensis* were used in different MFC systems MFC6, MFC7, MFC8, MFC9, MFC10, respectively. The membrane was 2 × 3 × 0.5 cm and the immobilization cell numbers were counted to be in the range 1.1 – 1.2 × 10^6 CFU. The voltage in MFC was measured with 500 Ohm external resistance and run until the output voltage decreased to the low values. The power density of all MFC system is illustrated in **Figure 4.24**. The power density rapidly increased in MFCs with BC/PANI/TiO_2 anode (MFC9 and MFC10) compared with the control system bare BC (MFC6). The power density of MFC10 reached the maximum value (38.89 W/m^3) after 8h of operation and maintained this power density for 28h. The power density of MFC10 was 15-fold higher than MFC6 with bare BC anode (2.57 W/m^3). MFC6 got a maximum value (7.09 W/m^3) after 16 hours of operation. In the case of BC/PANI/TiO_2 (MFC9) using $FeCl_3.6H_2O$ as an oxidant – the power density value peaked around 23.95 - 29.30 W/m^3, lower than MFC10. MFC7 and MFC8 also showed lower power density values in comparison with MFC9 and MFC10. The combination of BC/PANI and TiO_2 contributed to the increase in power density. Taşkan *et al.* (2013) used a Ti-TiO_2 electrode to enhance the electricity generation in MFC and their research showed that the current density achieved 15-fold higher than the carbon-based electrode. In the same year Wu *et al.* (2013b) reported a fabricated MFC with a three-dimensional nanostructure of carbon nanotube-gold-titanium-dioxide (CNT/Au/TiO_2) as anode modifier and the power density was 3-fold higher than the bare carbon paper electrode. Indeed, conducting polymers are often used as anode materials in MFC due to the large surface area, low cost and conductivity. For example, Szöllősi *et al.* (2017) successfully fabricated an alginate/PANI/TiO_2/graphite composite with high electrical conductivity and power density, stability in MFC. Li *et al.* (2012) also used modified carbon felt electrodes with four classes of conducting polymers, specifically polyaniline, poly(aniline aminophenol), poly(aniline-co-2,4-diaminophenol) (PANDAP) and poly(aniline-1,8-diaminonaphthalene) (PANDAN). Their method enhanced the power densities for both abiotic cathodes (increased by 300%) and biocathodes (increased by 180%) compared to unmodified carbon felts electrodes.

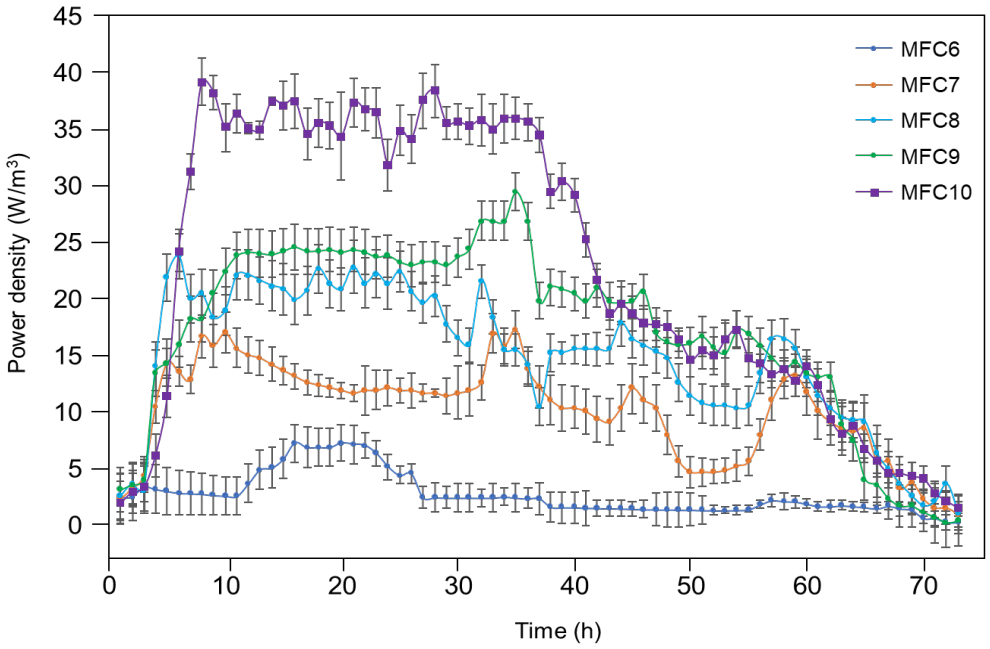

Figure 4.24. Power density of MFCs with different synthesized BC anode in simple batch

The polarization curve of all MFC systems was calculated and showed in. The maximum power density of MFC10 system was 40.66 W/m^3 with a current density of 116.72 A/m^3 **(Figure 4.25)**. Moreover, the power overshoot of MFC10 was absent. According to Peng *et al.,* (2013), the power overshoot in MFCs was present due to the lack of anodic capacitance or immature biofilm on the anode electrode. These results clearly substantiate the suitability of using BC/PANI/TiO_2/APS as anode for MFC.

To consider the effectiveness of BC/PANI/TiO_2/APS with immobilization of *S. xiamenensis*, semi-continuous batch was set-up after voltage output of MFC10 decreased to near nil. The anode chamber of the MFC10 was fed with fresh substrate. The maximum power density of each cycle peaked around 35.81 W/m^3 after 30th hour meaning the MFCs are able to produce electricity when the fuel was fed **(Figure 4.26)**. The cycle time of MFCs took about 70-72 hours from the feeding to exhaust of glucose.

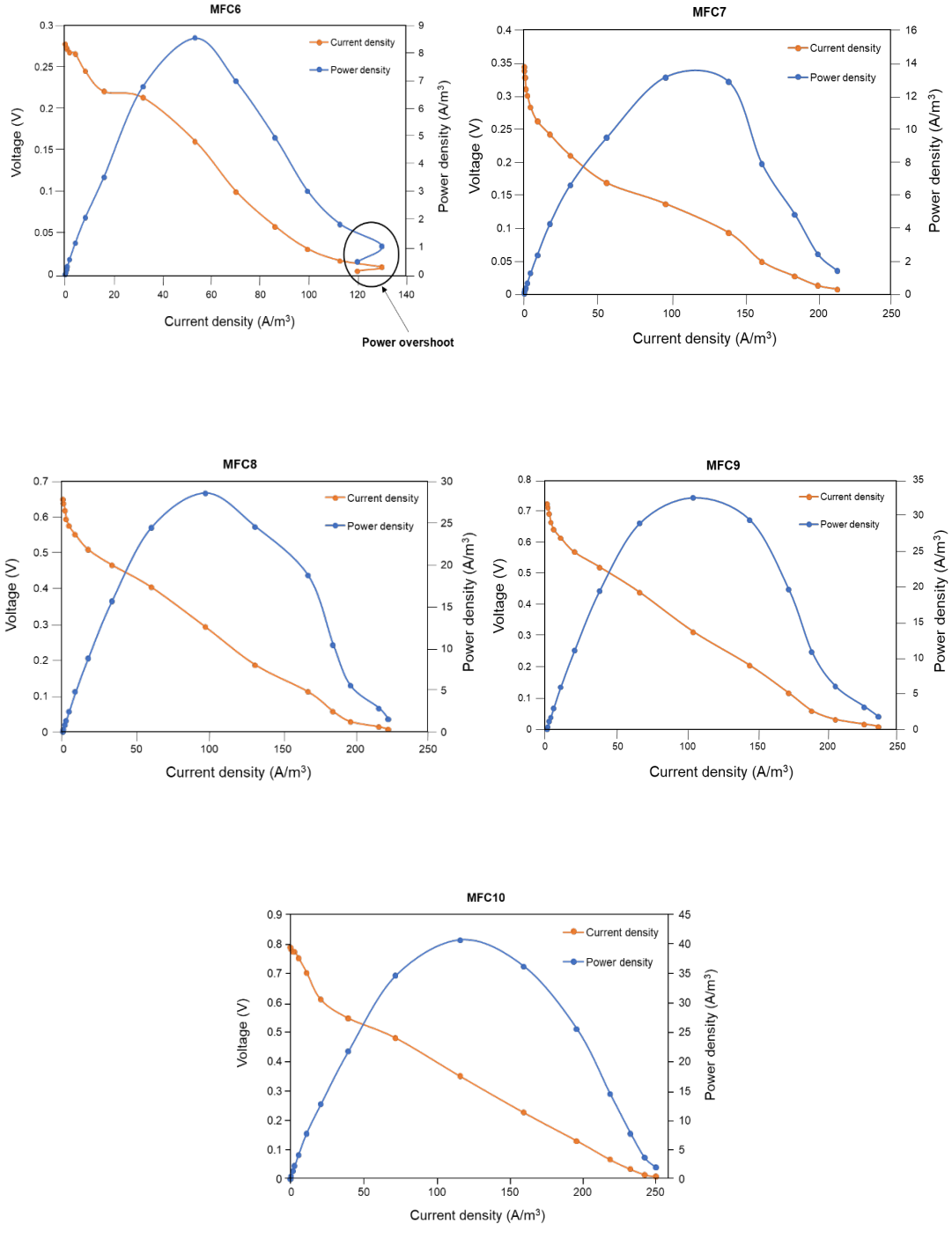

Figure 4.25. Polarization curve of MFCs with bare BC and synthesized BC composites

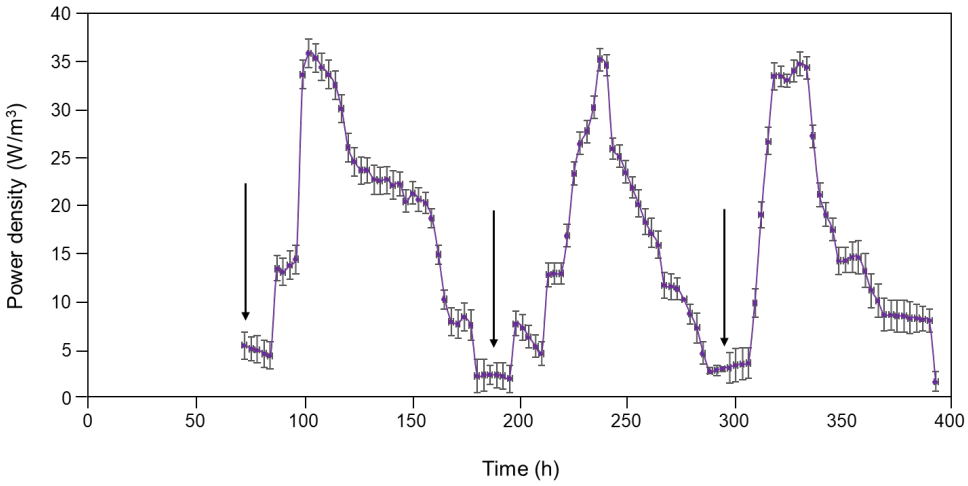

Figure 4.26. Power density of MFC with BC/PANI/TiO_2 in semi-continuous batch ("↓" indicate the new feeding cycle)

The CV response of MFC10 with BC/PANI/TiO_2/APS composite anode was calculated and drawn in **Figure 4.27**. The redox peaks were found for the systems of BC/PANI/TiO_2/APS anode. This result affirmed that c-type cytochromes were involved in the electron transfer process (Zhang *et al.*, 2017) and the successful fabrication of BC/PANI/TiO_2/APS was confirmed.

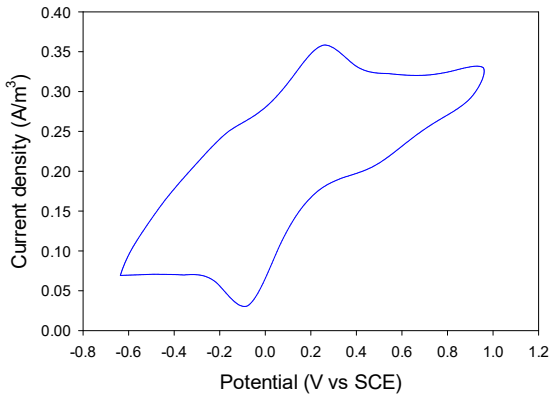

Figure 4.27. Cyclic voltammetry of MFC using BC/PANI/TiO_2/APS anode with potential (vs SCE)

4.3.2.2 Effect of exogenous iron(III) on the performance of MFC

The MFCs with BC/PANI/TiO_2/APS with immobilization of *S. xiamenensis* cells was applied. Fe(III) was added into anode chambers at the initiation with different concentration from 3 mM to 12 mM.

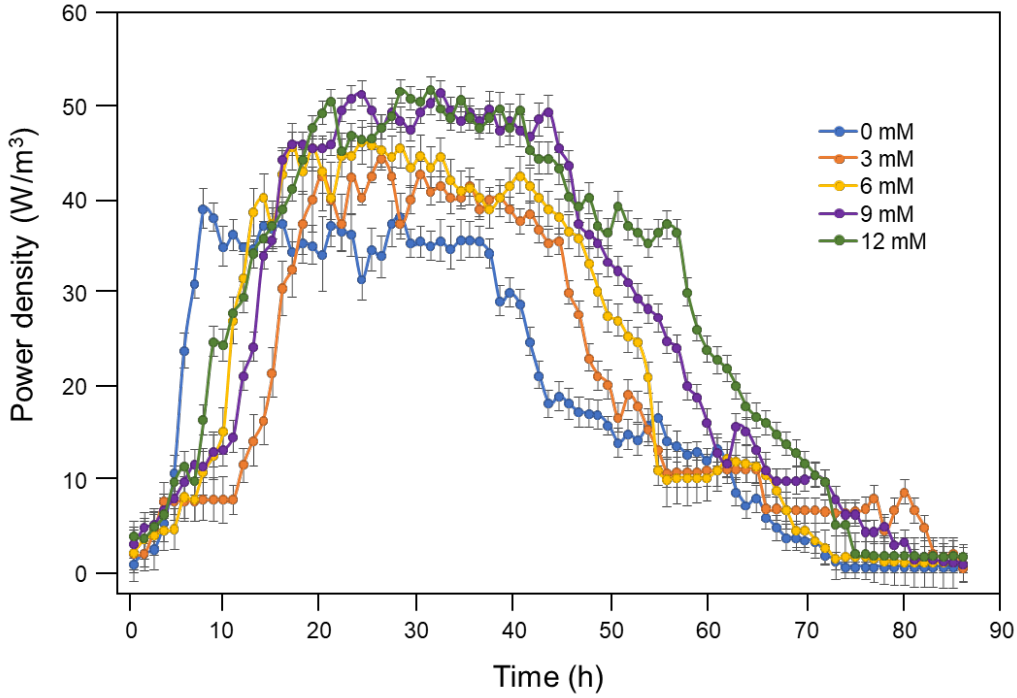

Figure 4.28. Power density of MFCs with different initial Fe(III) concentration

The power density rapidly increased in MFCs supplemented with different concentrations of Fe(III) after the inoculation **(Figure 4.28)**. The maximum of power density ranged from 49.05 ± 1.24 to 51.544 ± 1.29 W/m^3 between 20th hour and 40th hour in the MFC system with 12 mM Fe(III) concentration. These values were 1.3-fold and 1.4-fold higher than MFC systems with 3 mM and without Fe(III) concentration, respectively. The addition of Fe(III) to the anode chamber (up to 9 mM) resulted increase in the electricity generation. However, the higher concentration of Fe(III) did not increase the efficiency of MFCs. In our study, the improvements in MFCs performance were negligible when Fe(III) concentrations were higher than 9 mM. The maximum of power density in MFC with 9 mM Fe(III) was around 49.28 ± 2.34 to 51.11 ± 2.29 W/m^3.

Leu *et al.* (2016) found that the current using Fe_3O_4-modified carbon cloth electrode as the anode was 2-fold higher than bare carbon cloth electrode. This result verified that the Fe_3O_4-modifile carbon cloth electrode can enhance the current generation of MFC. In the

other study, Kim *et al.* (2015) demonstrated that the presence of ferric ions in anode electrode significantly increased power density (about 4-fold higher) of MFCs. Moreover, while Wei *et al.* (2013) pointed out that the presence of ferrous sulfate in anode improved power density of MFCs at the initiation, whereas Lin *et al.* (2014a) shown that the addition of FeCN in the anode enhanced voltage output (the voltage increased 39.3% higher than without FeCN).

In the carbon cycle process, iron plays an element role in the formation routes of pyruvate that is decarboxylated and forms thiamine pyrophosphate-enzyme complexes (Wei *et al.*, 2013). Additionally, the iron is the key of anaerobic bacteria metabolism and an enzyme activator. Many authors reported that the hydrogenase activity is affected by reduction of iron concentration (Junelles *et al.*, 1988; Peters, 1998; Volbeda *et al.*, 1995).

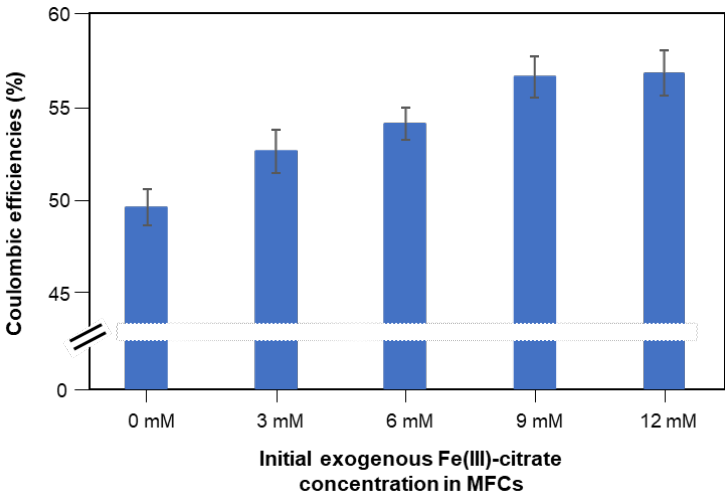

Figure 4.29. Maximum coulombic efficiencies in MFCs with different initial Fe(III) concentration

The CE reached 56.92 ± 1.21% of MFC with 12 mM Fe(III) concentration, compared to 49.71 ± 0.98% of the MFC without exogenous Fe(III) in anode chamber **(Figure 4.29)**. This result demonstrated that the supplement of exogenous Fe(III) into anode chamber of MFC was effectively increase in the CE of MFCs.

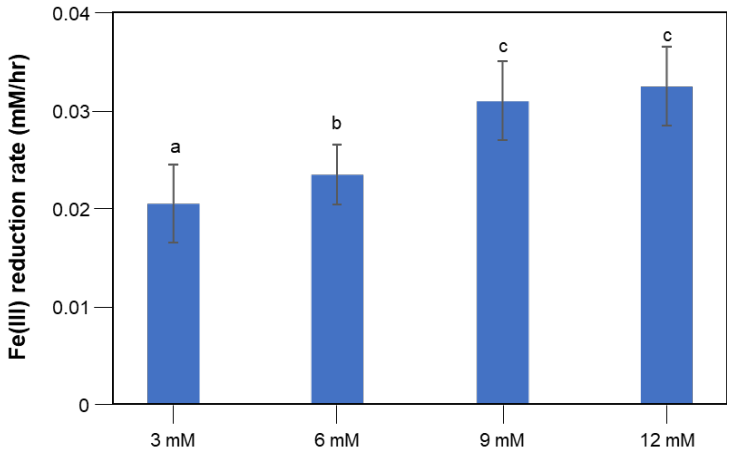

Figure 4.30. Reduction rate of Fe(III) in MFCs at different initial Fe(III) concentrations
[a, b, c] significant difference according to the Tukey's test ($p<0.05$)

In my case, the Fe(III) reduction rate in MFCs elevated with the increase of initial Fe(III) concentration **(Figure 4.30)**. The maximum reduction rate (0.033 ± 0.004 mM/hour) was detected in MFC at 12 mM of Fe(III) comparing with 0.021 ± 0.004 mM/hours and 0.024 ± 0.003 mM/hour in MFC at 3 mM and 6 mM of Fe(III), respectively. However, according to ANOVA analysis, there was not significant difference in Fe(III) reduction rate between MFC at 9 mM and MFC at 12 mM. The ability of reduction Fe(III) of *S. xiamenensis* was reported by Szöllősi *et al*. (2015). Similarly, Wu *et al.* (2013a) carried out the experiment with the supplementation of different Fe(III) concentrations (from 3 mM to 10 mM) in MFCs using *S. oneidensis* MR-1 and they reported that the maximum reduction rate of Fe(III) (25.0 ± 0.3%) appeared in MFC at 10 mM.

5 NOVEL CONTRIBUTION

1. The effect of exogenous riboflavin and pH on growth of *S. xiamenensis* and riboflavin production were studied. Exogenous riboflavin, initial pH and bacterial cell number were optimized for production of riboflavin by *S. xiamenensis*. The optimal conditions of exogenous riboflavin concentration, initial pH and inoculated cell numbers were initial 18 nmol/mL pH 8.2 and 10^5 CFU/mL, respectively in the LB fermented broth. The fermentation should be carried out for 72 hours.
2. Hydrogel bio-anode of alginate/polyaniline/titanium-dioxide/graphite composites with the immobilization of riboflavin mediator and *S. xiamenensis* cells was successfully fabricated and applied in MFC. The presence of riboflavin increased the transport of electrons from the cells to the electrode. New bio-anode improved the efficiency and stability of MFCs. The maximum power density (6.06 ± 0.15 W/m^3) was obtained in the case of MFC using hydrogel bio-anode with the immobilization of riboflavin concentration as 15 nmol/mL and 20 nmol/mL.
3. The fabrication of electrical conducting composites based on bacterial cellulose was successfully done. The effect of aniline concentration and ammonium persulfate or iron (III) chloride hexahydrate as an oxidant was determined. The highest electrical conductivity (2.62 ± 0.15 S/m) of BC/PANI composites using ammonium persulfate as an oxidant could be obtained when use of 0.2 mol/L aniline and molar ratio of ammonium persulfate to aniline was 1.2:1. In the case of use of iron (III) chloride hexahydrate as an oxidant, the electrical conductivity of BC/PANI composites was 2.21 ± 0.11 S/m at 0.2 mol/L aniline, and the molar ratio of iron(III) chloride hexahydrate to aniline was 1.5:1. The electrical conductivity of BC/PANI can be improved by coating with TiO_2. The electrical conductivity of TiO_2 coated BC/PANI/APS was 1.4-fold higher than sample without TiO_2.
4. New bio-anode of BC/PANI/APS/TiO_2 composites immobilized *S. xiamenensis* was fabricated and used in the MFC. This bio-anode significantly improved the power density of MFC from 2.57 W/m^3 (bare BC) to around 38.89 W/m^3 meaning 15-fold higher.
5. The performance of MFC was improved by supplement of Fe(III). With 9 mM initial Fe(III), the coulombic efficiency of MFC was 56.71 ± 1.13%, the maximum of power density was around 49.28 ± 2.34 to 51.11 ± 2.29 W/m^3 between 20th hour and 40th hour. The maximum Fe (III) reduction rate was 0.031 ± 0.004 mM/hour.

6 SUMMARY

Shewanella xiamenensis DSMZ 22215 (DSMZ, Braunschweig, Germany) was used as a main bacterium. The bacterium was grown anaerobically at 30 °C in Luria-Bertrani (LB) broth. The exogenous riboflavin with different concentration (ranging from 0-20 nmol/mL) was supplemented into LB broth to determine the effect of this component on growth and riboflavin production by *S. xiamenensis*. Bacterial cells number and riboflavin concentration was measured after 24 hours intervals. As the results, the higher initial exogenous riboflavin concentration present, the higher riboflavin production obtained. The maximum riboflavin production peaked at samples with exogenous riboflavin 15 nmL/mL and 20 nmol/mL after 72 hours of operation. Self-production of riboflavin by *S. xiamenensis* is apparent in sample without exogenous riboflavin. Bacteria grew better in exogenous riboflavin 15 nmol/mL and 20 nmol/mL. The kinetics of riboflavin production by *S. xiamenensis* in the sample without exogenous riboflavin was determined. Maximum specific cell growth rate (μ_{max}) of model was 0.079 1/h with substrate saturation constant (K_S) was 0.15 g/L. Biomass yield (Y_{XS}), riboflavin yield (Y_{PS}) were calculated as 0.001 g/g, 0.003 g/g, respectively. The growth-associated (α) and non-growth-associated (β) product formation coefficients during riboflavin production of Luedeking-Piret model was also determined as 3.3277 and 0.002, respectively. These values were significantly bigger than zero, thus both growth and biomass have effects on the product formation. In addition, the effect of pH condition was studied. LB broth with different pH values (from pH 6 to pH 10) was used. With the alkaline pH, there was an increase in riboflavin production. The riboflavin production at pH 9 was the highest (4.89 ± 0.51 nmol/mL). The *S. xiamenensis* cells growth with initial pH from 7 to 9 were similar, while they grew slowly at pH 6 and pH 10 after 24 hours of operation. Moreover, the combined effects of exogenous riboflavin (X_1) and initial pH (X_2) on riboflavin production (Y) of *S. xiamenensis* was investigated. Response Surface Methods (RSM) described the second-order polynomial equation of riboflavin production: $Y = 6.295 + 0.092X_1 + 0.12X_2 – 0.233X_2^2$, where Y is riboflavin production, X_1 is exogenous riboflavin and X_2 is initial pH value. The optimal condition value was pH 8.2 and exogenous riboflavin 18 nmol/mL.

The application of *S. xiamenensis* in MFCs was carry out with the immobilization them into hydrogel bio-anode composites. Alginate, polyaniline, titanium-dioxide and graphite was used to fabricated hydrogel bio-anode composites with the immobilization of riboflavin mediator and *S. xiamenensis* was investigated. The efficacy of using hydrogel bio-anode composites with the immobilization of riboflavin in improving the performance of MFCs was

outlined in this study. The presence of riboflavin enhanced the bioelectricity production in MFCs. The maximum power density was 6.06 ± 0.15 W/m^3 in MFCs at hydrogel bio-anode with 20 nmol/mL riboflavin, 1.7-fold higher than in MFC without riboflavin.

In addition, the new materials using for fabrication of anode electrode was studied to enhance the performance of MFCs. Bacterial cellulose (BC) was polymerized with aniline and oxidant (ammonium persulfate or iron (III) chloride hexahydrate) to make BC/PANI composites. These materials with the immobilization of *S. xiamenensis* was used as anode electrode in MFCs. Moreover, the coating titanium-dioxide on BC/PANI composites was carried out. Titanium-dioxide greatly improved electrical conductivity of BC/PANI. In the case of using ammonium persulfate as an oxidant, the electrical conductivity of BC/PANI/TiO_2 was 3.71 ± 0.2 S/m, 1.4-fold higher than the sample without coating TiO_2. The using BC/PANI/TiO_2 as anode improved the power density of MFCs. The power density in MFCs with BC/PANI/TiO_2/APS anode peaked at 38.89 W/m^3, 15-fold higher than MFC using bare BC anode.

To demonstrate the ability reducing Fe(III) of *S. xiamenensis* and the effect of Fe(III) on MFCs using BC/PANI/TiO_2/APS, Fe(III) was supplemented into anode chamber at the start-up of operation with different concentration from 3 mM to 12 mM. The coulombic efficiencies (CE) and power density of all MFC system increased with the increasing of initial Fe(III) concentration. The CE reached 56.92 ± 1.21% of MFC with 12 mM Fe(III) concentration, compared to 49.71 ± 0.98% of the MFC without Fe(III) in anode chamber. Besides, the Fe(III) reduction rate was 0.033 ± 0.004 mM/hour and 0.021 ± 0.004 mM/hours in MFC at 12 mM and MFC at 3 mM of Fe(III), respectively.

In conclusion, several conditions affected the ability of riboflavin production by *S. xiamenensis*, thus improving the electrochemical performance of this bacteria. New types of bio-anodes using different hydrogel composites were successfully engineered and applied. These bio-anodes improved significantly electric performance of MFCs.

7 REFERENCES

Adachi, M., Shimomura, T., Komatsu, M., Yakuwa, H., & Miya, A. (2008). A novel mediator–polymer-modified anode for microbial fuel cells. *Chemical communications (Cambridge, England), 7*, 2055-2057. doi:10.1039/b717773a

Aelterman, P., Rabaey, K., Pham, H. T., Boon, N., & Verstraete, W. (2006). Continuous electricity generation at high voltages and currents using stacked microbial fuel cells. *Environmental Science and Technology, 40*(10), 3388-3394. doi:10.1021/es0525511

Afsharpour, M., Rad, F. T., & Malekian, H. (2011). New cellulosic titanium dioxide nanocomposite as a protective coating for preserving paper-art-works. *Journal of Cultural Heritage, 12*(4), 380-383. doi:10.1016/j.culher.2011.03.001

Ahmed, E. M. (2015). Hydrogel: Preparation, characterization, and applications: A review. *Journal of Advanced Research, 6*(2), 105-121. doi:10.1016/j.jare.2013.07.006

Al-Shamary, E., & Khalaf, A. (2013). Influence of fermentation condition and Alkali treatment on the porosity and thickness of bacterial cellulose membranes. *The Online Journal of Science and Technology, 3*(2), 194–203.

Alonso, E., Faria, M., Mohammadkazemi, F., Resnik, M., Ferreira, A., & Cordeiro, N. (2018). Conductive bacterial cellulose-polyaniline blends: Influence of the matrix and synthesis conditions. *Carbohydrate Polymers, 183*, 254-262. doi:10.1016/j.carbpol.2017.12.025

Ansari, S., & Anis, A. (2018). Conducting polymer hydrogels. In *Polymeric Gels* (pp. 467-486): Elsevier.

Ateh, D., Navsaria, H., & Vadgama, P. (2007). Polypyrrole-based conducting polymers and interactions with biological tissues. *Journal of the Royal Society, Interface / the Royal Society, 3*, 741-752. doi:10.1098/rsif.2006.0141

Bacher, A., Eberhardt, S., Fischer, M., Kis, K., & Richter, G. (2000). Biosynthesis of vitamin B2 (riboflavin). *Annual review of nutrition, 20*, 153-167. doi:10.1146/annurev.nutr.20.1.153

Bajpai, A. K., Bajpai, J., & Soni, S. (2009). Designing polyaniline (PANI) and polyvinyl alcohol (PVA) based electrically conductive nanocomposites: preparation, characterization and blood compatible study. *Journal of Macromolecular Science®, Part A: Pure and Applied Chemistry*, 774-782. doi:10.1080/10601320903004533

Bakonyi, P., Koók, L., Kumar, G., Tóth, G., Rózsenberszki, T., Nguyen, D. D., . . . Nemestóthy, N. (2018). Architectural engineering of bioelectrochemical systems from the perspective of polymeric membrane separators: A comprehensive update on recent progress and future prospects. *Journal of Membrane Science, 564*, 508-522. doi:10.1016/j.memsci.2018.07.051

Baniasadi, H., Ramazani S.A, A., & Mashayekhan, S. (2015). Fabrication and characterization of conductive chitosan/gelatin-based scaffolds for nerve tissue engineering. *International Journal of Biological Macromolecules, 74*, 360-366. doi:10.1016/j.ijbiomac.2014.12.014

Barua, P. K., & Deka, D. (2010). Electricity generation from biowaste based microbial fuel cells. *Int J Energy Inf Commun, 1*, 77-92.

Bassas-Galia, M., Follonier, S., Pusnik, M., & Zinn, M. (2017). 2 - Natural polymers: A source of inspiration. In G. Perale & J. Hilborn (Eds.), *Bioresorbable Polymers for Biomedical Applications* (pp. 31-64): Woodhead Publishing.

Benabid, F. Z., & Zouai, F. (2016a). Natural polymers: Cellulose, chitin, chitosan, gelatin, starch, carrageenan, xylan and dextran. *Journal of Natural Products, 4*(3), 348-357.

Benabid, F. Z., & Zouai, F. (2016b). Natural polymers: cellulose, chitin, chitosan, gelatin, starch, carrageenan, xylan and dextran. *Journal of Natural Products, 4*, 348-357.

Bennetto, H. P., Stirling, J. L., Tanaka, K., & Vega, C. A. (1983). Anodic reactions in microbial fuel cells. *Biotechnology and Bioengineering, 25*(2), 559-568. doi:10.1002/bit.260250219

Bhadra, S., Khastgir, D., Singha, N. K., & Lee, J. H. (2009). Progress in preparation, processing and applications of polyaniline. *Progress in Polymer Science, 34*(8), 783-810. doi:10.1016/j.progpolymsci.2009.04.003

Bian, C., Yu, A., & Wu, H. (2009). Fibriform polyaniline/nano-TiO2 composite as an electrode material for aqueous redox supercapacitors. *Electrochemistry Communications, 11*(2), 266-269. doi:10.1016/j.elecom.2008.11.026

Bishop, C. (2007). *Vacuum deposition onto webs, films, and foils* (3rd edition ed.): Elsevier.

Bismarck, A., Aranberri, I., Springer, J., Lampke, T., Wielage, B., Stamboulis, A., . . . Limbach, H.-H. (2002). Surface characterization of flax, hemp and Cellulose Fibers; surface properties and the water uptake behavior. *Polymer Composites, 23*, 872-894. doi:10.1002/pc.10485

Bitsch, R., & Bitsch, I. (2011). *HPLC Determination of Riboflavin in Fortified Foods* (First ed.): WILEY-VHC Verlag GmbH & Co. KGaA.

Bodiga, V. L., Bodiga, S., Surampudi, S., Boindala, S., Putcha, U., Nagalla, B., . . . Manchala, R. (2012). Effect of vitamin supplementation on cisplatin-induced intestinal epithelial cell apoptosis in Wistar/NIN rats. *Nutrition, 28*(5), 572-580. doi:10.1016/j.nut.2011.09.007

Bond, D., & Lovley, D. (2003a). Electricity Production by Geobacter sulfurreducens Attached to Electrodes. *Applied and environmental microbiology, 69*, 1548-1555. doi:10.1128/AEM.69.3.1548-1555.2003

Bond, D. R., Holmes, D. E., Tender, L. M., & Lovley, D. R. (2002). Electrode-Reducing Microorganisms That Harvest Energy from Marine Sediments. *Science, 295*(5554), 483. doi:10.1126/science.1066771

Bond, D. R., & Lovley, D. R. (2003b). Electricity production by Geobacter sulfurreducens attached to electrodes. *Applied and environmental microbiology, 69*(3), 1548-1555. doi:10.1128/AEM.69.3.1548-1555.2003

Bradford, M. M. (1976). A rapid and sensitive method for the quantitation of microgram quantities of protein utilizing the principle of protein-dye binding. *Anal Biochem, 72*(1-2), 248-254. doi:10.1016/0003-2697(76)90527-3

Burgess, C., Smid, E., & Van Sinderen, D. (2009). Bacterial vitamin B2, B11 and B12 overproduction: An overview. *International journal of food microbiology, 133*, 1-7. doi:10.1016/j.ijfoodmicro.2009.04.012

Castro, C., Zuluaga, R., Putaux, J.-L., Caro, G., Mondragon, I., & Gañán, P. (2011). Structural characterization of bacterial cellulose produced by Gluconacetobacter swingsii sp. from Colombian agroindustrial wastes. *Carbohydrate Polymers, 84*(1), 96-102. doi:10.1016/j.carbpol.2010.10.072

Chang, I. S., Jang, J. K., Gil, G. C., Kim, M., Kim, H. J., Cho, B. W., & Kim, B. H. (2004). Continuous determination of biochemical oxygen demand using microbial fuel cell type biosensor. *Biosensors and Bioelectronics, 19*(6), 607-613. doi:10.1016/S0956-5663(03)00272-0

Chang, I. S., Moon, H., Jang, J. K., & Kim, B. H. (2005). Improvement of a microbial fuel cell performance as a BOD sensor using respiratory inhibitors. *Biosensors and Bioelectronics, 20*(9), 1856-1859. doi:10.1016/j.bios.2004.06.003

Chaudhuri, S. K., & Lovley, D. R. (2003). Electricity generation by direct oxidation of glucose in mediatorless microbial fuel cells. *Nature Biotechnology, 21*(10), 1229-1232. doi:10.1038/nbt867

Chen, J.-y., Li, N., & Zhao, L. (2014). Three-dimensional electrode microbial fuel cell for hydrogen peroxide synthesis coupled to wastewater treatment. *Journal of Power Sources, 254*, 316-322. doi:10.1016/j.jpowsour.2013.12.114

Chen, J., Hamon, M. A., Hu, H., Chen, Y., Rao, A. M., Eklund, P. C., & Haddon, R. C. (1998). Solution Properties of Single-Walled Carbon Nanotubes. *282*(5386), 95-98. doi:10.1126/science.282.5386.95 %J Science

Chen, Y., Cai, M., Lin, L., & Dong, J. (2005). Asp service lifecycle management technologies for networked manufacturing system. *Jisuanji Fuzhu Sheji Yu Tuxingxue Xuebao/Journal of Computer-Aided Design and Computer Graphics, 17*(11), 2518-2522.

Cheng, S., Liu, H., & Logan, B. E. (2006). Increased performance of single-chamber microbial fuel cells using an improved cathode structure. *Electrochemistry Communications, 8*(3), 489-494. doi:10.1016/j.elecom.2006.01.010

Cheng, S., & Logan, B. E. (2007). Ammonia treatment of carbon cloth anodes to enhance power generation of microbial fuel cells. *Electrochemistry Communications, 9*(3), 492-496. doi:10.1016/j.elecom.2006.10.023

Choi, Y.-J., Kim, N., Kim, S.-H., & Jung, S. (2003a). Dynamic Behaviors of Redox Mediators within the Hydrophobic Layers as an Important Factor for Effective Microbial Fuel Cell Operation. *Bulletin of the Korean Chemical Society, 24*, 437-440. doi:10.5012/bkcs.2003.24.4.437

Choi, Y., Jung, E., Kim, S., & Jung, S. (2003b). Membrane fluidity sensoring microbial fuel cell. *Bioelectrochemistry, 59*(1), 121-127. doi:10.1016/S1567-5394(03)00018-5

Choudhury, P., Ray, R. N., Bandyopadhyay, T. K., & Bhunia, B. (2020). Fed batch approach for stable generation of power from dairy wastewater using microbial fuel cell and its kinetic study. *Fuel, 266*, 117073. doi:10.1016/j.fuel.2020.117073

Ćirić-Marjanović, G. (2013). Recent advances in polyaniline composites with metals, metalloids and nonmetals. *Synthetic Metals, 170*, 31-56. doi:10.1016/j.synthmet.2013.02.028

Compton, O. C., & Nguyen, S. T. (2010). Graphene Oxide, Highly Reduced Graphene Oxide, and Graphene: Versatile Building Blocks for Carbon-Based Materials. *6*(6), 711-723. doi:10.1002/smll.200901934

Czaja, W., Krystynowicz, A., Bielecki, S., & Brown, R. M. (2006). Microbial cellulose—the natural power to heal wounds. *Biomaterials, 27*(2), 145-151. doi:10.1016/j.biomaterials.2005.07.035

Dai, L. (2004). Conducting Polymers. In *Intelligent Macromolecules for Smart Devices: From Materials Synthesis to Device Applications* (pp. 41-80). London: Springer London.

Dai, T., Jiang, X., Hua, S., Wang, X., & Lu, Y. (2008). Facile fabrication of conducting polymer hydrogels via supramolecular self-assembly. *Chemical Communications*(36), 4279-4281. doi:10.1039/B807116K

Davis, F., & Higson, S. P. J. (2007). Biofuel cells—Recent advances and applications. *Biosensors and Bioelectronics, 22*(7), 1224-1235. doi:10.1016/j.bios.2006.04.029

Dayal, M. S., Goswami, N., Sahai, A., Jain, V., Mathur, G., & Mathur, A. (2013). Effect of media components on cell growth and bacterial cellulose production from Acetobacter aceti MTCC 2623. *Carbohydrate Polymers, 94*(1), 12-16. doi:10.1016/j.carbpol.2013.01.018

Delaney, G., Bennetto, H., Mason, J., Roller, S., Stirling, J., & Thurston, C. (2008). Electron-transfer coupling in microbial fuel cells. 2. performance of fuel cells containing selected microorganism-mediator-substrate combinations. *Journal of Chemical Technology and Biotechnology. Biotechnology, 34*, 13-27. doi:10.1002/jctb.280340104

DeLong, E. F., & Chandler, P. (2002). Power from the deep. *Nature Biotechnology, 20*(8), 788-789. doi:10.1038/nbt0802-788

Dispenza, C., Leone, M., Presti, C. L., Librizzi, F., Spadaro, G., & Vetri, V. (2006). Optical properties of biocompatible polyaniline nano-composites. *Journal of Non-Crystalline Solids, 352*(36), 3835-3840. doi:10.1016/j.jnoncrysol.2006.06.017

Divya Priya, A., & Pydi Setty, Y. (2019). Cashew apple juice as substrate for microbial fuel cell. *Fuel, 246*, 75-78. doi:10.1016/j.fuel.2019.02.100

Dmytruk, K. V., Yatsyshyn, V. Y., Sybirna, N. O., Fedorovych, D. V., & Sibirny, A. A. (2011). Metabolic engineering and classic selection of the yeast Candida famata (Candida flareri) for construction of strains with enhanced riboflavin production. *Metabolic Engineering, 13*(1), 82-88. doi:10.1016/j.ymben.2010.10.005

Dou, P., Liu, Z., Cao, Z., Zheng, J., Wang, C., & Xu, X. (2016). Rapid synthesis of hierarchical nanostructured Polyaniline hydrogel for high power density energy storage application and three-dimensional multilayers printing. *Journal of Materials Science, 51*(9), 4274-4282. doi:10.1007/s10853-016-9727-8

Du, Z., Li, H., & Gu, T. (2007). A state of the art review on microbial fuel cells: A promising technology for wastewater treatment and bioenergy. *Biotechnology advances, 25*, 464-482. doi:10.1016/j.biotechadv.2007.05.004

Dumitru, A., & Scott, K. (2016). 4 - Anode materials for microbial fuel cells. In K. Scott & E. H. Yu (Eds.), *Microbial Electrochemical and Fuel Cells* (pp. 117-152). Boston: Woodhead Publishing.

Duraiarasan, S., Vijay, M., Sivaprakash, B., & Razack, S. (2015). Kinetic modeling of microalgal growth and lipid synthesis for biodiesel production. *3 Biotech, 5*. doi:10.1007/s13205-014-0264-3

Dutta, S., Bhunia, B., Raju, A., Maity, N., & Dey, A. (2019). Enhanced rapamycin production through kinetic and purification studies by mutant strain of Streptomyces hygroscopicus NTG-30-27. *Chemical Papers, 73*(8), 2053-2063. doi:10.1007/s11696-019-00767-0

El-Saied, H., Basta, A., & Gobran, R. (2004). Research Progress in Friendly Environmental Technology for the Production of Cellulose Products (Bacterial Cellulose and Its Application). *Polymer-plastics Technology and Engineering - POLYM-PLAST TECHNOL ENG, 43*, 797-820. doi:10.1081/PPT-120038065

Fan, L., & Xue, S. (2016). Overview on Electricigens for Microbial Fuel Cell. *The Open Biotechnology Journal, 10*, 398-406. doi:10.2174/1874070701610010398

Feng, X., Ullah, N., Wang, X., Sun, X., Li, C., Bai, Y., . . . Li, Z. (2015). Characterization of Bacterial Cellulose by Gluconacetobacter hansenii CGMCC 3917. *Journal of Food Science, 80*(10), E2217-E2227. doi:10.1111/1750-3841.13010

Fijałkowski, K., Peitler, D., Rakoczy, R., & Żywicka, A. (2015). Survival of probiotic lactic acid bacteria immobilized in different forms of bacterial cellulose in simulated gastric juices and bile salt solution. *LWT - Food Science and Technology, 68*. doi:10.1016/j.lwt.2015.12.038

Flimban, S., Ismail, I., Kim, T., & Oh, S.-E. (2019). Overview of Recent Advancements in the Microbial Fuel Cell from Fundamentals to Applications: Design, Major Elements, and Scalability. *Energies, 12*, 3390. doi:10.3390/en12173390

Fredrickson, J. K., Romine, M. F., Beliaev, A. S., Auchtung, J. M., Driscoll, M. E., Gardner, T. S., . . . Tiedje, J. M. (2008). Towards environmental systems biology of Shewanella. *Nature Reviews Microbiology, 6*(8), 592-603. doi:10.1038/nrmicro1947

Gaden, E. (2000). Fermentation Process Kinetics. *Journal of Biochemical and Microbiological Technology and Engineering, 1*, 413-429. doi:10.1002/jbmte.390010407

Gajda, I., Greenman, J., & Ieropoulos, I. A. (2018). Recent advancements in real-world microbial fuel cell applications. *Current Opinion in Electrochemistry, 11*, 78-83. doi:10.1016/j.coelec.2018.09.006

Gao, Z., Yang, W., Wang, J., Wang, B., Li, Z., Liu, Q., . . . Liu, L. (2013). A New Partially Reduced Graphene Oxide Nanosheet/Polyaniline Nanowafer Hybrid as Supercapacitor Electrode Material. *Energy & Fuels, 27*(1), 568-575. doi:10.1021/ef301795g

García-Angulo, V. A. (2017). Overlapping riboflavin supply pathways in bacteria. *Critical Reviews in Microbiology, 43*(2), 196-209. doi:10.1080/1040841X.2016.1192578

Genet, M., Stokes, A., Salin, F., Mickovski, S., Fourcaud, T., Dumail, J.-F., & Beek, R. (2007). The Influence of Cellulose Content on Tensile Strength in Tree Roots. *Plant and Soil, 278*(1/2), 3-11. doi:10.1007/978-1-4020-5593-5_1

Ghasemi, B., Yaghmaei, S., Ghaderi, S., Bayat, A., & Mardanpour, M. M. (2020). Effects of chemical, electrochemical, and electrospun deposition of polyaniline coatings on surface of anode electrodes for evaluation of MFCs' performance. *Journal of Environmental Chemical Engineering, 8*(5), 104039. doi:10.1016/j.jece.2020.104039

Ghasemi, M., Daud, W. R. W., Mokhtarian, N., Mayahi, A., Ismail, M., Anisi, F., . . . Alam, J. (2013). The effect of nitric acid, ethylenediamine, and diethanolamine modified polyaniline nanoparticles anode electrode in a microbial fuel cell. *International Journal of Hydrogen Energy, 38*(22), 9525-9532. doi:10.1016/j.ijhydene.2012.12.016

Ghassemi, Z., & Slaughter, G. (2017). Biological Fuel Cells and Membranes. *Membranes, 7*, 3. doi:10.3390/membranes7010003

Gibson, L. J. (2012). The hierarchical structure and mechanics of plant materials. *Journal of the Royal Society Interface, 9*(76), 2749-2766. doi:doi:10.1098/rsif.2012.0341

Gil, G.-C., Chang, I.-S., Kim, B. H., Kim, M., Jang, J.-K., Park, H. S., & Kim, H. J. (2003). Operational parameters affecting the performannce of a mediator-less microbial fuel cell. *Biosensors and Bioelectronics, 18*(4), 327-334. doi:10.1016/S0956-5663(02)00110-0

Gnana kumar, G., Kirubaharan, C. J., Udhayakumar, S., Karthikeyan, C., & Nahm, K. S. (2014). Conductive Polymer/Graphene Supported Platinum Nanoparticles as Anode Catalysts for the Extended Power Generation of Microbial Fuel Cells. *Industrial & Engineering Chemistry Research, 53*(43), 16883-16893. doi:10.1021/ie502399y

Gorby, Y. A., Yanina, S., McLean, J. S., Rosso, K. M., Moyles, D., Dohnalkova, A., . . . Fredrickson, J. K. (2006). Electrically conductive bacterial nanowires produced by Shewanella oneidensis strain MR-1 and other microorganisms. *Proceedings of the National Academy of Sciences of the United States of America, 103*(30), 11358-11363. doi:10.1073/pnas.0604517103

Grzebyk, M., & Poźniak, G. (2005). Microbial fuel cells (MFCs) with interpolymer cation exchange membranes. *Separation and Purification Technology, 41*(3), 321-328. doi:10.1016/j.seppur.2004.04.009

Guiseppi-Elie, A. (2010). Electroconductive hydrogels: Synthesis, characterization and biomedical applications. *Biomaterials, 31*(10), 2701-2716. doi:10.1016/j.biomaterials.2009.12.052

Gulrez, S., Al-Assaf, S., & Phillips, G. (2011). Hydrogels: Methods of Preparation, Characterisation and Applications. In (Vol. 51).

Guo, H., He, W., Lu, Y., & Zhang, X. (2015). Self-crosslinked polyaniline hydrogel electrodes for electrochemical energy storage. *Carbon, 92*, 133-141. doi:10.1016/j.carbon.2015.03.062

Habermann, W., & Pommer, E. H. (1991). Biological fuel cells with sulphide storage capacity. *Applied Microbiology and Biotechnology, 35*(1), 128-133. doi:10.1007/BF00180650

Hacker, M. C., & Nawaz, H. A. (2015). Multi-Functional Macromers for Hydrogel Design in Biomedical Engineering and Regenerative Medicine. *International Journal of Molecular Sciences, 16*(11), 27677-27706.

Han, J., Ding, Q., Mei, C., Wu, Q., Yue, Y., & Xu, X. (2019). An intrinsically self-healing and biocompatible electroconductive hydrogel based on nanostructured nanocellulose-polyaniline complexes embedded in a viscoelastic polymer network towards flexible conductors and electrodes. *Electrochimica Acta, 318*, 660-672. doi:10.1016/j.electacta.2019.06.132

Han, T. H., Parveen, N., Shim, J. H., Nguyen, A. T. N., Mahato, N., & Cho, M. H. (2018). Ternary Composite of Polyaniline Graphene and TiO2 as a Bifunctional Catalyst to Enhance the Performance of Both the Bioanode and Cathode of a Microbial Fuel Cell. *Industrial & Engineering Chemistry Research, 57*(19), 6705-6713. doi:10.1021/acs.iecr.7b05314

Harnisch, F., Warmbier, R., Schneider, R., & Schröder, U. (2009). Modeling the ion transfer and polarization of ion exchange membranes in bioelectrochemical systems. *Bioelectrochemistry, 75*(2), 136-141. doi:10.1016/j.bioelechem.2009.03.001

Hasan, K., Grattieri, M., Wang, T., Milton, R. D., & Minteer, S. D. (2017). Enhanced Bioelectrocatalysis of Shewanella oneidensis MR-1 by a Naphthoquinone Redox Polymer. *ACS Energy Letters, 2*(9), 1947-1951. doi:10.1021/acsenergylett.7b00585

He, L., Du, P., Chen, Y., Lu, H., Cheng, X., Chang, B., & Wang, Z. (2017). Advances in microbial fuel cells for wastewater treatment. *Renewable and Sustainable Energy Reviews, 71*, 388-403. doi:10.1016/j.rser.2016.12.069

He, M., Zheng, Y., & Du, Q. (2013a). Three-dimensional polypyrrole/MnO2 composite networks deposited on graphite felt as free-standing electrode for supercapacitors. *Materials Letters, 104*, 48-52. doi:10.1016/j.matlet.2013.04.008

He, W., & Benson, R. (2013b). 5 - Polymeric Biomaterials. In S. Ebnesajjad (Ed.), *Handbook of Biopolymers and Biodegradable Plastics* (pp. 87-107). Boston: William Andrew Publishing.

Holzman, D. C. (2005). Microbe power. *Environmental health perspectives, 113*(11), A754-A757. doi:10.1289/ehp.113-a754

Hu, R., Zhao, J., Jiang, R., & Zheng, J. (2017). Preparation of high strain polyaniline/polyvinyl alcohol composite and its applications in stretchable supercapacitor. *Journal of Materials Science: Materials in Electronics, 28*(19), 14568-14574. doi:10.1007/s10854-017-7320-9

Hu, Z. (2008). Electricity generation by a baffle-chamber membraneless microbial fuel cell. *Journal of Power Sources, 179*(1), 27-33. doi:10.1016/j.jpowsour.2007.12.094

Huang, H., Yao, J., Li, L., Zhu, F., Liu, Z., Zeng, X., . . . Huang, Z. (2016). Reinforced polyaniline/polyvinyl alcohol conducting hydrogel from a freezing–thawing method as self-supported electrode for supercapacitors. *Journal of Materials Science, 51*(18), 8728-8736. doi:10.1007/s10853-016-0137-8

Huang, L., Zeng, R. J., & Angelidaki, I. (2008). Electricity production from xylose using a mediator-less microbial fuel cell. *Bioresource Technology, 99*(10), 4178-4184. doi:10.1016/j.biortech.2007.08.067

Huggins, T., Wang, H., Kearns, J., Jenkins, P., & Ren, Z. J. (2014). Biochar as a sustainable electrode material for electricity production in microbial fuel cells. *Bioresource Technology, 157*, 114-119. doi:10.1016/j.biortech.2014.01.058

Hümbelin, M., Griesser, V., Keller, T., Schurter, W., Haiker, M., Hohmann, H. P., . . . van Loon, A. P. G. M. (1999). GTP cyclohydrolase II and 3,4-dihydroxy-2-butanone 4-phosphate synthase are rate-limiting enzymes in riboflavin synthesis of an industrial Bacillus subtilis strain used for riboflavin production. *Journal of Industrial Microbiology and Biotechnology, 22*(1), 1-7. doi:10.1038/sj.jim.2900590

Ieropoulos, I., Greenman, J., & Melhuish, C. (2003). Imitating Metabolism: Energy Autonomy in Biologically Inspired Robots. *Proceedings of the AISB '03*, 191-194.

Ieropoulos, I., Winfield, J., & Greenman, J. (2010). Effects of flow-rate, inoculum and time on the internal resistance of microbial fuel cells. *Bioresource Technology, 101*(10), 3520-3525. doi:10.1016/j.biortech.2009.12.108

Ieropoulos, I. A., Greenman, J., Melhuish, C., & Hart, J. (2005). Comparative study of three types of microbial fuel cell. *Enzyme and Microbial Technology, 37*(2), 238-245. doi:10.1016/j.enzmictec.2005.03.006

Iizawa, T., Taketa, H., Maruta, M., Ishido, T., Gotoh, T., & Sakohara, S. (2007). Synthesis of porous poly(N-isopropylacrylamide) gel beads by sedimentation polymerization and their morphology. *104*(2), 842-850. doi:10.1002/app.25605

Ikeda, T., & Kano, K. (2003). Bioelectrocatalysis-based application of quinoproteins and quinoprotein-containing bacterial cells in biosensors and biofuel cells. *Biochimica et Biophysica Acta (BBA) - Proteins and Proteomics, 1647*(1), 121-126. doi:10.1016/S1570-9639(03)00075-X

Ishii, S. i., Watanabe, K., Yabuki, S., Logan, B. E., & Sekiguchi, Y. (2008). Comparison of Electrode Reduction Activities of Geobacter sulfurreducens and an Enriched Consortium in an Air-Cathode Microbial Fuel Cell. *Applied and environmental microbiology, 74*(23), 7348-7355. doi:10.1128/AEM.01639-08

Jabłońska, A., & Pałys, B. (2017). Effect of the polymerization bath on structure and electrochemical properties of polyaniline-poly(styrene sulfonate) hydrogels. *Journal of Electroanalytical Chemistry, 784*, 115-123. doi:10.1016/j.jelechem.2016.11.050

Jahan, M. S., Saeed, A., He, Z., & Ni, Y. (2011). Jute as raw material for the preparation of microcrystalline cellulose. *Cellulose, 18*(2), 451-459. doi:10.1007/s10570-010-9481-z

Jayakumar, A., Yoon, Y.-J., Wang, R., & Lee, J.-M. (2015). Novel graphene/polyaniline/MnOx 3D-hydrogels obtained by controlled morphology of MnOx in the graphene/polyaniline matrix for high performance binder-free supercapacitor electrodes. *RSC Advances, 5*(114), 94388-94396. doi:10.1039/C5RA16884H

Jia, Y., Jiang, J., Sun, K., & Dai, T. (2012). Electrocatalytic performance of Pt supported on polyaniline-poly(styrene sulfonate) hydrogel. *Journal of Applied Polymer Science, 125*. doi:10.1002/app.36712

John, A., Palaniappan, S., Djurado, D., & Pron, A. (2008). One-step preparation of solution processable conducting polyaniline by inverted emulsion polymerization using didecyl ester of 4-sulfophthalic acid as multifunctional dopant. *Journal of Polymer Science Part A: Polymer Chemistry, 46*, 1051-1057. doi:10.1002/pola.22448

Junelles, A. M., Janati-Idrissi, R., Petitdemange, H., & Gay, R. (1988). Iron effect on acetone-butanol fermentation. *Current Microbiology, 17*(5), 299-303. doi:10.1007/BF01571332

Kaewnopparat, S., Sansernluk, K., & Faroongsarng, D. (2008). Behavior of Freezable Bound Water in the Bacterial Cellulose Produced by Acetobacter xylinum: An Approach

Using Thermoporosimetry. *AAPS PharmSciTech, 9*, 701-707. doi:10.1208/s12249-008-9104-2

Kalathil, S., Nguyen, V. H., Shim, J.-J., Khan, M. M., Lee, J., & Cho, M. H. (2013). Enhanced Performance of a Microbial Fuel Cell Using CNT/MnO2 Nanocomposite as a Bioanode Material. *Journal of Nanoscience and Nanotechnology*. doi:10.1166/jnn.2013.7832

Kalingan, A. E., & Krishnan, M. R. V. (1997). Application of agro-industrial by-products for riboflavin production by Eremothecium ashbyii NRRL 1363. *Applied Microbiology and Biotechnology, 47*(3), 226-230. doi:10.1007/s002530050917

Kamalesh, S., Tan, P., Wang, J., Lee, T., Kang, E. T., & Wang, C.-H. (2001). Biocompatibility of electroactive polymer in tissue. *Journal of biomedical materials research, 52*, 467-478. doi:10.1002/1097-4636(20001205)52:33.0.CO;2-6

Karthick, S., & Haribabu, K. (2020). Bioelectricity generation in a microbial fuel cell using polypyrrole-molybdenum oxide composite as an effective cathode catalyst. *Fuel, 275*, 117994. doi:10.1016/j.fuel.2020.117994

Karube, I., Matsunaga, T., Tsuru, S., & Suzuki, S. (1977). Biochemical fuel cell utilizing immobilized cells of clostridium butyricum. *Biotechnology and Bioengineering, 19*(11), 1727-1733. doi:10.1002/bit.260191112

Keshk, S., M A Razek, T., & Sameshima, K. (2006). Bacterial Cellulose Production from Beet Molasses. *African Journal of Biotechnology (ISSN: 1684-5315) Vol 5 Num 17, 5*. doi:10.4314/ajb.v5i17.43149

Khodamoradi, N., Babaeipour, V., & Sirousazar, M. (2019). Bacterial cellulose/montmorillonite bionanocomposites prepared by immersion and in-situ methods: structural, mechanical, thermal, swelling and dehydration properties. *Cellulose, 26*(13), 7847-7861. doi:10.1007/s10570-019-02666-9

Kim, B. H., Chang, I. S., Cheol Gil, G., Park, H. S., & Kim, H. J. (2003). Novel BOD (biological oxygen demand) sensor using mediator-less microbial fuel cell. *Biotechnology Letters, 25*(7), 541-545. doi:10.1023/A:1022891231369

Kim, B. H., Ikeda, T., Park, H. S., Kim, H. J., Hyun, M. S., Kano, K., . . . Tatsumi, H. (1999a). Electrochemical activity of an Fe(III)-reducing bacterium, Shewanella putrefaciens IR-1, in the presence of alternative electron acceptors. *Biotechnology Techniques, 13*(7), 475-478. doi:10.1023/A:1008993029309

Kim, B. H., Kim, H. J., Hyun, M. S., & Park, D. H. (1999b). Direct electrode reaction of Fe(III)-reducing bacterium, Shewanella putrefaciens. *Journal of Microbiology and Biotechnology, 9*(2), 127-131.

Kim, H.-W., Lee, K.-S., Razzaq, A., Lee, S. H., Grimes, C. A., & In, S.-I. (2018). Photocoupled Bioanode: A New Approach for Improved Microbial Fuel Cell Performance. *Energy Technology, 6*(2), 257-262. doi:10.1002/ente.201700177

Kim, H., Eun Song, J., Silva, C., & Kim, H. R. Production of conductive bacterial cellulose-polyaniline membranes in the presence of metal salts. *Textile Research Journal, 0*(0), 0040517519893717. doi:10.1177/0040517519893717

Kim, H. J., Hyun, M. S., Chang, I. S., & Kim, B. H. (1999c). A microbial fuel cell type lactate biosensor using a metal-reducing bacterium, Shewanella putrefaciens. *Journal of Microbiology and Biotechnology, 9*(3), 365-367.

Kim, H. J., Park, H. S., Hyun, M. S., Chang, I. S., Kim, M., & Kim, B. H. (2002). A mediator-less microbial fuel cell using a metal reducing bacterium, Shewanella putrefaciens. *Enzyme and Microbial Technology, 30*(2), 145-152. doi:10.1016/S0141-0229(01)00478-1

Kim, J. R., Min, B., & Logan, B. E. (2005). Evaluation of procedures to acclimate a microbial fuel cell for electricity production. *Applied Microbiology and Biotechnology, 68*(1), 23-30. doi:10.1007/s00253-004-1845-6

Kimura, S., Chen, H., Saxena, I., Brown, R., & Itoh, T. (2001). Localization of c-di-GMP-Binding Protein with the Linear Terminal Complexes of Acetobacter xylinum. *Journal of bacteriology, 183*, 5668-5674. doi:10.1128/JB.183.19.5668-5674.2001

Kis, K., & Bacher, A. (1995). Substrate Channeling in the Lumazine Synthase/Riboflavin Synthase Complex of Bacillus subtilis. *The Journal of biological chemistry, 270*, 16788-16795. doi:10.1074/jbc.270.28.16788

Klemm, D., Heublein, B., Fink, H.-P., & Bohn, A. (2005). Cellulose: Fascinating Biopolymer and Sustainable Raw Material. *Angewandte Chemie (International ed. in English), 44*, 3358-3393. doi:10.1002/anie.200460587

Koizumi, S., Yue, Z., Tomita, Y., Kondo, T., Iwase, H., Yamaguchi, D., & Hashimoto, T. (2008). Bacterium organizes hierarchical amorphous structure in microbial cellulose. *The European Physical Journal E, 26*(1), 137-142. doi:10.1140/epje/i2007-10259-3

Kojima, Y., Seto, A., Tonouchi, N., Tsuchida, T., & Yoshinaga, F. (1997). High Rate Production in Static Culture of Bacterial Cellulose from Sucrose by a Newly Isolated Acetobacter Strain. *Bioscience, Biotechnology, and Biochemistry, 61*(9), 1585-1586. doi:10.1271/bbb.61.1585

Kolonne, S., Seviour, R. J., & McDougall, B. M. (1994). Effect of pH on exocellular riboflavin production byEremothecium ashbyii. *Biotechnology Letters, 16*(1), 79-84. doi:10.1007/BF01022628

Kotloski, N. J., & Gralnick, J. A. (2013). Flavin Electron Shuttles Dominate Extracellular Electron Transfer by Shewanella oneidensis. *Mbio, 4*(1), e00553-00512. doi:10.1128/mBio.00553-12

Kumar, G., Hashmi, S., Karthikeyan, C., Ghavaminejad, A., Vatankhah-varnoosfaderani, M., & Stadler, F. (2014). Graphene Oxide/Carbon Nanotube Composite Hydrogels—Versatile Materials for Microbial Fuel Cell Applications. *Macromolecular Rapid Communications, 35*. doi:10.1002/marc.201400332

Kumar, R., Singh, L., Wahid, Z., & Md Din, M. F. (2015a). Exoelectrogens in microbial fuel cells toward bioelectricity generation: A review. *International Journal of Energy Research, 39*. doi:10.1002/er.3305

Kumar, R., Singh, L., & Wahid, Z. A. (2015b). Role of Microorganisms in Microbial Fuel Cells for Bioelectricity Production. In V. C. Kalia (Ed.), *Microbial Factories: Biofuels, Waste treatment: Volume 1* (pp. 135-154). New Delhi: Springer India.

Kumar, R., Singh, L., & Zularisam, A. W. (2016). Exoelectrogens: Recent advances in molecular drivers involved in extracellular electron transfer and strategies used to improve it for microbial fuel cell applications. *Renewable and Sustainable Energy Reviews, 56*, 1322-1336. doi:10.1016/j.rser.2015.12.029

Kumar, S. S., Kumar, V., Kumar, R., Malyan, S. K., & Pugazhendhi, A. (2019a). Microbial fuel cells as a sustainable platform technology for bioenergy, biosensing, environmental monitoring, and other low power device applications. *Fuel, 255*, 115682. doi:10.1016/j.fuel.2019.115682

Kumar, S. S., Kumar, V., Malyan, S. K., Sharma, J., Mathimani, T., Maskarenj, M. S., . . . Pugazhendhi, A. (2019b). Microbial fuel cells (MFCs) for bioelectrochemical treatment of different wastewater streams. *Fuel, 254*, 115526. doi:10.1016/j.fuel.2019.05.109

Lai, B., Tang, X., Li, H., Du, Z., Liu, X., & Zhang, Q. (2011). Power production enhancement with a polyaniline modified anode in microbial fuel cells. *Biosensors and Bioelectronics, 28*(1), 373-377. doi:10.1016/j.bios.2011.07.050

Lee, S. A., Choi, Y., Jung, S., & Kim, S. (2002). Effect of initial carbon sources on the electrochemical detection of glucose by Gluconobacter oxydans. *Bioelectrochemistry, 57*(2), 173-178. doi:10.1016/S1567-5394(02)00115-9

Lee, Y.-Y., Kang, H.-Y., Gwon, S. H., Choi, G. M., Lim, S.-M., Sun, J.-Y., & Joo, Y.-C. (2016a). A Strain-Insensitive Stretchable Electronic Conductor: PEDOT:PSS/Acrylamide Organogels. *Advanced materials, 28*(8), 1636-1643. doi:10.1002/adma.201504606

Lee, Y.-Y., Kang, H.-Y., Gwon, S. H., Choi, G. M., Lim, S.-M., Sun, J.-Y., & Joo, Y.-C. (2016b). A Strain-Insensitive Stretchable Electronic Conductor: PEDOT:PSS/Acrylamide Organogels. *28*(8), 1636-1643. doi:10.1002/adma.201504606

Lehmann, M., Degen, S., Hohmann, H.-P., Wyss, M., Bacher, A., & Schramek, N. (2009). Biosynthesis of riboflavin. Screening for an improved GTP cyclohydrolase II mutant. *The FEBS journal, 276*, 4119-4129.

Leong, J. X., Daud, W. R. W., Ghasemi, M., Liew, K. B., & Ismail, M. (2013). Ion exchange membranes as separators in microbial fuel cells for bioenergy conversion: A comprehensive review. *Renewable and Sustainable Energy Reviews, 28*, 575-587. doi:10.1016/j.rser.2013.08.052

Leu, H.-J., Lin, C.-Y., Chang, F.-C., & Tsai, M.-J. (2016). Fe3O4-modified carbon cloth electrode for microbial fuel cells from organic wastewaters. *Desalination and Water Treatment, 57*(60), 29371-29376. doi:10.1080/19443994.2016.1202867

Levine, H., Oyaas, J. E., Wasserman, L., Hoogerheide, J. C., & Stern, R. M. (1949). Riboflavin Production by Candida Yeasts. *Industrial & Engineering Chemistry, 41*(8), 1665-1668. doi:10.1021/ie50476a034

Li, C., Ding, L., Cui, H., Zhang, L., Xu, K., & Ren, H. (2012). Application of conductive polymers in biocathode of microbial fuel cells and microbial community. *Bioresource Technology, 116*, 459-465. doi:10.1016/j.biortech.2012.03.115

Li, C., Zhang, L., Ding, L., Ren, H., & Cui, H. (2011). Effect of conductive polymers coated anode on the performance of microbial fuel cells (MFCs) and its biodiversity analysis. *Biosensors and Bioelectronics, 26*(10), 4169-4176. doi:10.1016/j.bios.2011.04.018

Li, F., Li, Y.-X., Cao, Y.-X., Wang, L., Liu, C.-G., Shi, L., & Song, H. (2018). Modular engineering to increase intracellular NAD(H/+) promotes rate of extracellular electron transfer of Shewanella oneidensis. *Nature Communications, 9*. doi:10.1038/s41467-018-05995-8

Li, L., Ge, J., Guo, B., & Ma, P. X. (2014a). In situ forming biodegradable electroactive hydrogels. *Polymer Chemistry, 5*(8), 2880-2890. doi:10.1039/C3PY01634J

Li, M., Guo, Y., Wei, Y., MacDiarmid, A. G., & Lelkes, P. I. (2006). Electrospinning polyaniline-contained gelatin nanofibers for tissue engineering applications. *Biomaterials, 27*(13), 2705-2715. doi:10.1016/j.biomaterials.2005.11.037

Li, P., Yang, Y., Shi, E., Shen, Q., Shang, Y., Wu, S., . . . Wu, D. (2014b). Core-Double-Shell, Carbon Nanotube-Polypyrrole-MnO2 Sponge as Freestanding, Compressible Supercapacitor Electrode. *ACS Applied Materials & Interfaces, 6*(7), 5228-5234. doi:10.1021/am500579c

Li, S.-W., Zeng, R., & Sheng, G.-P. (2016). An excellent anaerobic respiration mode for chitin degradation by Shewanella oneidensis MR-1 in microbial fuel cells. *Biochemical Engineering Journal, 118*. doi:10.1016/j.bej.2016.11.010

Li, Z., Wang, L., Hua, J., Jia, S., Zhang, J., & Liu, H. (2015). Production of nano bacterial cellulose from waste water of candied jujube-processing industry using Acetobacter xylinum. *Carbohydrate Polymers, 120*, 115-119. doi:10.1016/j.carbpol.2014.11.061

Liang, P., Wang, H., Xia, X., Huang, X., Mo, Y., Cao, X., & Fan, M. (2011). Carbon nanotube powders as electrode modifier to enhance the activity of anodic biofilm in microbial fuel cells. *Biosensors and Bioelectronics, 26*(6), 3000-3004. doi:10.1016/j.bios.2010.12.002

Lim, S., Choi, J., & Park, E. (2001). Microbial Production of Riboflavin Using Riboflavin Overproducers, Ashbya gossypii, Bacillus subtilis, and Candida famate: An Overview. *Biotechnology Bioprocess Engineering, 6*, 75-88. doi:10.1007/BF02931951

Lin, C.-W., Wu, C.-H., Chiu, Y.-H., & Tsai, S.-L. (2014a). Effects of different mediators on electricity generation and microbial structure of a toluene powered microbial fuel cell. *Fuel, 125*, 30-35. doi:10.1016/j.fuel.2014.02.018

Lin, D., Lopez-Sanchez, P., Li, R., & Li, Z. (2014b). Production of bacterial cellulose by Gluconacetobacter hansenii CGMCC 3917 using only waste beer yeast as nutrient source. *Bioresource Technology, 151*, 113-119. doi:10.1016/j.biortech.2013.10.052

Liu, H., Cheng, S., & Logan, B. (2005a). Production of Electricity from Acetate or Butyrate Using a Single-Chamber Microbial Fuel Cell. *Environmental Science & Technology, 39*, 658-662. doi:10.1021/es048927c

Liu, H., Grot, S., & Logan, B. E. (2005b). Electrochemically Assisted Microbial Production of Hydrogen from Acetate. *Environmental Science & Technology, 39*(11), 4317-4320. doi:10.1021/es050244p

Liu, H., & Logan, B. (2004a). Electricity Generation Using an Air-Cathode Single Chamber Microbial Fuel Cell in the Presence and Absence of a Proton Exchange Membrane. *Environmental Science & Technology, 38*, 4040-4046. doi:10.1021/es0499344

Liu, H., Ramnarayanan, R., & Logan, B. E. (2004b). Production of Electricity during Wastewater Treatment Using a Single Chamber Microbial Fuel Cell. *Environmental Science & Technology, 38*(7), 2281-2285. doi:10.1021/es034923g

Liu, Q., Bai, Z., Fan, J., Sun, Z., Mi, H., Zhang, Q., & Qiu, J. (2018). A hydrogel-mediated scalable strategy toward core-shell polyaniline/poly(acrylic acid)-modified carbon nanotube hybrids as efficient electrodes for supercapacitor applications. *Applied Surface Science, 436*, 189-197. doi:10.1016/j.apsusc.2017.11.209

Liu, Z.-D., Lian, J., Du, Z.-W., & Li, H.-R. (2006). Construction of Sugar-based Microbial Fuel Cells by Dissimilatory Metal Reduction Bacteria. *Chinese Journal of Biotechnology, 22*(1), 131-137. doi:10.1016/S1872-2075(06)60010-1

Logan, B., Cheng, S., Watson, V., & Estadt, G. (2007). Graphite Fiber Brush Anodes for Increased Power Production in Air-Cathode Microbial Fuel Cells. *Environmental Science & Technology, 41*, 3341-3346. doi:10.1021/es062644y

Logan, B. E. (2004). Peer Reviewed: Extracting Hydrogen and Electricity from Renewable Resources. *Environmental Science & Technology, 38*(9), 160A-167A. doi:10.1021/es040468s

Logan, B. E. (2007a). Architecture. In *Microbial Fuel Cells* (pp. 85-110): John Wiley & Sons.

Logan, B. E. (2007b). Introduction. In *Microbial Fuel Cells* (pp. 1-11): John Wiley & Sons.

Logan, B. E. (2007c). Materials. In *Microbial Fuel Cells* (pp. 61-84): John Wiley & Sons.

Logan, B. E. (2007d). Power Generation. In *Microbial Fuel Cells* (pp. 44-60): John Wiley & Sons.

Logan, B. E., Hamelers, B., Rozendal, R., Schröder, U., Keller, J., Freguia, S., . . . Rabaey, K. (2006a). Microbial fuel cells: Methodology and technology. *Environmental Science and Technology, 40*(17), 5181-5192. doi:10.1021/es0605016

Logan, B. E., Hamelers, B., Rozendal, R., Schröder, U., Keller, J., Freguia, S., . . . Rabaey, K. (2006b). Microbial Fuel Cells: Methodology and Technology. *Environmental Science & Technology, 40*(17), 5181-5192. doi:10.1021/es0605016

Long, X., Wang, H., Wang, C., Cao, X., & Li, X. (2019). Enhancement of azo dye degradation and power generation in a photoelectrocatalytic microbial fuel cell by simple cathodic reduction on titania nanotube arrays electrode. *Journal of Power Sources, 415*, 145-153. doi:10.1016/j.jpowsour.2019.01.069

Lovley, D. R. (2006). Microbial fuel cells: novel microbial physiologies and engineering approaches. *Current Opinion in Biotechnology, 17*(3), 327-332. doi:10.1016/j.copbio.2006.04.006

Lovley, D. R. (2008). The microbe electric: conversion of organic matter to electricity. *Current Opinion in Biotechnology, 19*(6), 564-571. doi:10.1016/j.copbio.2008.10.005

Luo, H., Yu, S., Liu, G., Zhang, R., & Teng, W. (2016). Effect of in-situ immobilized anode on performance of the microbial fuel cell with high concentration of sodium acetate. *Fuel, 182*, 732-739. doi:10.1016/j.fuel.2016.06.032

Lv, P., Feng, Q., Wang, Q., Li, D., Zhou, J., & Wei, Q. (2016). Preparation of bacterial cellulose/carbon nanotube nanocomposite for biological fuel cell. *Fibers and Polymers, 17*, 1858-1865. doi:10.1007/s12221-016-6337-7

Lynd, L. R., Weimer, P. J., van Zyl, W. H., & Pretorius, I. S. (2002). Microbial Cellulose Utilization: Fundamentals and Biotechnology. *Microbiology and Molecular Biology Reviews, 66*(3), 506-577. doi:10.1128/MMBR.66.3.506-577.2002

Mal, P., Dutta, K., Bandyopadhyay, D., Basu, A., Khan, R., & Bishayi, B. (2013). Azithromycin in combination with riboflavin decreases the severity of Staphylococcus aureus infection induced septic arthritis by modulating the production of free radicals and endogenous cytokines. *Inflammation Research, 62*(3), 259-273. doi:10.1007/s00011-012-0574-z

Manoukian, O., Sardashti, N., Stedman, T., Gailiunas, K., Ojha, A., Penalosa, A., . . . Kumbar, S. (2018). Biomaterials for Tissue Engineering and Regenerative Medicine. In.

Manoukian, O. S., Sardashti, N., Stedman, T., Gailiunas, K., Ojha, A., Penalosa, A., . . . Kumbar, S. G. (2019). Biomaterials for Tissue Engineering and Regenerative Medicine. In R. Narayan (Ed.), *Encyclopedia of Biomedical Engineering* (pp. 462-482). Oxford: Elsevier.

Maolin, Z., Jun, L., Min, Y., & Hongfei, H. (2000). The swelling behavior of radiation prepared semi-interpenetrating polymer networks composed of polyNIPAAm and hydrophilic polymers. *Radiation Physics and Chemistry, 58*(4), 397-400. doi:10.1016/S0969-806X(99)00491-0

Mardiana, U., Innocent, C., Cretin, M., Buchari, Setiyanto, H., Nurpalah, R., & Kusmiati, M. (2019). Applicability of Alginate Film Entrapped Yeast for Microbial Fuel Cell. *Russian Journal of Electrochemistry, 55*(2), 78-87. doi:10.1134/S1023193519010075

Marsili, E., Baron, D. B., Shikhare, I. D., Coursolle, D., Gralnick, J. A., & Bond, D. R. (2008). Shewanella secretes flavins that mediate extracellular electron transfer. *Proceedings of the National Academy of Sciences of the United States of America, 105*(10), 3968-3973. doi:10.1073/pnas.0710525105

Martínez, M. V., Bongiovanni Abel, S., Rivero, R., Miras, M. C., Rivarola, C. R., & Barbero, C. A. (2015). Polymeric nanocomposites made of a conductive polymer and a thermosensitive hydrogel: Strong effect of the preparation procedure on the properties. *Polymer, 78*, 94-103. doi:10.1016/j.polymer.2015.09.054

Mashkour, M., Rahimnejad, M., & Mashkour, M. (2016). Bacterial cellulose-polyaniline nano-biocomposite: A porous media hydrogel bioanode enhancing the performance of microbial fuel cell. *Journal of Power Sources, 325*, 322-328. doi:10.1016/j.jpowsour.2016.06.063

Mashkour, M., Rahimnejad, M., Mashkour, M., Bakeri, G., Luque, R., & Oh, S.-E. (2017). Application of Wet Nanostructured Bacterial Cellulose as a Novel Hydrogel Bioanode for Microbial Fuel Cells. *4*(3), 648-654. doi:10.1002/celc.201600868

Massey, V. (2000). The Chemical and Biological Versatility of Riboflavin. *Biochemical Society transactions, 28*, 283-296. doi:10.1042/0300-5127:0280283

Mawad, D., Lauto, A., & Wallace, G. G. (2016). Conductive Polymer Hydrogels. In S. Kalia (Ed.), *Polymeric Hydrogels as Smart Biomaterials* (pp. 19-44). Cham: Springer International Publishing.

Mehdina, A., Dejaloud, M., & Jabbari, A. (2013). Nanostructured polyaniline-coated anode for improving microbial fuel cell power output. *Chemical Papers- Slovak Academy of Sciences, 67*. doi:10.2478/s11696-013-0381-1

Menicucci, J., Beyenal, H., Marsili, E., Veluchamy, Demir, G., & Lewandowski, Z. (2006). Procedure for Determining Maximum Sustainable Power Generated by Microbial Fuel Cells. *Environmental Science & Technology, 40*(3), 1062-1068. doi:10.1021/es051180l

Min, B., Cheng, S., & Logan, B. E. (2005a). Electricity generation using membrane and salt bridge microbial fuel cells. *Water Research, 39*(9), 1675-1686. doi:10.1016/j.watres.2005.02.002

Min, B., Kim, J., Oh, S., Regan, J. M., & Logan, B. E. (2005b). Electricity generation from swine wastewater using microbial fuel cells. *Water Research, 39*(20), 4961-4968. doi:10.1016/j.watres.2005.09.039

Moon, H., Chang, I. S., Jang, J. K., & Kim, B. H. (2005). Residence time distribution in microbial fuel cell and its influence on COD removal with electricity generation. *Biochemical Engineering Journal, 27*(1), 59-65. doi:10.1016/j.bej.2005.02.010

Mullai, P., Rene, E., & Kothandapani, S. (2013). Biohydrogen Production and Kinetic Modeling Using Sediment Microorganisms of Pichavaram Mangroves, India. *BioMed Research International, 2013*, 265618. doi:10.1155/2013/265618

Müller, D., Mandelli, J., Marins, J., Soares, B., Porto, L., Rambo, C., & Barra, G. (2012). Electrically conducting nanocomposites: Preparation and properties of polyaniline (PAni)-coated bacterial cellulose nanofibers (BC). *Cellulose, 19*. doi:10.1007/s10570-012-9754-9

Naina Mohamed, S., Thomas, N., Tamilmani, J., Boobalan, T., Matheswaran, M., Kalaichelvi, P., . . . Pugazhendhi, A. (2020). Bioelectricity generation using iron(II) molybdate nanocatalyst coated anode during treatment of sugar wastewater in microbial fuel cell. *Fuel, 277*, 118119. doi:10.1016/j.fuel.2020.118119

Najafpour, G. (2015). Chapter 8 - Microbial Fuel Cells - A New Source of Power. In *Biochemical Engineering and Biotechnology* (pp. 527-555): Elsevier Science.

Najafpour, G., Rahimnejad, M., & Ghoreyshi, A. A. (2011). The Enhancement of a Microbial Fuel Cell for Electrical Output Using Mediators and Oxidizing Agents. *Energy Sources Part A Recovery Utilization and Environmental Effects, 33*. doi:10.1080/15567036.2010.518223

News. (2007). Project to turn beer wastewater into power. *Fuel Cells Bulletin, 2007*(7), 11. doi:10.1016/S1464-2859(07)70297-3

Nguyen, V. T., Gidley, M. J., & Dykes, G. A. (2008). Potential of a nisin-containing bacterial cellulose film to inhibit Listeria monocytogenes on processed meats. *Food Microbiology, 25*(3), 471-478. doi:10.1016/j.fm.2008.01.004

Nien, P.-C., Lee, C.-Y., Ho, K.-C., Adav, S. S., Liu, L., Wang, A., . . . Lee, D.-J. (2011). Power overshoot in two-chambered microbial fuel cell (MFC). *Bioresource Technology, 102*(7), 4742-4746. doi:10.1016/j.biortech.2010.12.015

Nishi, Y., Uryu, M., Yamanaka, S., Watanabe, K., Kitamura, N., Iguchi, M., & Mitsuhashi, S. (1990). The structure and mechanical properties of sheets prepared from bacterial cellulose. *Journal of Materials Science, 25*(6), 2997-3001. doi:10.1007/BF00584917

O'Connell, M. J., Boul, P., Ericson, L. M., Huffman, C., Wang, Y., Haroz, E., . . . Smalley, R. E. (2001). Reversible water-solubilization of single-walled carbon nanotubes by polymer wrapping. *Chemical Physics Letters, 342*(3), 265-271. doi:10.1016/S0009-2614(01)00490-0

O'Connor, T. F., Rajan, K. M., Printz, A. D., & Lipomi, D. J. (2015). Toward organic electronics with properties inspired by biological tissue. *Journal of Materials Chemistry B, 3*(25), 4947-4952. doi:10.1039/C5TB00173K

Oh, H. S., Jeong, H. M., Park, J. H., Ock, I.-W., & Kang, J. K. (2015). Hierarchical Si hydrogel architecture with conductive polyaniline channels on sulfonated-graphene for high-performance Li ion battery anodes having a robust cycle life. *Journal of Materials Chemistry A, 3*(19), 10238-10242. doi:10.1039/C5TA01825K

Oh, S., & Logan, B. E. (2005). Hydrogen and electricity production from a food processing wastewater using fermentation and microbial fuel cell technologies. *Water Research, 39*(19), 4673-4682. doi:10.1016/j.watres.2005.09.019

Oh, S., Min, B., & Logan, B. E. (2004). Cathode performance as a factor in electricity generation in microbial fuel cells. *Environmental Science and Technology, 38*(18), 4900-4904. doi:10.1021/es049422p

Okamoto, A., Hashimoto, K., & Nakamura, R. (2012). Long-range electron conduction of Shewanella biofilms mediated by outer membrane C-type cytochromes. *Bioelectrochemistry, 85*, 61-65. doi:10.1016/j.bioelechem.2011.12.003

Oliot, M., Galier, S., Roux de Balmann, H., & Bergel, A. (2016). Ion transport in microbial fuel cells: Key roles, theory and critical review. *Applied Energy, 183*, 1682-1704. doi:10.1016/j.apenergy.2016.09.043

Oliveira, V. B., Simões, M., Melo, L. F., & Pinto, A. M. F. R. (2013). Overview on the developments of microbial fuel cells. *Biochemical Engineering Journal, 73*, 53-64. doi:10.1016/j.bej.2013.01.012

Oueiny, C., Berlioz, S., & Perrin, F.-X. (2014). Carbon nanotube–polyaniline composites. *Progress in Polymer Science, 39*(4), 707-748. doi:10.1016/j.progpolymsci.2013.08.009

Palanisamy, G., Jung, H.-Y., Sadhasivam, T., Kurkuri, M. D., Kim, S. C., & Roh, S.-H. (2019). A comprehensive review on microbial fuel cell technologies: Processes, utilization, and advanced developments in electrodes and membranes. *Journal of Cleaner Production, 221*, 598-621. doi:10.1016/j.jclepro.2019.02.172

Pandit, S., Khilari, S., Roy, S., Pradhan, D., & Das, D. (2014). Improvement of power generation using Shewanella putrefaciens mediated bioanode in a single chambered microbial fuel cell: Effect of different anodic operating conditions. *Bioresource Technology, 166*, 451-457. doi:10.1016/j.biortech.2014.05.075

Park, D., & Zeikus, J. (2002). Impact of electrode composition on electricity generation in a single-compartment fuel cell using Shewanella putrefaciens. *Applied Microbiology and Biotechnology, 59*(1), 58-61. doi:10.1007/s00253-002-0972-1

Park, D. H., Kim, B. H., Moore, B., Hill, H. A. O., Song, M. K., & Rhee, H. W. (1997). Electrode reaction of Desulfovibrio desulfuricans modified with organic conductive compounds. *Biotechnology Techniques, 11*(3), 145-148. doi:10.1023/A:1018441127733

Park, D. H., Laivenieks, M., Guettler, M. V., Jain, M. K., & Zeikus, J. G. (1999a). Microbial utilization of electrically reduced neutral red as the sole electron donor for growth and

metabolite production. *Applied and environmental microbiology, 65*(7), 2912-2917. doi:10.1128/AEM.65.7.2912-2917.1999

Park, D. H., & Zeikus, J. (2003). Improved Fuel Cell and Electrode Designs for Producing Electricity from Microbial Degradation. *Biotechnology and Bioengineering, 81*, 348-355. doi:10.1002/bit.10501

Park, D. H., & Zeikus, J. G. (1999b). Utilization of electrically reduced neutral red by Actinobacillus succinogenes: physiological function of neutral red in membrane-driven fumarate reduction and energy conservation. *Journal of bacteriology, 181*(8), 2403-2410.

Park, D. H., & Zeikus, J. G. (2000). Electricity Generation in Microbial Fuel Cells Using Neutral Red as an Electronophore. *Applied and environmental microbiology, 66*(4), 1292-1297. doi:10.1128/AEM.66.4.1292-1297.2000

Park, H. S., Kim, B. H., Kim, H. S., Kim, H. J., Kim, G. T., Kim, M., . . . Chang, H. I. (2001). A Novel Electrochemically Active and Fe(III)-reducing Bacterium Phylogenetically Related to Clostridium butyricum Isolated from a Microbial Fuel Cell. *Anaerobe, 7*(6), 297-306. doi:10.1006/anae.2001.0399

Park, I. H., Christy, M., Kim, P., & Nahm, K. S. (2014). Enhanced electrical contact of microbes using Fe3O4/CNT nanocomposite anode in mediator-less microbial fuel cell. *Biosensors and Bioelectronics, 58*, 75-80. doi:10.1016/j.bios.2014.02.044

Park, J. K., Jung, J. Y., & Khan, T. (2009). 26 - Bacterial cellulose. In G. O. Phillips & P. A. Williams (Eds.), *Handbook of Hydrocolloids (Second Edition)* (pp. 724-739): Woodhead Publishing.

Park, S., Baker, J. O., Himmel, M. E., Parilla, P. A., & Johnson, D. K. (2010). Cellulose crystallinity index: measurement techniques and their impact on interpreting cellulase performance. *Biotechnology for Biofuels, 3*(1), 10. doi:10.1186/1754-6834-3-10

Peng, X., Yu, H., Yu, H., & Wang, X. (2013). Lack of anodic capacitance causes power overshoot in microbial fuel cells. *Bioresource Technology, 138*, 353-358. doi:10.1016/j.biortech.2013.03.187

Peppas, N. A., Bures, P., Leobandung, W., & Ichikawa, H. (2000). Hydrogels in pharmaceutical formulations. *European Journal of Pharmaceutics and Biopharmaceutics, 50*(1), 27-46. doi:10.1016/S0939-6411(00)00090-4

Peters, J. W. (1998). X-ray crystal structure of the Fe-only hydrogenase (Cpl) from Clostridium pasteurianum to 1.8 angstrom resolution. *Science, 282*(5395), 1853-1858.

Petrov, P., Mokreva, P., Kostov, I., Uzunova, V., & Tzoneva, R. (2016). Novel electrically conducting 2-hydroxyethylcellulose/polyaniline nanocomposite cryogels: Synthesis and application in tissue engineering. *Carbohydrate Polymers, 140*, 349-355. doi:10.1016/j.carbpol.2015.12.069

Pham, C. A., Jung, S. J., Phung, N. T., Lee, J., Chang, I. S., Kim, B. H., . . . Chun, J. (2003). A novel electrochemically active and Fe(III)-reducing bacterium phylogenetically related to Aeromonas hydrophila, isolated from a microbial fuel cell. *FEMS Microbiology Letters, 223*(1), 129-134. doi:10.1016/s0378-1097(03)00354-9

Pourramezan, Z., Roayaei, A., & Ghezelbash, G. (2009). Optimization of Culture Conditions for Bacterial Cellulose Production by Acetobacter sp. 4B-2. *Biotechnology, 8*, 151-154. doi:10.3923/biotech.2009.150.154

Prestigiacomo, C., Fernandez-Marchante, C. M., Fernández-Morales, F. J., Cañizares, P., Scialdone, O., & Rodrigo, M. A. (2016). New prototypes for the isolation of the anodic chambers in microbial fuel cells. *Fuel, 181*, 704-710. doi:10.1016/j.fuel.2016.04.122

Puig, S., Serra, M., Coma, M., Cabré, M., Dolors Balaguer, M., & Colprim, J. (2011). Microbial fuel cell application in landfill leachate treatment. *Journal of Hazardous Materials, 185*(2), 763-767. doi:10.1016/j.jhazmat.2010.09.086

Pyarasani, R. D., Jayaramudu, T., & John, A. (2019). Polyaniline-based conducting hydrogels. *Journal of Materials Science, 54*(2), 974-996. doi:10.1007/s10853-018-2977-x

Qiao, Y., Li, C. M., Bao, S.-J., & Bao, Q.-L. (2007). Carbon nanotube/polyaniline composite as anode material for microbial fuel cells. *Journal of Power Sources, 170*(1), 79-84. doi:10.1016/j.jpowsour.2007.03.048

Rabaey, K., Boon, N., Höfte, M., & Verstraete, W. (2005a). Microbial Phenazine Production Enhances Electron Transfer in Biofuel Cells. *Environmental Science & Technology, 39*(9), 3401-3408. doi:10.1021/es048563o

Rabaey, K., Boon, N., Siciliano, S. D., Verhaege, M., & Verstraete, W. (2004). Biofuel cells select for microbial consortia that self-mediate electron transfer. *Applied and environmental microbiology, 70*(9), 5373-5382. doi:10.1128/AEM.70.9.5373-5382.2004

Rabaey, K., Clauwaert, P., Aelterman, P., & Verstraete, W. (2005b). Tubular Microbial Fuel Cells for Efficient Electricity Generation. *Environmental Science & Technology, 39*, 8077-8082. doi:10.1021/es050986i

Rabaey, K., Lissens, G., Siciliano, S., & Verstraete, W. (2003). A microbial fuel cell capable of converting glucose to electricity at high rate and efficiency. *Biotechnology Letters, 25*, 1531-1535. doi:10.1023/A:1025484009367

Rabaey, K., Van de Sompel, K., Maignien, L., Boon, N., Aelterman, P., Clauwaert, P., . . . Verstraete, W. (2006). Microbial Fuel Cells for Sulfide Removal. *Environmental Science & Technology, 40*(17), 5218-5224. doi:10.1021/es060382u

Rabaey, K., & Verstraete, W. (2005c). Microbial fuel cells: novel biotechnology for energy generation. *Trends in Biotechnology, 23*(6), 291-298. doi:10.1016/j.tibtech.2005.04.008

Rahimnejad, M., Adhami, A., Darvari, S., Zirepour, A., & Oh, S.-E. (2015). Microbial fuel cell as new technology for bioelectricity generation: A review. *Alexandria Engineering Journal, 54*(3), 745-756. doi:10.1016/j.aej.2015.03.031

Rahimnejad, M., Ghasemi, M., Najafpour, G. D., Ismail, M., Mohammad, A. W., Ghoreyshi, A. A., & Hassan, S. H. A. (2012). Synthesis, characterization and application studies of self-made Fe3O4/PES nanocomposite membranes in microbial fuel cell. *Electrochimica Acta, 85*, 700-706. doi:10.1016/j.electacta.2011.08.036

Rani, M. U., & Appaiah, A. (2011). Optimization of culture conditions for bacterial cellulose production from Gluconacetobacter hansenii UAC09. *Annals of Microbiology, 61*(4), 781-787. doi:10.1007/s13213-011-0196-7

Rebelo, A., Archer, A., Chen, X., Liu, C., Yang, G., & Liu, Y. (2018). Dehydration of bacterial cellulose and the water content effects on its viscoelastic and electrochemical properties. *Science and Technology of Advanced Materials, 19*, 203-211. doi:10.1080/14686996.2018.1430981

Reguera, G., Nevin, K. P., Nicoll, J. S., Covalla, S. F., Woodard, T. L., & Lovley, D. R. (2006). Biofilm and nanowire production leads to increased current in Geobacter sulfurreducens fuel cells. *Applied and environmental microbiology, 72*(11), 7345-7348. doi:10.1128/AEM.01444-06

Revin, V., Liyaskina, E., Nazarkina, M., Bogatyreva, A., & Shchankin, M. (2018). Cost-effective production of bacterial cellulose using acidic food industry by-products. *Brazilian Journal of Microbiology, 49*, 151-159. doi:10.1016/j.bjm.2017.12.012

Rezaee, A., Godini, H., & Bakhtou, H. (2008). Microbial cellulose as support material for the immobilization of denitrifying bacteria. *Environmental Engineering and Management Journal, 7*. doi:10.30638/eemj.2008.082

Rhoads, A., Beyenal, H., & Lewandowski, Z. (2005). Microbial Fuel Cell using Anaerobic Respiration as an Anodic Reaction and Biomineralized Manganese as a Cathodic Reactant. *Environmental Science & Technology, 39*(12), 4666-4671. doi:10.1021/es048386r

Ringeisen, B., Henderson, E., Wu, P., Pietron, J., Ray, R., Little, B., . . . Jones-Meehan, J. (2006). High Power Density From a Miniature Microbial Fuel Cell Using Shewanella oneidensis DSP10. *Environmental Science & Technology, 40*, 2629-2634. doi:10.1021/es052254w

Rosenbaum, M., Schröder, U., & Scholz, F. (2006). Investigation of the electrocatalytic oxidation of formate and ethanol at platinum black under microbial fuel cell conditions. *Journal of Solid State Electrochemistry, 10*, 872-878. doi:10.1007/s10008-006-0167-2

Rosenbaum, M., Zhao, F., Quaas, M., Wulff, H., Schröder, U., & Scholz, F. (2007). Evaluation of catalytic properties of tungsten carbide for the anode of microbial fuel cells. *Applied Catalysis B: Environmental, 74*(3), 261-269. doi:10.1016/j.apcatb.2007.02.013

Rozendal, R. A., Sleutels, T., Hamelers, H. V. M., & Buisman, C. (2008). Effect of the type of ion exchange membrane on performance, ion transport, and pH in biocatalyzed electrolysis of wastewater. *Water science and technology : a journal of the International Association on Water Pollution Research, 57*, 1757-1762. doi:10.2166/wst.2008.043

Sabry, S., Ghanem, k., & Ghozlan, H. (1994). Riboflavin production by Aspergillus terreus from beet molasses. *Microbiología (Madrid, Spain), 9*, 118-124.

Sauer, U., Hatzimanikatis, V., Hohmann, H.-P., Manneberg, M., Loon, A., & Bailey, J. (1996). Physiology and metabolic fluxes of wild-type and riboflavin-producing Bacillus subtilis. *Applied and environmental microbiology, 62*. doi:10.1128/AEM.62.10.3687-3696.1996

Schröder, U. (2007). Anodic electron transfer mechanisms in microbial fuel cells and their energy efficiency. *Physical Chemistry Chemical Physics, 9*(21), 2619-2629. doi:10.1039/b703627m

Schröder, U., Nießen, J., & Scholz, F. (2003). A generation of microbial fuel cells with current outputs boosted by more than one order of magnitude. *Angewandte Chemie - International Edition, 42*(25), 2880-2883. doi:10.1002/anie.200350918

Seviour, R., & McDougall, B. (1994). Effect of pH on exocellular riboflavin production by Eremothecium ashbyii. *Biotechnology Letters - BIOTECHNOL LETT, 16*, 79-84. doi:10.1007/BF01022628

Sharma, K., Kaith, B. S., Kumar, V., Kalia, S., Kumar, V., & Swart, H. C. (2014). Water retention and dye adsorption behavior of Gg-cl-poly(acrylic acid-aniline) based conductive hydrogels. *Geoderma, 232-234*, 45-55. doi:10.1016/j.geoderma.2014.04.035

Sharma, K., Kumar, V., Kaith, B. S., Kalia, S., & Swart, H. (2016). Conducting Polymer Hydrogels and Their Applications. In.

Shi, Z., Li, Y., Chen, X., Han, H., & Yang, G. (2014). Double network bacterial cellulose hydrogel to build a biology–device interface. *Nanoscale, 6*(2), 970-977. doi:10.1039/C3NR05214A

Shi, Z., Zang, S., Jiang, F., Huang, L., Lu, D., Ma, Y., & Yang, G. (2012). In situ nano-assembly of bacterial cellulose–polyaniline composites. *RSC Advances, 2*, 1040. doi:10.1039/c1ra00719j

Shirakawa, H., Louis, E. J., MacDiarmid, A. G., Chiang, C. K., & Heeger, A. J. (1977). Synthesis of electrically conducting organic polymers: halogen derivatives of polyacetylene, (CH). *Journal of the Chemical Society, Chemical Communications*(16), 578-580. doi:10.1039/C39770000578

Shukla, A., Suresh, P., Berchmans, S., & Rajendran, A. (2004). Biological Fuel Cells and Their Applications. *Current Science, 87*.

Singh, M., Kumar, P., & Karthikeyan, S. (2011). Structural basis for pH dependent monomer–dimer transition of 3,4-dihydroxy 2-butanone-4-phosphate synthase domain from Mycobacterium tuberculosis. *Journal of Structural Biology, 174*(2), 374-384. doi:10.1016/j.jsb.2011.01.013

Sleutels, T. H. J. A., ter Heijne, A., Kuntke, P., Buisman, C. J. N., & Hamelers, H. V. M. (2017). Membrane Selectivity Determines Energetic Losses for Ion Transport in Bioelectrochemical Systems. *Chemistry select, 2*(12), 3462-3470. doi:10.1002/slct.201700064

Słoniewska, A., & Pałys, B. (2014). Supramolecular polyaniline hydrogel as a support for urease. *Electrochimica Acta, 126*, 90-97. doi:10.1016/j.electacta.2013.10.164

Solonaru, A., & Grigoras, M. (2017). Water-soluble polyaniline/graphene composites as materials for energy storage applications. *Express Polymer Letters, 11*, 127-139. doi:10.3144/expresspolymlett.2017.14

Stahmann, K. P., Revuelta, J. L., & Seulberger, H. (2000). Three biotechnical processes using Ashbya gossypii, Candida famata, or Bacillus subtilis compete with chemical riboflavin production. *Applied Microbiology and Biotechnology, 53*(5), 509-516. doi:10.1007/s002530051649

Stejskal, J. (2017). Conducting polymer hydrogels. *Chemical Papers, 71*(2), 269-291. doi:10.1007/s11696-016-0072-9

Stejskal, J., Exnerová, M., Moravkova, Z., Trchová, M., Hromádková, J., & Prokeš, J. (2012). Oxidative stability of polyaniline. *Polymer Degradation and Stability, 97*, 1026–1033. doi:10.1016/j.polymdegradstab.2012.03.006

Stejskal, J., & Gilbert, R. G. (2002). Polyaniline. Preparation of a conducting polymer(IUPAC Technical Report). *Pure and Applied Chemistry, 74*(5). doi:10.1351/pac200274050857

Stejskal, J., & Sapurina, I. (2005). Polyaniline: Thin films and colloidal dispersions (IUPAC Technical Report). *Pure and Applied Chemistry - PURE APPL CHEM, 77*, 815-826. doi:10.1351/pac200577050815

Stejskal, J., Sapurina, I., & Trchová, M. (2010). Polyaniline nanostructures and the role of aniline oligomers in their formation. *Progress in Polymer Science, 35*(12), 1420-1481. doi:10.1016/j.progpolymsci.2010.07.006

Subha, C., Kavitha, S., Abisheka, S., Tamilarasan, K., Arulazhagan, P., & Rajesh Banu, J. (2019). Bioelectricity generation and effect studies from organic rich chocolaterie wastewater using continuous upflow anaerobic microbial fuel cell. *Fuel, 251*, 224-232. doi:10.1016/j.fuel.2019.04.052

Sun, J., Hu, Y., Bi, Z., & Cao, Y. (2009). Improved performance of air-cathode single-chamber microbial fuel cell for wastewater treatment using microfiltration membranes and multiple sludge inoculation. *Journal of Power Sources, 187*(2), 471-479. doi:10.1016/j.jpowsour.2008.11.022

Sun, R., Sun, X. F., Liu, G. Q., Fowler, P., & Tomkinson, J. (2002). Structural and physicochemical characterization of hemicelluloses isolated by alkaline peroxide from barley straw. *Polymer International, 51*(2), 117-124. doi:10.1002/pi.815

Szöllősi, A., Hoschke, Á., Rezessy-Szabó, J. M., Bujna, E., Kun, S., & Nguyen, Q. D. (2017). Formation of novel hydrogel bio-anode by immobilization of biocatalyst in alginate/polyaniline/titanium-dioxide/graphite composites and its electrical performance. *Chemosphere, 174*, 58-65. doi:10.1016/j.chemosphere.2017.01.095

Szöllősi, A., Narr, L., Kovács, A., & Styevkó, G. (2015a). Relationship between kinetics of growth and production of exo-electrons: Case study with Geobacter toluenoxydans. *Acta Microbiologica et Immunologica Hungarica, 62*, 307-316. doi:10.1556/030.62.2015.3.8

Szöllősi, A., Rezessy-Szabó, J. M., Hoschke, Á., & Nguyen, Q. D. (2015b). Novel method for screening microbes for application in microbial fuel cell. *Bioresource Technology, 179*, 123-127. doi:10.1016/j.biortech.2014.12.004

Szymanska-Chargot, M., Cybulska, J., & Zdunek, A. (2011). Sensing the Structural Differences in Cellulose from Apple and Bacterial Cell Wall Materials by Raman and FT-IR Spectroscopy. *Sensors (Basel, Switzerland), 11*, 5543-5560. doi:10.3390/s110605543

Tahara, N., Tabuchi, M., Watanabe, K., Yano, H., Morinaga, Y., & Yoshinaga, F. (1997). Degree of Polymerization of Cellulose from Acetobacter xylinum BPR2001 Decreased by Cellulase Produced by the Strain. *Bioscience, Biotechnology, and Biochemistry, 61*(11), 1862-1865. doi:10.1271/bbb.61.1862

Tamayo, L., Palza, H., Bejarano, J., & Zapata, P. A. (2019). Chapter 8 - Polymer Composites With Metal Nanoparticles: Synthesis, Properties, and Applications. In K. Pielichowski & T. M. Majka (Eds.), *Polymer Composites with Functionalized Nanoparticles* (pp. 249-286): Elsevier.

Tamer, I. M., Özilgen, M., & Ungan, S. (1988). Kinetics of riboflavin production by Brewers' yeasts. *Enzyme and Microbial Technology, 10*(12), 754-756. doi:10.1016/0141-0229(88)90121-4

Tang, Q., Wu, J., Sun, H., Fan, S., Hu, D., & Lin, J. (2008). Superabsorbent conducting hydrogel from poly(acrylamide-aniline) with thermo-sensitivity and release properties. *Carbohydrate Polymers, 73*(3), 473-481. doi:10.1016/j.carbpol.2007.12.030

Tang, X., Li, H., Du, Z., Wang, W., & Ng, H. Y. (2015). Conductive polypyrrole hydrogels and carbon nanotubes composite as an anode for microbial fuel cells. *RSC Advances, 5*(63), 50968-50974. doi:10.1039/C5RA06064H

Tang, Y. J., Martin, H. G., Dehal, P. S., Deutschbauer, A., Llora, X., Meadows, A., . . . Keasling, J. D. (2009). Metabolic flux analysis of Shewanella spp. reveals evolutionary robustness in central carbon metabolism. *Biotechnology and Bioengineering, 102*(4), 1161-1169. doi:10.1002/bit.22129

Tanisho, S., Kamiya, N., & Wakao, N. (1989). Microbial fuel cell using Enterobacter aerogenes. *Journal of Electroanalytical Chemistry and Interfacial Electrochemistry, 275*(1), 25-32. doi:10.1016/0022-0728(89)87189-X

Tao, H.-C., Liang, M., Li, W., Zhang, L.-J., Ni, J.-R., & Wu, W.-M. (2011). Removal of copper from aqueous solution by electrodeposition in cathode chamber of microbial fuel cell. *Journal of Hazardous Materials, 189*(1), 186-192. doi:10.1016/j.jhazmat.2011.02.018

Taşkan, E., Hasar, H., & Ozkaya, B. (2013). Usage of Ti-TiO2 electrode in microbial fuel cell to enhance the electricity generation and its biocompatibility. *Applied Mechanics and Materials, 404*, 371-376. doi:10.4028/www.scientific.net/AMM.404.371

Tender, L. M., Reimers, C. E., Stecher, H. A., Holmes, D. E., Bond, D. R., Lowy, D. A., . . . Lovley, D. R. (2002). Harnessing microbially generated power on the seafloor. *Nature Biotechnology, 20*(8), 821-825. doi:10.1038/nbt716

Tharali, A. D., Sain, N., & Osborne, W. J. (2016). Microbial fuel cells in bioelectricity production. *Frontiers in Life Science, 9*(4), 252-266. doi:10.1080/21553769.2016.1230787

Thulasinathan, B., Nainamohamed, S., Ebenezer Samuel, J. O., Soorangkattan, S., Muthuramalingam, J., Kulanthaisamy, M., . . . Alagarsamy, A. (2019). Comparative study on Cronobacter sakazakii and Pseudomonas otitidis isolated from septic tank wastewater in microbial fuel cell for bioelectricity generation. *Fuel, 248*, 47-55. doi:10.1016/j.fuel.2019.03.060

Thygesen, A., Poulsen, F. W., Min, B., Angelidaki, I., & Thomsen, A. B. (2009). The effect of different substrates and humic acid on power generation in microbial fuel cell operation. *Bioresource Technology, 100*(3), 1186-1191. doi:10.1016/j.biortech.2008.07.067

Trchová, M., Šeděnková, I., Tomsik, E., Stejskal, J., Holler, P., & Cirić-Marjanović, G. (2006). Evolution of Polyaniline Nanotubes: The Oxidation of Aniline in Water. *The journal of physical chemistry. B, 110*, 9461-9468. doi:10.1021/jp057528g

Ul-Islam, M., Khan, T., & Park, J. K. (2012). Water holding and release properties of bacterial cellulose obtained by in situ and ex situ modification. *Carbohydrate Polymers, 88*(2), 596-603. doi:10.1016/j.carbpol.2012.01.006

Ullah, M., Manan, S., Kiprono, S., Islam, M., & Yang, G. (2019). Synthesis, Structure, and Properties of Bacterial Cellulose. In *Nanocellulose: From Fundamentals to Advanced Materials* (pp. 81-113): Wiley-VCH Verlag GmbH & Co. KGaA.

Valencia Castro, L. E., Pérez Martínez, C. J., del Castillo Castro, T., Castillo Ortega, M. M., & Encinas, J. C. (2015). Chemical polymerization of pyrrole in the presence of l-serine or l-glutamic acid: Electrically controlled amoxicillin release from composite hydrogel. *Journal of Applied Polymer Science, 132*(15). doi:10.1002/app.41804

Vandamme, E. J. (1992). Production of vitamins, coenzymes and related biochemicals by biotechnological processes. *Journal of Chemical Technology and Biotechnology, 53*(4), 313-327. doi:10.1002/jctb.280530402

Vandamme, E. J., De Baets, S., Vanbaelen, A., Joris, K., & De Wulf, P. (1998). Improved production of bacterial cellulose and its application potential. *Polymer Degradation and Stability, 59*(1), 93-99. doi:10.1016/S0141-3910(97)00185-7

Vargas, I., Albert, I., & Regan, J. (2013). Spatial Distribution of Bacterial Communities on Volumetric and Planar Anodes in Single-Chamber Air-Cathode Microbial Fuel Cells. *Biotechnology and Bioengineering, 110*. doi:10.1002/bit.24949

Vega, C. A., & Fernández, I. (1987). Mediating effect of ferric chelate compounds in microbial fuel cells with Lactobacillus plantarum, Streptococcus lactis, and Erwinia dissolvens. *Bioelectrochemistry and Bioenergetics, 17*(2), 217-222. doi:10.1016/0302-4598(87)80026-0

Virdis, B., Rabaey, K., Yuan, Z., & Keller, J. (2008). Microbial fuel cells for simultaneous carbon and nitrogen removal. *Water Research, 42*(12), 3013-3024. doi:10.1016/j.watres.2008.03.017

Vogl, C., Grill, S., Schilling, O., Stülke, J., Mack, M., & Stolz, J. (2007). Characterization of riboflavin (vitamin B2) transport proteins from Bacillus subtilis and Corynebacterium glutamicum. *Journal of bacteriology, 189*(20), 7367-7375. doi:10.1128/JB.00590-07

Volbeda, A., Charon, M. H., Piras, C., Hatchikian, E. C., Frey, M., & Fontecilla-Camps, J. C. (1995). Crystal structure of the nickel-iron hydrogenase from Desulfovibrio gigas. *Nature, 373*(6515), 580-587. doi:10.1038/373580a0

von Canstein, H., Ogawa, J., Shimizu, S., & Lloyd, J. R. (2008). Secretion of Flavins by Shewanella Species and Their Role in Extracellular Electron Transfer. *Applied and environmental microbiology, 74*(3), 615-623. doi:10.1128/AEM.01387-07 %J Applied and Environmental Microbiology

Waller, M., & Trabold, T. (2013). Review of Microbial Fuel Cells for Wastewater Treatment: Large-Scale Applications, Future Needs and Current Research Gaps. *Conference: ASME 2013 11th International Conference on Fuel Cell Science, Engineering and Technology collocated with the ASME 2013 Heat Transfer Summer Conference and the ASME 2013 7th International Conference on Energy Sustainability*. doi:10.1115/FuelCell2013-18185

Wan, Y., Wang, J., Gama, M., Guo, R., Zhang, Q., Zhang, P., . . . Luo, H. (2019). Biofabrication of a novel bacteria/bacterial cellulose composite for improved adsorption capacity. *Composites Part A: Applied Science and Manufacturing, 125*, 105560. doi:10.1016/j.compositesa.2019.105560

Wang, H., Wang, Q., Li, X., Wang, Y., Jin, P., Zheng, Y., . . . Qingbiao, L. (2019a). Bioelectricity generation from the decolorization of reactive blue 19 by using microbial fuel cell. *Journal of Environmental Management, 248*, 109310. doi:10.1016/j.jenvman.2019.109310

Wang, H., Zhu, E., Yang, J., Zhou, P., Sun, D., & Tang, W. (2012a). Bacterial cellulose nanofiber-supported polyaniline nanocomposites with flake-shaped morphology as supercapacitor electrodes. *The Journal of Physical Chemistry C, 116*(24), 13013-13019. doi:10.1021/jp301099r

Wang, J., Tavakoli, J., & Tang, Y. (2019b). Bacterial cellulose production, properties and applications with different culture methods – A review. *Carbohydrate Polymers, 219*, 63-76. doi:10.1016/j.carbpol.2019.05.008

Wang, L., Lu, X., Lei, S., & Song, Y. (2014). Graphene-based polyaniline nanocomposites: preparation, properties and applications. *Journal of Materials Chemistry A, 2*(13), 4491-4509. doi:10.1039/C3TA13462H

Wang, Q.-Q., Wu, X.-Y., Yu, Y.-Y., Sun, D.-Z., Jia, H.-H., & Yong, Y.-C. (2017). Facile in-situ fabrication of graphene/riboflavin electrode for microbial fuel cells. *Electrochimica Acta, 232*. doi:10.1016/j.electacta.2017.03.008

Wang, Y.-P., Liu, X.-W., Li, W.-W., Li, F., Wang, Y.-K., Sheng, G.-P., . . . Yu, H.-Q. (2012b). A microbial fuel cell–membrane bioreactor integrated system for cost-effective wastewater treatment. *Applied Energy, 98*, 230-235. doi:10.1016/j.apenergy.2012.03.029

Wang, Y., Zheng, H., Chen, Y., Wen, Q., & Wu, J. (2020). Macroporous composite capacitive bioanode applied in microbial fuel cells. *Chinese Chemical Letters, 31*(1), 205-209. doi:10.1016/j.cclet.2019.05.052

Watanabe, K. (2008). Recent Developments in Microbial Fuel Cell Technologies for Sustainable Bioenergy. *Journal of Bioscience and Bioengineering, 106*(6), 528-536. doi:10.1263/jbb.106.528

Watanabe, K., Tabuchi, M., Morinaga, Y., & Yoshinaga, F. (1998). Structural Features and Properties of Bacterial Cellulose Produced in Agitated Culture. *Cellulose, 5*(3), 187-200. doi:10.1023/A:1009272904582

Wei, L., Han, H., & Shen, J. (2013). Effects of temperature and ferrous sulfate concentrations on the performance of microbial fuel cell. *International Journal of Hydrogen Energy, 38*(25), 11110-11116. doi:10.1016/j.ijhydene.2013.01.019

Wen, J., & Huang, Y. (2013). *Robust speed control of permanent magnet synchronous motor.* Paper presented at the Proceedings of the 2013 IEEE 8th Conference on Industrial Electronics and Applications, ICIEA 2013.

Wijsboom, Y. H., Patra, A., Zade, S. S., Sheynin, Y., Li, M., Shimon, L. J. W., & Bendikov, M. (2009). Controlling Rigidity and Planarity in Conjugated Polymers: Poly(3,4-ethylenedithioselenophene). *Angewandte Chemie - International Edition, 48*(30), 5443-5447. doi:10.1002/anie.200901231

Wilkinson, S. (2000). "Gastrobots"—Benefits and Challenges of Microbial Fuel Cells in FoodPowered Robot Applications. *Autonomous Robots, 9*(2), 99-111. doi:10.1023/A:1008984516499

Woodward, J. (1988). Methods of immobilization of microbial cells. *Journal of Microbiological Methods, 8*(1), 91-102. doi:10.1016/0167-7012(88)90041-3

Wu, D., Xing, D., Lu, L., Wei, M., Liu, B., & Ren, N. (2013a). Ferric iron enhances electricity generation by Shewanella oneidensis MR-1 in MFCs. *Bioresource Technology, 135*, 630-634. doi:10.1016/j.biortech.2012.09.106

Wu, S., Xiao, Y., Song, P., Wang, C., Yang, Z., Slade, R. C. T., & Zhao, F. (2016). Riboflavin-mediated extracellular electron transfer process involving Pachysolen tannophilus. *Electrochimica Acta, 210*, 117-121. doi:10.1016/j.electacta.2016.05.139

Wu, Y., Zhang, X., Li, S., Lv, X., Cheng, Y., & Wang, X. (2013b). Microbial biofuel cell operating effectively through carbon nanotube blended with gold–titania nanocomposites modified electrode. *Electrochimica Acta, 109*, 328-332. doi:10.1016/j.electacta.2013.07.166

Xie, X., Ye, M., Hu, L., Liu, N., McDonough, J. R., Chen, W., . . . Cui, Y. (2012). Carbon nanotube-coated macroporous sponge for microbial fuel cell electrodes. *Energy and Environmental Science, 5*(1), 5265-5270. doi:10.1039/c1ee02122b

Xu, H., Wang, L., Wen, Q., Chen, Y., Qi, L., Huang, J., & Tang, Z. (2019). A 3D porous NCNT sponge anode modified with chitosan and Polyaniline for high-performance microbial fuel cell. *Bioelectrochemistry, 129*, 144-153. doi:10.1016/j.bioelechem.2019.05.008

Xu, S., Liu, H., Fan, Y., Schaller, R., Jiao, J., & Chaplen, F. (2011). Enhanced performance and mechanism study of microbial electrolysis cells using Fe nanoparticle-decorated anodes. *Applied Microbiology and Biotechnology, 93*, 871-880. doi:10.1007/s00253-011-3643-2

Yadav, A. K., Dash, P., Mohanty, A., Abbassi, R., & Mishra, B. K. (2012). Performance assessment of innovative constructed wetland-microbial fuel cell for electricity production and dye removal. *Ecological Engineering, 47*, 126-131. doi:10.1016/j.ecoleng.2012.06.029

Yamane, Y., Nakamura, Y., Okamoto, H., Ooshima, H., & Kato, J. (1995). Overproduction of riboflavin by anArthrobacter sp. mutant resistant to 5-fluorouracil. *Applied Biochemistry and Biotechnology, 50*(3), 317-322. doi:10.1007/BF02788101

Yan, B., Chen, Z., Cai, L., Chen, Z., Fu, J., & Xu, Q. (2015). Fabrication of polyaniline hydrogel: Synthesis, characterization and adsorption of methylene blue. *Applied Surface Science, 356*, 39-47. doi:10.1016/j.apsusc.2015.08.024

Yang, L., Chu, J. S., & Fix, J. A. (2002). Colon-specific drug delivery: new approaches and in vitro/in vivo evaluation. *International Journal of Pharmaceutics, 235*(1), 1-15. doi:10.1016/S0378-5173(02)00004-2

Yong, Y.-C., Cai, Z., Yu, Y.-Y., Chen, P., Jiang, R., Cao, B., . . . Song, H. (2013a). Increase of riboflavin biosynthesis underlies enhancement of extracellular electron transfer of Shewanella in alkaline microbial fuel cells. *Bioresource Technology, 130*, 763-768. doi:10.1016/j.biortech.2012.11.145

Yong, Y.-C., Liao, Z.-H., Sun, J.-Z., Zheng, T., Jiang, R.-R., & Song, H. (2013b). Enhancement of coulombic efficiency and salt tolerance in microbial fuel cells by

graphite/alginate granules immobilization of Shewanella oneidensis MR-1. *Process Biochemistry, 48*(12), 1947-1951. doi:10.1016/j.procbio.2013.09.008

Yoon, S. H., Jin, H.-J., Kook, M.-C., & Pyun, Y. R. (2006). Electrically Conductive Bacterial Cellulose by Incorporation of Carbon Nanotubes. *Biomacromolecules, 7*(4), 1280-1284. doi:10.1021/bm050597g

Yuan, H., Deng, L., Chen, Y., & Yuan, Y. (2016). MnO2/Polypyrrole/MnO2 multi-walled-nanotube-modified anode for high-performance microbial fuel cells. *Electrochimica Acta, 196*, 280-285. doi:10.1016/j.electacta.2016.02.183

Zeng, X., Small, D. P., & Wan, W. (2011). Statistical optimization of culture conditions for bacterial cellulose production by Acetobacter xylinum BPR 2001 from maple syrup. *Carbohydrate Polymers, 85*(3), 506-513. doi:10.1016/j.carbpol.2011.02.034

Zhai, D., Liu, B., Shi, Y., Pan, L., Wang, Y., Li, W., . . . Yu, G. (2013). Highly Sensitive Glucose Sensor Based on Pt Nanoparticle/Polyaniline Hydrogel Heterostructures. *ACS Nano, 7*(4), 3540-3546. doi:10.1021/nn400482d

Zhang, H., Xu, X., Chen, C., Chen, X., Huang, Y., & Sun, D. (2019). In situ controllable fabrication of porous bacterial cellulose. *Materials Letters, 249*, 104-107. doi:10.1016/j.matlet.2019.04.026

Zhang, L., Zhou, S., Zhuang, L., Li, W., Zhang, J., Lu, N., & Deng, L. (2008). Microbial fuel cell based on Klebsiella pneumoniae biofilm. *Electrochemistry Communications, 10*(10), 1641-1643. doi:10.1016/j.elecom.2008.08.030

Zhang, P., Liu, J., Qu, Y., & Feng, Y. (2017). Enhanced Shewanella oneidensis MR-1 anode performance by adding fumarate in microbial fuel cell. *Chemical Engineering Journal, 328*, 697-702. doi:10.1016/j.cej.2017.07.008

Zhang, X., Chechik, V., Smith, D. K., Walton, P. H., Duhme-Klair, A.-K., & Luo, Y. (2009). Nanocomposite hydrogels—Controlled synthesis of chiral polyaniline nanofibers and their inclusion in agarose. *Synthetic Metals, 159*(19), 2135-2140. doi:10.1016/j.synthmet.2009.08.002

Zhang, Z., Liang, M., Liu, X., Zhao, F., Wang, B., Li, W., & Wang, Q. (2015). A hybrid gel of hypergravity prepared NiO and polyaniline as Li-ion battery anodes. *RSC Advances, 5*(107), 88419-88424. doi:10.1039/C5RA17929G

Zhao, H.-B., Yuan, L., Fu, Z.-B., Wang, C.-Y., Yang, X., Zhu, J.-Y., . . . Schiraldi, D. A. (2016). Biomass-Based Mechanically Strong and Electrically Conductive Polymer Aerogels and Their Application for Supercapacitors. *ACS Applied Materials & Interfaces, 8*(15), 9917-9924. doi:10.1021/acsami.6b00510

Zheng, J., Yu, X., Wang, C., Cao, Z., Yang, H., Ma, D., & Xu, X. (2016). Facile synthesis of three-dimensional reinforced Sn/polyaniline/sodium alginate nanofiber hydrogel network for high performance lithium-ion battery. *Journal of Materials Science: Materials in Electronics, 27*(5), 4457-4464. doi:10.1007/s10854-016-4317-8

Acknowledgements

Firstly, I would like to express my deep and sincere gratitude to my supervisor **Prof. Quang D. Nguyen** for giving me the opportunity to do research and proving invaluable guidance throughout this research. His dynamism, vision, sincerity and motivation have deeply inspired me. He has taught me the methodology to carry out the research and to present the research works as clearly as possible. His guidance helped me in all the time of research and writing of this thesis.

My thankfulness goes to my co-supervisor **Assoc. Prof. Dam Sao Mai** for introducing me to the world of science and for helping me during research as well.

I would like to thank **all members of the Department of Distilling and Brewing: Rezessyné Dr. Szabó Judit, Prof. Hoschke Ágoston,** and **Hegyesné Dr. Vecseri Beáta** for supporting me and giving me encouragements during the study; **Dr. Bujna Erika; Dr. Farkas Csilla, Dr. Kun Szilárd, Dr. Kun-Farkas Gabriella, Kiss Zsuzsanna, Kilin Ákos** for their kind of help and share, especially **Dr. Nagy Edina Szandra** for her continuous help and supporting me in the laboratory. In additions, I would like to thank all my colleagues at Institute of Food Technology and Biotechnology, Industrial University of Ho Chi Minh city, especially **Dr. Dieu-Hanh Nguyen**, **Dr. Tan-Viet Pham**, **Ms. Huynh Nguyen Tuong An** for supporting me to complete some experiments in Vietnam.

I would like to give my sincere thanks to **Professors** in **the Food Science Doctoral School** for giving me the opportunity to carry out my Ph.D. study.

I am thankful to **Professors** in **Faculty of Food Science**, who gave me scientific lectures.
I also have learned from them the kind of working and studying as well.

Last but not least, I would like to thank my fellow lab-mates **Ta Phuong Linh, Koren Dániel, Pham Minh Tuan, Tran Thi Mai Anh, Nguyen Bao Toan, Vu Ngoc Ha Vi** for their help during the experiments.